

**The synthesis of xanthene-based transition metal complexes and
their application in the oxidation reaction of *n*-octane**

By

Nonjabulo Nyalungu

BSc(Hons)

Dissertation submitted in fulfillment of the academic requirements for the degree of Master of
Science in the School of Chemistry, University of KwaZulu-Natal, Durban, South Africa

As the candidate's supervisor we have approved this dissertation for submission.

Signed: _____ Name: Prof. H. B. Friedrich Date: _____ (supervisor)

Signed: _____ Name: Dr M. D. Bala Date: _____ (co-supervisor)

November 2014

Abstract

The oxidation of alkanes into valuable products such as alcohols, ketones and aldehydes is very important to industry for detergents and perfumes. One of the challenges with alkanes is their inertness which results from the strong and localized C-C and C-H bonds. There are few methods that are known to transform alkanes into products of value. Therefore in this study xanthene-based ligands were used in an attempt to transform alkanes into products of value. Xanthene-based ligands are known to produce catalysts that are highly active and selective in reactions such as hydroformylation and hydrocyanation. These ligands are bidentate and their structure consists of a xanthene backbone with two phosphorus donor atoms and a rigid backbone. Five xanthene-based ligands were synthesized, characterized and complexed to cobalt and nickel. In this study modification at position X was done by using a sulphur atom, a methyl group as well as an isopropyl group in order to observe the effect this has on the activation of *n*-octane.

Crystal structures of ligand (4,5-bis(di-*p*-tolylphosphino)-9,9-dimethyl xanthene) and complex (Co(4,5-bis(di-*p*-tolylphosphino)-9,9-dimethylxanthene)Cl₂) and (Ni(4,5-bis(di-*p*-tolylphosphino)-9,9-dimethylxanthene)Cl₂) were obtained. The five cobalt and five nickel complexes were catalytically tested in the oxidation of *n*-octane, using three oxidants *tert*-butyl hydroperoxide, hydrogen peroxide and *meta*-chloroperbenzoic acid. This was carried out in tetrahydrofuran solvent at varying temperatures.

Hydrogen peroxide and *meta*-chloroperbenzoic acid gave no substantial activation, while *tert*-butyl hydroperoxide showed activity. Modifications to the backbone at position X brought changes to the bite angle and minor changes to activity. Selectivity at 50 and 60 °C favoured the C-2 position with 2-octanone as the dominant product. Terminal position showed no products of alkane oxygenation. Alcohols (3-octanol and 4-octanol) were observed at higher temperatures. Steric factors had no significance effect on activity while temperature had a greater effect. The temperature that was best to work with was 50 °C since all catalysts were active. Sulphur had a deactivating effect on efficacy of both cobalt and nickel catalysts.

Preface

The experimental work described in this dissertation was carried out in the School of Chemistry, University of KwaZulu-Natal, Westville Campus, Durban, from February 2012 to November 2014, under the supervision of Prof. H. B. Friedrich and Dr M. D. Bala. These studies represent original work by the author and have not otherwise been submitted in any form or degree or diploma to any tertiary institution. Where use has been made of the work of others it is duly acknowledged in the text.

Signed: _____

Nonjabulo Nyalungu

B. Sc (Honours) (UKZN-Westville Campus)

Declaration - Plagiarism

I, _____ declare that

1. The research reported in this thesis, except where otherwise indicated is my original research.
2. This thesis has not been submitted for any degree or examination at any other university.
3. This thesis does not contain other persons' data, pictures, graphs or other information, unless specifically acknowledged as being sourced from other person.
4. This thesis does not contain other persons' writing, unless specifically acknowledged as being sourced from other researchers. Where other written sources have been quoted, then:
 - a. Their words have been re-written but the general information attributed to them has been referenced.
 - b. Where their exact words have been used, then their writing has been placed in italics and inside quotation marks, and referenced.
5. This thesis does not contain text, graphics or tables copied and pasted from the Internet, unless specifically acknowledged, and the source being detailed in the thesis and in the References sections.

Signed: _____

Nonjabulo Nyalungu

Conference Contributions

Part of the work discussed in this dissertation has been presented as a poster presentation at the following conferences:

CATSA Conference 2012, Cape Town, poster presentation, *Synthesis of xanthene-based pincer ligands*, N. Nyalungu, H. B. Friedrich and M. D. Bala

SACI Conference 2013, Durban, poster presentation, *Synthesis of xanthene-based pincer ligands*, N. Nyalungu, H. B. Friedrich and M. D. Bala.

CATSA Conference 2013, Wild Coast, poster presentation, *Synthesis of xanthene-based pincer ligands and their application in oxidation of n-octane*, N. Nyalungu, H. B. Friedrich and M. D. Bala.

Table of Contents

List of Figures	x
List of Tables	xii
List of Schemes.....	xiii
Acknowledgements.....	xiv
List of Abbreviations.....	xv
Chapter 1: Introduction	1
1.1 Catalysis	1
1.2 History of C-H Activation.....	2
1.3 C-H Activation.....	2
1.4 Ligand design for C-H activation.....	5
1.4.1 Ligand of choice	5
1.4.2 Ligand design parameters	6
1.4.3 Ligand backbone.....	7
1.4.4 Donor atoms.....	7
1.4.5 Transition metals in homogeneous catalysis.....	8
1.4.6 Electronic effect.....	9
1.4.7 Steric effect.....	9
1.4.8 Natural bite angle.....	10
1.5 Diphosphine complexes	11
1.5.1 Application of diphosphine ligands in catalysis	12
1.5.2 Xanthene-based ligands.....	13
1.6 Biological catalysis	14
1.6.1 Biomimetic catalysis.....	14

1.6.2	Methane monooxygenase in C-H activation.....	15
1.6.3	Cytochrome P450 monooxygenase in C-H activation.....	16
1.7	Heterogeneous catalysis in C-H Activation	18
1.8	Homogenous catalysis.....	19
1.9	Methods of C-H bond activation using homogeneous catalysis	20
1.9.1	Oxidative addition of paraffins	20
I	Concerted oxidative addition.....	20
II	S _N 2 oxidative addition	21
III	Radical oxidative addition	21
1.9.2	Reductive elimination	22
1.10	Future use of Hydrocarbons in Catalysis.....	23
1.11	The project aims and goal.....	23
1.12	References	26
Chapter 2:	Experimental.....	30
2.1	General	30
2.1.1	Instrumentation	31
2.1.2	Experimental Methods.....	31
2.1.2.1	4,5-bis(diphenylphosphino)-9,9-dimethyl xanthene.....	31
2.1.2.2	4,5-bis(di- <i>p</i> -tolylphosphino)-9,9-dimethyl xanthene	32
2.1.2.3	(2,7-di- <i>n</i> -hexanoyl-9,9-dimethyl xanthene)	33
2.1.2.4	2,7-di- <i>n</i> -hexyl-9,9-dimethyl xanthene.....	34
2.1.2.5	4,5-bis(diphenylphosphino)-2,7-dihexyl-9,9-dimethyl xanthene.....	35
2.1.2.6	9-isopropyl-9H-xanthen-9-ol.....	36
2.1.2.7	10-isopropylidene xanthene.....	37
2.1.2.8	4, 5-bis(diphenylphosphino) 10-isopropylidene xanthene	38

2.1.2.9	Co(4,5-bis(diphenylphosphino)-9,9-dimethyl xanthene)Cl ₂	39
2.1.2.10	Co(4,5-bis(di- <i>p</i> -tolylphosphino)-9,9-dimethyl xanthene)Cl ₂	40
2.1.2.11	Co(4,5-bis(diphenylphosphino)-2,7-dihexyl-9,9-dimethyl xanthene)Cl ₂	41
2.1.2.12	Co(Thixantphos)Cl ₂	41
2.1.2.13	Co(4,5-bis(diphenylphosphino) 10-isopropylidene xanthene)Cl ₂	42
2.1.2.14	Ni(4,5-bis(diphenylphosphino)-9,9-dimethyl xanthene)Cl ₂	43
2.1.2.15	Ni(4,5-bis(di- <i>p</i> -tolylphosphino)-9,9-dimethyl xanthene)Cl ₂	43
2.1.2.16	Ni(4,5-bis(diphenylphosphino)-2,7-dihexyl-9,9-dimethyl xanthene)Cl ₂	44
2.1.2.17	Ni(thixantphos)Cl ₂	45
2.1.2.18	Ni(4,5-bis(diphenylphosphino) 10-isopropylidene xanthene)Cl ₂	45
2.2	References	47
Chapter 3: Results and Discussion		48
3.1	Introduction	48
3.1.1	Preparation of Ligands.....	48
3.1.2	NMR Analysis	49
3.1.3	IR Analysis.....	59
3.1.4	Melting points	61
3.2	Complexes.....	62
3.2.1	Elemental Analysis	63
3.2.2	XRD	63
3.2.2.1	Crystal Structures	64
3.3	Summary	71
3.4	References	72
Chapter 4: Oxidation of alkanes.....		74
4.1	Introduction.....	74

4.2	Instrumentation	76
4.3	General Procedure.....	76
4.4	Optimization	77
4.4.1	Optimization results for cobalt and nickel catalysts.....	77
4.4.2	Oxidation of <i>n</i> -octane in the presence of H ₂ O ₂ as the oxidant.....	79
4.4.3	Oxidation of <i>n</i> -octane in the presence of <i>m</i> -CPBA as the oxidant.....	79
4.5	Results & Discussion	80
4.5.1	Efficiency of the cobalt based catalyst using TBHP as oxidant at 50 °C.....	80
4.5.2	Catalyst efficiency at 60 °C.....	84
4.5.3	Efficiency of the nickel based catalysts using TBHP as the oxidant at 50 °C.....	85
4.5.4	Catalyst efficiency at 60 °C.....	88
4.6	Effects of oxidant.....	90
4.7	Catalyst Efficiency.....	90
4.8	Summary	92
4.9	References.....	94
Chapter 5:	General Conclusion	96

List of Figures

Figure 1.1: Parameters for bidentate design	6
Figure 1.2: Some xanthene-based ligands	7
Figure 1.3: Electronic effects of ligands	9
Figure 1.4: Illustration of the Tolman's cone angle	10
Figure 1.5: Illustration of the P-P distance determined by the backbone, which can be measured by bite angle using dummy atoms.	11
Figure 1.6: Diphosphine ligands.	13
Figure 1.7: Generic structure of xanthene-based ligands with flexibility and rigid backbones. .	14
Figure 1.8: Oxidation of alkanes by monooxygenase.....	15
Figure 1.9: Structure of cytochrome P450 showing the heme structure.....	16
Figure 1.10: The concerted oxidative addition mechanism.	21
Figure 1.11: S _N 2 oxidative addition mechanism.....	21
Figure 1.12: Non-radical chain oxidative addition mechanism.	22
Figure 1.13: Radical chain oxidative addition mechanism.....	22
Figure 1.14: Reductive elimination mechanism	23
Figure 3.1: General structure of the ligands studied in this project.....	48
Figure 3.2: ¹ H NMR of ligands 4,5-bis(diphenylphosphino)-9,9-dimethyl xanthene	55
Figure 3.3: ¹ H NMR of ligand 4,5-bis(di- <i>p</i> -tolylphosphino)-9,9-dimethyl xanthene.....	56
Figure 3.4: ¹ H NMR of ligand 2,7-di- <i>n</i> -hexyl-9,9-dimethyl xanthene	56
Figure 3.5: ¹ H NMR of ligand 4,5-bis(diphenylphosphino)-10- <i>isopropylidene</i> xanthene.	57
Figure 3.6: ORTEP diagram of ligand 2.3 showing the atom numbering scheme. Thermal ellipsoids are represented at the 50% probability levels.....	67
Figure 3.7: ORTEP diagram of complex 2.12 showing the atom numbering scheme. Thermal ellipsoids are represented at the 50% probability levels.....	69
Figure 3.8: ORTEP diagram of complex 2.17 showing the atom numbering scheme. Thermal ellipsoids are represented at the 50% probability levels.....	70
Figure 4.1: Conversion on <i>n</i> -octane over the blank reaction and over the catalysts at different substrate to oxidant ratios.	78
Figure 4.2: Selectivities at two substrate to oxidant ratios over catalyst 2.11	78

Figure 4.3: Conversion of <i>n</i> -octane over the cobalt catalysts at 50 °C.....	81
Figure 4.4: Selectivity to products over the cobalt catalysts at 50 °C.....	83
Figure 4.5: Conversion over the cobalt catalysts in the presence of TBHP at 60 °C.....	84
Figure 4.6: Selectivity over the cobalt catalysts in the presence of TBHP at 60 °C.....	85
Figure 4.7: Nickel catalysts activity in the presence of TBHP as oxidant.....	86
Figure 4.8: Selectivity over the nickel catalysts in the presence of TBHP as oxidant.	87
Figure 4.9: Conversion over the nickel catalysts in the presence of TBHP as oxidant.	88
Figure 4.10: Selectivity of the nickel based catalysts in the presence of TBHP as oxidant.	89
Figure 4.11: Conversion over the nickel catalysts when TBHP was added slowly at the interval of 24 h.....	90

List of Tables

Table 3.1: Precursors and their percentage yields.	51
Table 3.2: Ligand structures and their percentage yields.	52
Table 3.3: Cobalt complexes and their percentage yields.....	53
Table 3.4: Nickel complexes and their percentage yields.....	54
Table 3.5: ¹ H NMR peaks of representative ligands and their integration.	58
Table 3.6: ³¹ P NMR data of ligands 2.2 , 2.3 , 2.6 and 2.10	59
Table 3.7: IR data of ligands and corresponding complexes.	61
Table 3.8: Melting point of ligands and their complexes.	62
Table 3.9: Elemental analysis data for complexes 2.11-2.20	63
Table 3.10: Crystallographic and structure refinement data for ligand 2.3 , complexes 2.12 and 2.17	65
Table 3.11: Selected bond lengths and bond angles of ligand 2.3	67
Table 3.12: Selected bond lengths and bond angles for complex 2.12 and 2.17	71
Table 4.1: GC parameters and column specifications.	76
Table 4.2: Optimization conditions used for catalysis.	80
Table 4.3: Natural bite angle of ligands.	82
Table 4.4: Regioselectivity of cobalt catalysts at 50 °C.	83
Table 4.5: Regioselectivity of cobalt catalysts at 60 °C.	85
Table 4.6: Selectivity parameters in <i>n</i> -octane activation by nickel catalysts at 50 °C.	87
Table 4.7: Selectivity parameters in <i>n</i> -octane activation by the nickel catalysts at 60 °C.	89
Table 4.8: Turn over numbers of various catalysts at 50 and 60 °C.	91

List of Schemes

Scheme 1.1: The catalytic cycle proposed for alkane oxidation by O ₂ promoted by cytochrome P450	18
Scheme 3.1: General procedure for the synthesis of ligands (2.2, 2.3, 2.6 & 2.10).	49
Scheme 4.1: Adapted mechanism for the oxidation of <i>n</i> -octane (RH) by cobalt and nickel complexes and TBHP as oxidant	92

Acknowledgements

- I would like to give glory to God as this would have not been a success without Him. For giving me strength and patience this has now come to completion.
- I would like to give equal thanks and appreciation to both my supervisors, Professor H. B. Friedrich and Dr M. D. Bala for their valuable input, constant support and guidance throughout my MSc study.
- To my parents mom (Nomadeli Nyalungu) and dad (Sebatatzi Nyalungu) your support has been amazing I have never seen people that sacrificed so much for their children. I'm very grateful for having you in my life.
- To all of my siblings (Cindy, Dumisani, Slindile and Khulekani), cousins (Mbali, Bandile and Nto), nephews (Lunga, Londi, Mpumelelo, Bulela and Nqubeko) and nieces (Linda and Namisa) I love the way you showed me support and love. I hope I have been a great example and you will keep the culture of education alive.
- To a very close friend of mine Samkelo Mthlane, thank you for your endless support and for believing in me. You have inspired me to be where I am and for that I will always treasure you.
- To my mentor and my friend Dunesha Naicker, your input towards my MSc have been valuable. At times you were more than just a colleague you were more like my supervisor. You have guided me from the structure to the end of my project. For that I would like to say thank you.
- To Dr Sooboo Singh, Dr Sam Mahommed, Mr Mzamo Shozi and members of the CRG-UKZN we have worked well together, you guys were more like my second family.
- To Greg Moodley, Jay, Raj, Dr Owaga, Neil, Anita, Unathi, and Dilip thank you for your individual part into making this project a success.
- For funding I would like to thank, c*change, NRF and Thrip.

List of Abbreviations

AlCl ₃	= Aluminium chloride
ATR	= Attenuated total reflectance
arom	= Aromatic
Å	= Angstrom
<i>n</i> -BuLi	= <i>n</i> -Butyllithium
CPK	= Corey-Pauling-Koltun
d	= Doublet
DCM	= Dichloromethane
DFT	= Density functional theory
Et ₂ O	= Diethyl ether
DSC	= Differential scanning calorimetry
eqn	= Equation
ESI	= Electron spray ionization
Et ₃ N	= Triethylamine
EtOH	= Ethanol
FID	= Flame ionization detector
IR	= Infrared
g	= Gram
GC	= Gas Chromatography
HOMO	= Highest Occupied Molecular Orbital

HRMS	= High resolution mass spectroscopy
Hz	= Hertz
<i>J</i>	= Coupling constant
Kcal/mol	= Kilocalories per mole
L	= Ligand
l	= Litre
LUMO	= Lowest Unoccupied Molecular Orbital
LLDPE	= Linear low density polyethylene
M	= Metal
m	= Multiplet
MeCN	= Acetonitrile
MeOH	= Methanol
min	= Minute
ml	= Milliliter (10^{-3} liter)
mmol	= Millimolar
MMO	= Methane monooxygenase
mol	= Moles
Mp	= Melting point
mV	= Millivolts
MW	= Molecular weight
NMR	= Nuclear magnetic resonance

Ph	= Phenyl
ppm	= Parts per million
por	= Porphyrin
qui	= Quintet
RF	= Response factor
rt	= Room temperature
<i>s</i>	= Strong
TLC	= Thin layer chromatography
t	= Triplet
<i>t</i> -BuOOH	= <i>Tert</i> -butyl hydroperoxide
THF	= Tetrahydrofuran
TMEDA	= N, N, N', N'-tetramethylenediamine
TON	= Turn over number
<i>w</i>	= weak
XRD	= X-ray diffraction
μL	= Microliter (10 ⁻⁶ liter)

Chapter 1

Introduction

1.1 Catalysis

The term catalysis was coined by Berzelius in 1836. Many years later Ostwald described it as :“*a substance which increases the rate at which a chemical reaction approaches equilibrium without becoming itself permanently involved*” [1]. In simple terms, a catalyst is a substance that speeds up a reaction without itself being consumed in the reaction. It does this by lowering the activation energy, making it easier for reactants to reach the final stage as products [2, 3]. Catalysis is the core of many chemical processes that convert inexpensive raw materials into products of value that are relevant to human needs in energy, transportation, health and comfort. Catalysis is important in the industrial chemistry in the production of liquid fuels and bulk chemicals. The more established areas of industrial catalysis include pharmaceutical, environmental and petrochemicals [4]. In a catalytic process, a catalyst usually goes through many cycles, meaning that it converts many substrates into products, hence the term turn-over number is used. In reality, a catalyst is not active forever, because substances called poisons may hinder its activity. A catalyst can be organic in nature, inorganic or a mixture of the two. In the context of this study, in the main three types of catalysis are relevant:

- biological (enzymatic)
- heterogeneous
- homogeneous

Enzymatic catalysis is involved in many commercial applications even though it is a relatively new emerging discipline. Heterogeneous catalysis by definition refers to a system whereby a substrate and the catalyst are brought together in different phases. It was the first to be applied commercially in a large scale and heterogeneous catalysis still dominates. In homogeneous catalysis a substrate and a catalyst are in one phase. About 85% of chemical processes are run catalytically and the ratio of heterogeneous to homogeneous is 75:25. In homogeneous catalysis,

proper ligand design is vital and an appropriate choice of ligand is important for tuning the catalytic activity and selectivity [5].

1.2 History of C-H Activation

The activation of C-H compounds started in the 1930s with the involvement of transition metal complexes. It was only in the 1970s that metals like Pt, Pd, Ru, Co, Ir and Ti were used in the oxidation of alkanes. At the end of 1980 and 1990, C-H activation by low valent metal complexes was replaced by high valent metal oxo-compounds and oxygen. In the early 2000s attention was also growing on biological oxidation and its chemical models [6, 7].

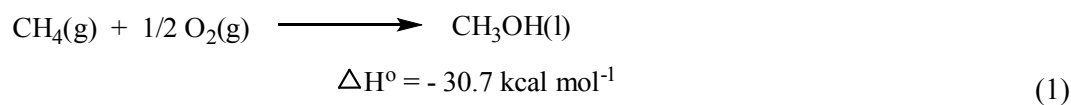
1.3 C-H Activation

The oxidation of alkanes into valuable products such as alcohols, ketones and aldehydes is very important to industry for detergents and perfumes [8]. The problem is, few methods for transforming alkanes into products of value exist. This is due to the inertness of alkanes which results from the strong and localized C-C and C-H bonds [9]. Saturated hydrocarbons lack empty orbitals of low lying energy or filled orbitals of high energy that could participate in a chemical reaction. Another factor attributing to this is that the reactions that use alkanes are thermodynamically unfavorable at mild temperatures of 30 to 40 °C [10, 11].

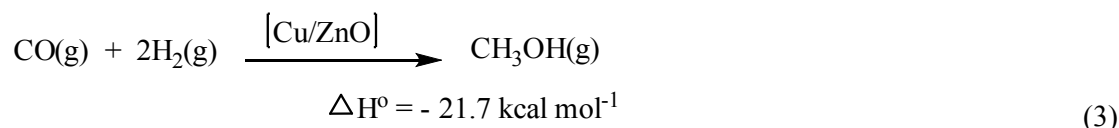
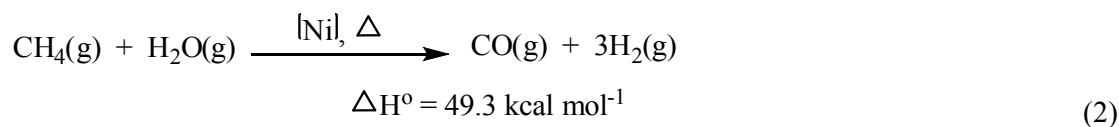
Selectivity is a major problem in C-H activation and there are two challenges associated with this:

- chemoselectivity and
- regioselectivity

In chemoselectivity the product of alkane activation is more reactive than the starting material. An example, in (equation 1), shows a direct oxidation of methane to methanol. Methanol is more reactive than methane and, as a result, the product formed is over-oxidized, since the strength of the C-H bond in methanol is weaker than that of methane itself.

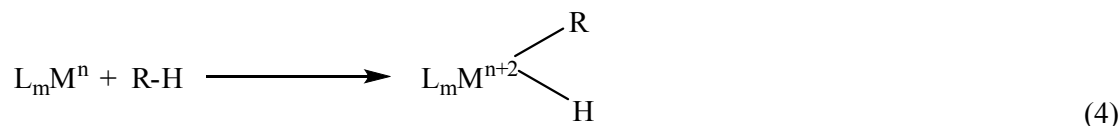


Therefore, a more efficient way of methanol production is by first forming syngas and then using it to produce methanol as shown in (equation 2 and 3) [10].



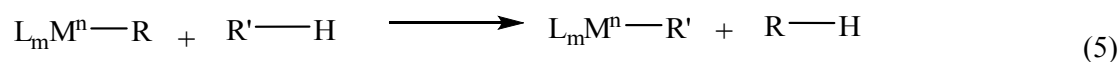
The use of radicals and electrophilic reagents for C-H activation shows that tertiary C-H bonds are attacked first over primary or secondary bonds. As a result, the selectivity is not so high. Selectivity problems could be overcome by using organometallic systems. These systems show that C-H bond activation in a reversed regioselectivity can be obtained [10-12]. The variety of organometallic systems includes:

I Oxidative addition

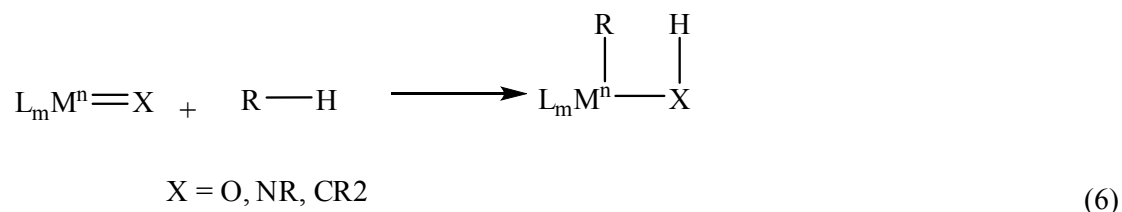


L = ligand (PMe₃), M = metal, R = alkyl

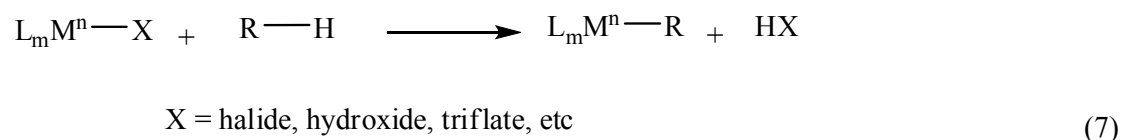
II Sigma bond metathesis



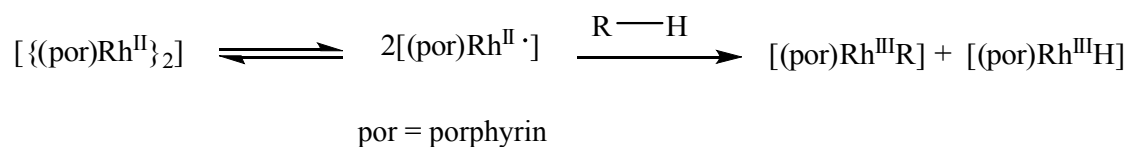
III 1,2 addition



IV Electrophilic activation



V Metalloradical activation



The main disadvantage of these organometallic systems is that the metal in the complex does not tolerate oxidants such as hydrogen peroxide, which are also required for oxidation catalysis. The only complex that is an exception to this is a platinum complex, which was introduced by Shilov and co-workers in 1969 [6]. This platinum complex is soluble in water, robust to air and moisture and can still attain the selectivity pattern similar to the organometallic systems [6, 7, 10].

The chemical inertness of alkanes can be overcome, if the transformations are done at high temperatures between 300 – 500 °C. The key disadvantage to this is that unwanted products are produced and the reactions are uncontrollable. Alkanes such as methane are similar to molecular

hydrogen at room temperature. Molecular hydrogen does not combine with oxygen in air at low temperatures to give water, however, this is possible at high temperatures [9].

There are a few other methods such as cracking and thermal dehydrogenation that can be used to transform hydrocarbons into valuable products, but their drawback is that high energy is required, therefore making them expensive processes. Such reactions, from an economic viewpoint, are unproductive as they also lack selectivity. This has been a motivation to chemists to search for new ways to transform alkanes into valuable products under mild conditions with high selectivity. A new method used highly reactive species such as superacids and free radicals, however, these species are expensive and the selectivity did not improve [13-15]. Furthermore, a method developed for alkane activation used coordination metal complex catalysis. In this method, a molecule or its fragment enters the coordination sphere of the metal complex where it is chemically activated. The mechanism involves a metal complex coordinating to the alkane C-H bond resulting in an unstable product, which comprises of a carbon-metal bond and a metal-hydride bond. In addition to coordination complexes, biological systems are well-established for C-H activation [6, 8, 10, 12, 16]. It has been discovered that many enzymes can catalyze alkanes into valuable products at physiological temperatures, however a problem is volume limitation which limits this to small scale production only [12, 16, 17].

1.4 Ligand design for C-H activation

1.4.1 Ligand of choice

Ligands are very important in transition metal complexes, because they control features such as stability, selectivity and activity by using their electronic and steric properties. A lot of work on monodentate ligands has been done and it showed that various metal complexes e.g CAMP- (methylcyclohexyl-o-anisylphosphane) were highly active catalysts on reactions such as hydrocyanation, hydrogenation and hydroformylation. In the early seventies, bidentate ligands such as DIPAMP were introduced and they showed superior selectivity and activity compared to monodentate ligands in reactions such as asymmetric hydrogenation. Therefore, various transition metal complexes which contained bidentate ligands such as DIPAMP- ethane-1,2-diylbis[(2-methoxyphenyl) phenylphosphane)], DIOP- (2,3-o-isopropylidene-2,3-dihydroxy-1,4-

bis(diphenylphosphino) butane), BISBI-[2,2-bis((diphenylphosphino)methyl)-1,1-biphenyl] and duxantphos have been investigated and they all showed excellent performance in several catalytic reactions [18, 19]. In this work, bidentate ligands were chosen, because most of them such as xanthene-based are known to be stable and show superior selectivity and activity in several reactions.

1.4.2 Ligand design parameters

Ligand design is very important in synthetic organometallic chemistry. This is because the ligand controls the manner in which the metal center coordinates in the complex. Ligands can contain different chemical donor functions, such as hard and soft donor atoms. Figure 1.1 shows that there are many variables to consider when one designs a ligand, in this case a bidentate ligand [18]. The main tools to look at when designing a complex are ligand parameters as they play a vital role in the structure and reactivity of the metal complex.

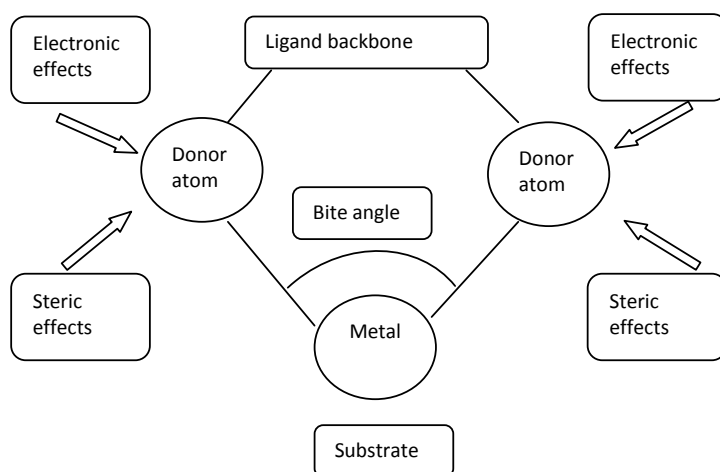


Figure 1.1: Parameters for bidentate design [18].

In bidentate phosphorus ligands the key parameters are contained in Figure 1.1 [18]. Electronic effects determine the behavior of the ligands and complexes in reactions and their stability is largely determined by the steric effects. Another parameter that is used to describe the rigidity of a bidentate ligand is the flexibility range. This is defined as the bite angles that can be reached within the energy barrier of 3 kcal.mol⁻¹ [20].

1.4.3 Ligand backbone

Typically a ligand is a Lewis base that consists of a backbone and donor atoms. The backbone is often a scaffolding of carbon atoms (linear, ring, etc), that keeps the donor atoms at a certain distance or orientation. For diphosphine ligands different backbones result in different P...P distances. A change in the P...P distance may affect catalytic activity, hence for these types of ligands, the P...P distance is significant in their design, coordination chemistry and application in catalysis. The most common backbones are either straight chain or composed of aromatic rings [21-23].

Recent studies on bidentate ligands have shifted to the backbones that have heteroatoms such as silicon, nitrogen, oxygen and many others. This is due to the effect they have on the selectivity and rates of the reaction. Amongst these are different types of xanthene-based ligands (Figure 1.2) [22, 24].

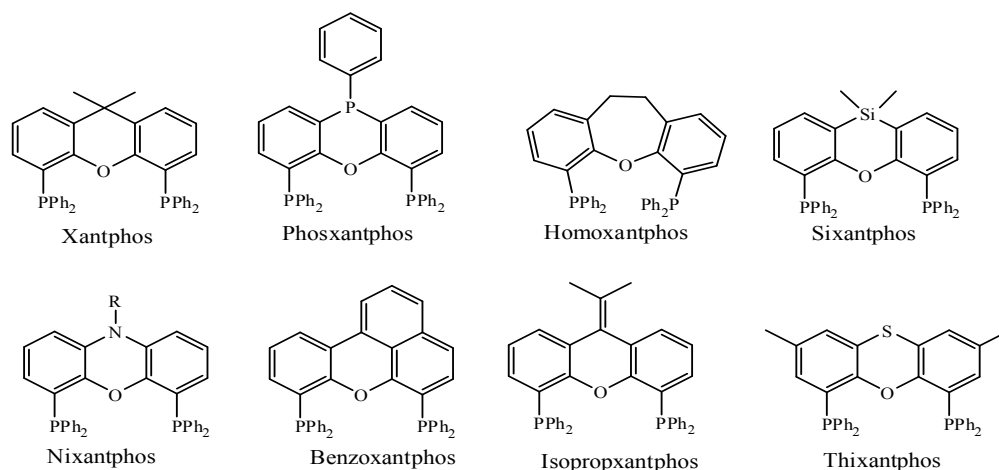


Figure 1.2: Some xanthene-based ligands [22].

1.4.4 Donor atoms

Donor atoms in a ligand are very important as they play a major role in catalytic performance. Generally, the donor atom is a heteroatom that binds to the central metal. In a chemical transformation, it is the donor atom and its substituents that control accessibility to the metal for potential substrates [25]. Phosphorus is a soft donor atom that has been known for decades as a strongly ligating atom for late transition metals. Their easy coordination to metal centres

through the lone pair of electrons on the phosphorus atoms and the variety of coordination modes makes phosphorus based ligands important and popular in catalysis [1, 26, 27].

Commonly, phosphorus containing ligands have been observed to coordinate to metal centres in one of the following manner:

- monodentate
- bidentate
- tridentate

A major difference between these coordination modes is the number of donor atoms used to bind to a metal [27]. In the terdentate fashion, the ligand coordinates in a pincer manner. The most common types of pincer skeletons are NCN, NON, SCS, CNC, PNP, PONOP as well as PCP [28-30]. These donor atoms provide different chemical functions such as N, which is intermediate donor and P, a soft donor atom. The pincer skeleton PCP was first reported by Moulton and Shaw 35 years ago [31, 32]. Phosphine ligands are good sigma donors and good pi-acceptors. Alkyl phosphines are good sigma donors and that makes them strong bases, whereby phosphites are good pi-acceptors [33].

In terms of applications, phosphine based ligands are the most popular in hydroformylation and hydrogenation studies, an example is the known Wilkinson's catalyst [1]. In the Shell process for alkene hydroformylation it was observed that the use of catalysts with phosphorus as donor atoms resulted in the formation of linear products, which is observed to a far lesser extent with the use of phosphine free catalyst [34].

1.4.5 Transition metals in homogeneous catalysis

Transition metals play a major role in homogeneous processes as they are incorporated in these systems. They are divided into early and late transition metals, depending on their reactivity and coordination to other atoms. Early transition metals are electronically hard metals that generally are intolerant of many functional groups in ligands. Late transition metals are electronically soft metals that tolerate many functional groups. Every ligand has a bonding motif, which originates from the type of donor atoms. Early transition metals are suitable for hard ligands and late transition metal prefers soft ligand [35].

1.4.6 Electronic effect

This parameter gives an insight to how chemical bonds influence reactivity. Electronics and sterics are inter-related parameters where a change in one may affect the other. It shows how electrons move around the complex and the term electronic refers to the changes at the metal centre due to the movement of electrons (Figure 1.3) [18]. Donor atoms such as phosphines are known to have σ -basicity and π -acidity. This put simply, phosphorus as a donor atom can act as a base through its lone pair by simply donating the lone pair to a metal. When possessing π -acidity properties, it allows π -back donation from the metal to its anti-bonding σ^* -orbitals which play the role of π -acceptor orbitals. The bond lengths are altered due to the transfer of electron density. Therefore, this property classifies some ligands as basic and some as acidic and ultimately determines the stability of a complex. This parameter focuses on the type of bonds created between complexes and differs from one metal to the other [1, 18, 22, 27].

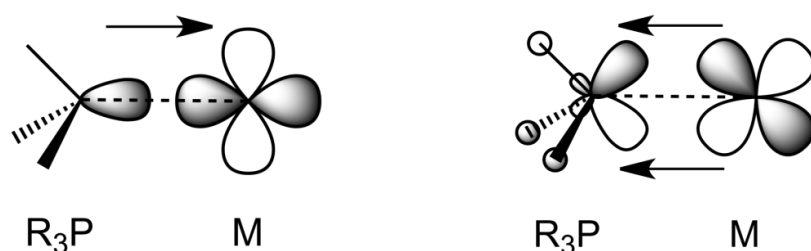


Figure 1.3: Electronic effects of ligands [18].

1.4.7 Steric effect

The steric effect is defined by the Tolman's steric parameter that measures the bulkiness of a ligand. Tolman (Figure 1.4) measured cone angles by using CPK models, which is calculated based on the distance between the metal to the phosphorus and the substituents around the phosphorus [27]. It is a measurement of steric bulkiness in a metal-ligand complex. Systematic studies have revealed that steric effects are as important as electronic effects, however, steric effects are better at explaining the stability of complexes. The bigger the cone angle the bulkier the ligand, which in many cases can give rise to stable complexes. This parameter can have a

major influence on the activity and selectivity of transition metal complexes in catalysis [18, 21, 22, 25, 27, 36].

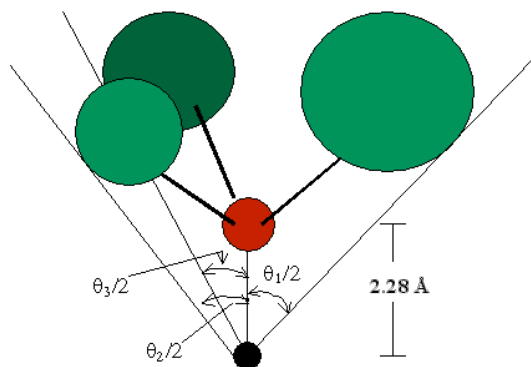


Figure 1.4: Illustration of the Tolman's cone angle [37].

1.4.8 Natural bite angle

This concept was introduced in 1990 by Whiteker and Casey, it a concept used to define diphosphine ligands such as the BISBI- [2,2-bis((diphenylphosphino)methyl)-1,1-biphenyl] ligand in hydroformylation [36, 38]. This concept is defined as the preferred chelation angle that is controlled by the ligand backbone and not by the metal valence angles. It is believed to have an effect on the reactivity of the metal complexes [39]. Ligands with a wide bite angle are stable and favourable to catalytic performance[40]. In bidentate diphosphines based on xanthene, the backbone induces large bite angles, due to the rigidity in the backbone. It shows possible changes to the central ring as the xanthene backbone changes the natural bite angle automatically (Figure 1.5), but the sterics and electronics are not affected [22]. Another parameter which goes with natural bite angle is the flexibility range, which is the range in which the bite angle can reach or have access to, within 3 kcal.mol⁻¹ [1].

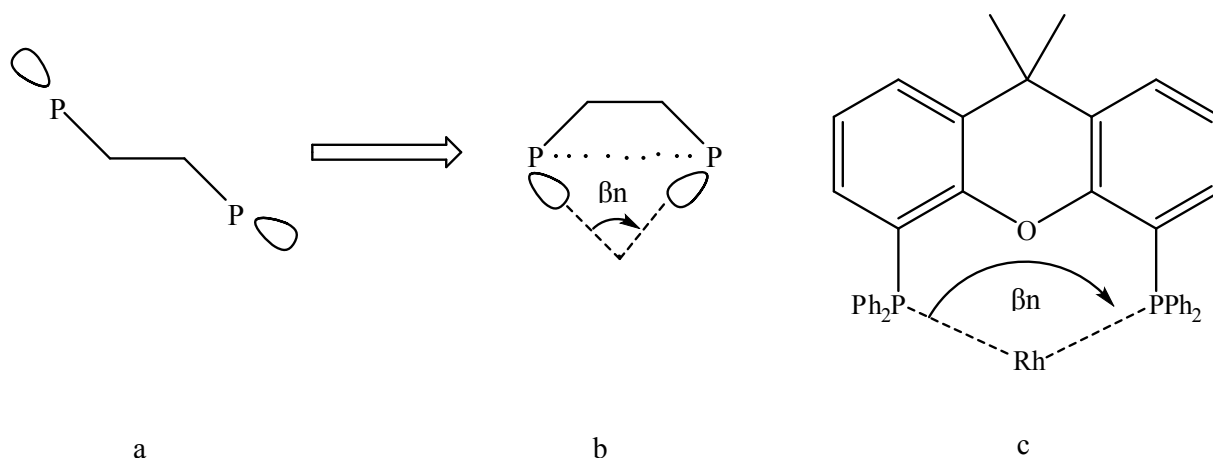


Figure 1.5: Bite angle measured using bidentate ligand (a) and (b) and the example of the P-P distance determined by the xantphos backbone (c) [22].

1.5 Diphosphine complexes

A complex is a metal ion surrounded by a set of ligands. The metal ion is the Lewis acid in the complex and is also known as the acceptor atom. Coordination complexes are of many different geometries, the most common being octahedral, tetrahedral, square planar and trigonal bipyramidal. The type of bonding between a metal and a ligand can be through a sigma or pi-bond. In general, bidentate diphosphine ligands form stable complexes, as some phosphine based ligands are good sigma donors while others are strong pi-acceptors.

About a decade ago, the most reported diphosphines were those in which the carbon chain was longer than two carbons and those with an aromatic link between donor atoms. This was mainly due to their ease of coordination to metal centres as well as variability of coordination modes. Lately, the more desired diphosphine ligands are those with larger bite angles and rigid backbones as they are believed to increase the migration rate. Rigid backbone ligands have constrained geometries and certain coordination behavior that can affect the catalytic cycle by stabilization or destabilization of the initial, transition or final state [21].

The first diphosphine to meet required properties mentioned was Venanzi's transphos as it had a rigid polyaromatic backbone which enforces the formation of trans chelates [21, 41]. The use of

fused ring hydrocarbon bridges such as anthracene was common. Therefore, the most promising backbones are those that are heterocyclic such as xanthene-based backbone [21, 26, 27].

1.5.1 Application of diphosphine ligands in catalysis

Research has shown that diphosphine ligands based on the simple alkyl linkers dppe - (diphenylphosphino) ethane and dppp - (diphenylphosphino) propane were amongst those reported as highly stable [1]. They were reported to form stable organometallic complexes due to their chelating effect. Their application in catalysis was reported by many, but Iwamoto and Yuguchi were the first to report promising results for the co-dimerization of butadiene and ethene using an iron catalyst in 1966 [22]. The results showed that when ligands of varying bridge length, such as dppe, were used instead of PPh₃ (monophosphine) low activity was obtained and this is explained by the chelate effect. This effect showed a decline in the activity of these ligands. Monophosphines then became the dominant field of study. Years later, the introduction of BISBI in the late 1980's was a major breakthrough, as this showed high regioselectivity in the formation of linear aldehydes in hydroformylation. This was followed by other bidentate ligands such as DIOP - (2,3-o-isopropylidene-2,3-dihydroxy-1,4-bis(diphenylphosphino) butane) and DIPAMP - ethane-1,2-diylbis[(2-methoxyphenyl) phenylphosphane]) which became popular as effective asymmetric hydrogenation catalysts [1, 20].

In catalysis, diphosphine ligands (Figure 1.6) based on xanthene have mostly been applied in hydroformylation, cross-coupling, allylic alkylation, hydrocyanation, hydroamination and hydrogen transfer reactions. In hydroformylation it was observed that application of ligands with a large bite angle (rhodium catalysed) favoured the formation of linear aldehydes [20, 22, 24]. The DBFPhos - 4,6-bis(diphenylphosphino)dibenzofuran ligand was the only exception and this is explained by the way it coordinated to the metal centre. At higher temperatures high selectivity was obtained. Due to the rigid backbone of the ligand, coordination occurred in a bisequatorial manner that was maintained even at high temperatures [20, 24, 40, 42]. Apart from hydroformylation, these bidentate ligands were also used in hydrocyanation by Du Pont, carbonylation chemistry and copolymerization of butadiene [1, 43].

Recent work has revealed that diphosphines of xanthene-based ligands were applied industrially for the manufacture of sulphuric acid *via* the chamber process. This led to renewed interest in bidentate ligands, which is still sustained to date [38].

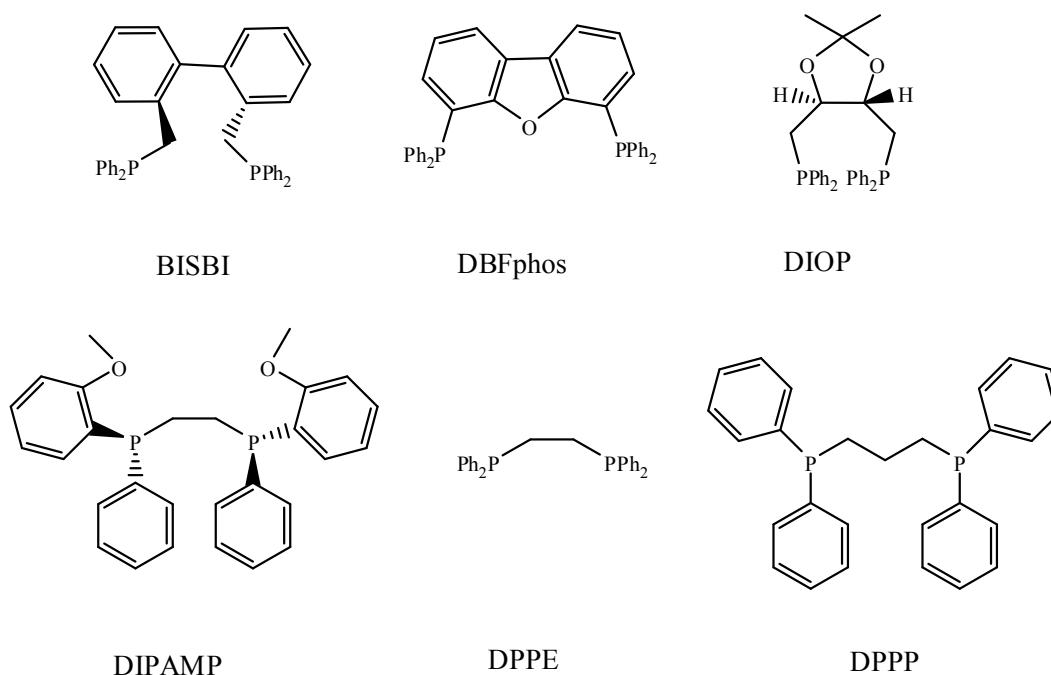


Figure 1.6: Diphosphine ligands [18, 44].

1.5.2 Xanthene-based ligands

Xanthenes are a family of diphosphine ligands with wide natural bite angles. Xanthene-based ligands resemble a butterfly in their structure and have bite angles larger than 90°. When the bridge at the X-position (Figure 1.7(b)) is varied, small changes are observed with the bite angle, whilst the sterics and electronics remain unaffected [21, 23]. These ligands have a heterocyclic backbone, which makes them efficient catalysts. Xanthene-based scaffolds can be flexible as in Fig 1.7 (a) or rigid as in Fig 1.7 (b). The backbone is functionalized by donor atoms, which include amines, phosphines, sulfur, etc. A donor atom of interest to this study is phosphorus. It is the donor atom in conjunction with its substituents that controls the accessibility of the metal to a potential substrate as well as the electron density around the metal [25].

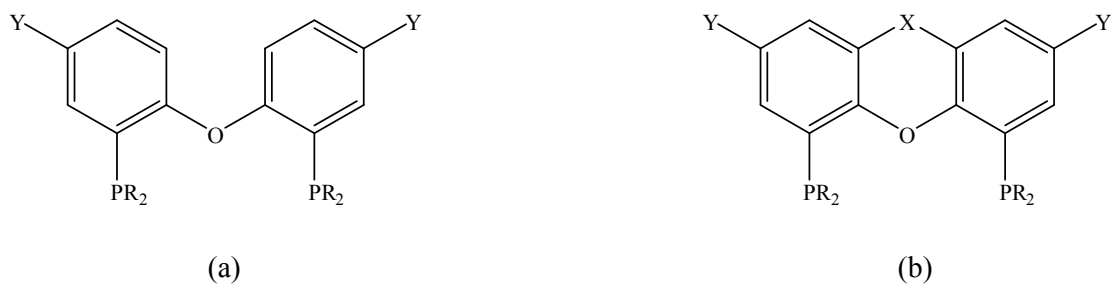


Figure 1.7: Generic structure of xanthene-based ligands with flexibility (a) and rigid (b) backbones.

Xanthene based catalysts exhibit luminescence properties.. Those complexed to gold show rich photochemistry and they are used in the development of molecular sensors and switches or energy storage devices [45]. Other uses include dyes, and in the pharmaceutical and catalysis industries.

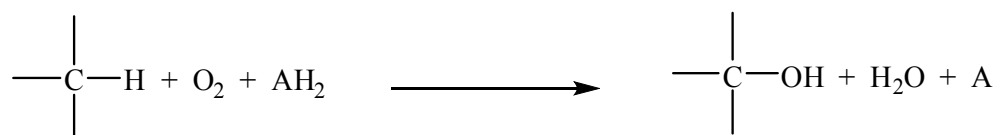
In cross-coupling and allylic alkylation, the type of ligand used has a large impact on the catalysis. In terms of reaction rate and selectivity, an increase was observed when catalysts with natural bite angles up to 102.7° were used. Catalysts with natural bite angles larger than 102.7° result in decreased reaction rates and selectivities. Steric hindrance induced by the ligand determines the reaction rate as well as the selectivities of the catalyst. An increased natural bite angle was observed to increase steric hindrance to the substrate, thereby limiting access to the metal centre, resulting in high regioselectivity [27, 36].

1.6 Biological catalysis

1.6.1 Biomimetic catalysis

In natural systems, the oxidation of alkanes is performed in two ways: through aerobic oxidation and anaerobic oxidation. Enzymes that catalyse via activation of oxygen are referred to as monooxygenases. The term monooxygenase simple means a group of enzymes catalyzing

alkanes by molecular oxygen. These monooxygenases insert one oxygen from O₂ into the C-H bond, while the other oxygen is reduced to form water (see Figure 1.8) [9].



AH₂ = hydrogen donor

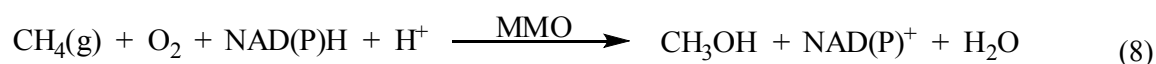
Figure 1.8: Oxidation of alkanes by monooxygenase [6].

Many monooxygenases contain metals as part of their active sites for biological transformations. The majority of metals found in active sites of enzymes are iron and copper. Examples of such enzymes are methane monooxygenase and cytochrome P450 [6, 46]. For a monooxygenase cycle to be complete a reducing agent from an organic component is required in the system. This biological reductant will activate the molecular oxygen of the metalloenzyme. These reductants transfer the electrons to the metal of the metalloenzyme, reducing it to react with the molecular oxygen and thereafter activating it, to react with alkanes. Molecular oxygen activation creates peroxy and oxo-complexes which initiate the catalytic effect of monooxygenases [9].

Therefore in a biomimetic study chemical analogues of enzymes are synthesized and used in C-H activation. Even though there have been analogues of enzymes, they have not been able to mimic the exact behavior of these enzymes. Selectivity has been observed, but does not match that of the naturally occurring enzymes. One offsetting condition about biomimetic catalysts is that they cannot accomplish the activation of C-H bonds under mild conditions [9].

1.6.2 Methane monooxygenase in C-H activation

The methane monooxygenases are those enzymes that are extracted from methane oxidizing bacteria. The oxidation occurs as shown in (Equation 8):



NADPH = hydrogen donor

Methane monooxygenase is known as a non-heme enzyme, which means it does not require any heme-group for the activation of hydrocarbons. Its mechanism involves the transfer of oxygen from a high valent metal oxo species into the alkane. It oxidizes alkanes and shows highest activity of methane conversion to methanol. It fails to oxidize aromatic hydrocarbons. Many mimics of methane monooxygenase show high activity in alkane conversion but they all fail to oxidize methane to methanol under mild conditions [6, 7, 9, 47].

1.6.3 Cytochrome P450 monooxygenase in C-H activation

The family of cytochrome P450 is a vast and diverse set of enzymes. To date about 3800 microbial P450 are known. Only about 10-17% of these are said to be active towards degradations of fatty acids and alkanes. There are approximately 500 cytochrome P450 suprafamily that are known today. They all differ from each other in the structure of their globular protein in the region of the active center and have similar prosthetic groups. It is the most abundant in nature and it oxidizes saturated and unsaturated hydrocarbons. P450 is a heme type methane monooxygenase (Figure 1.9).

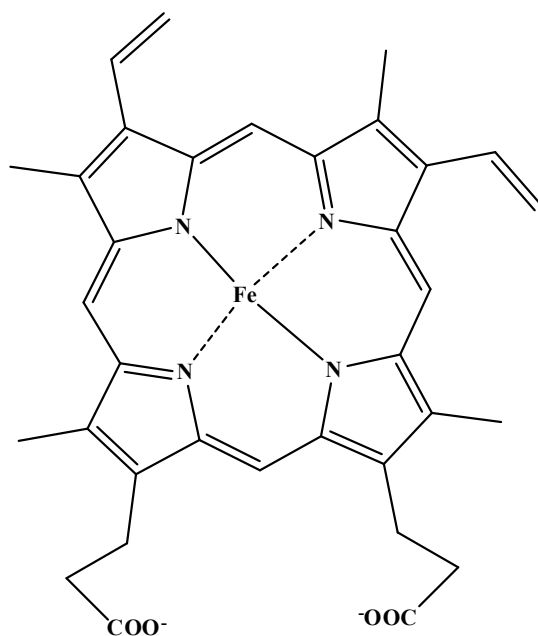
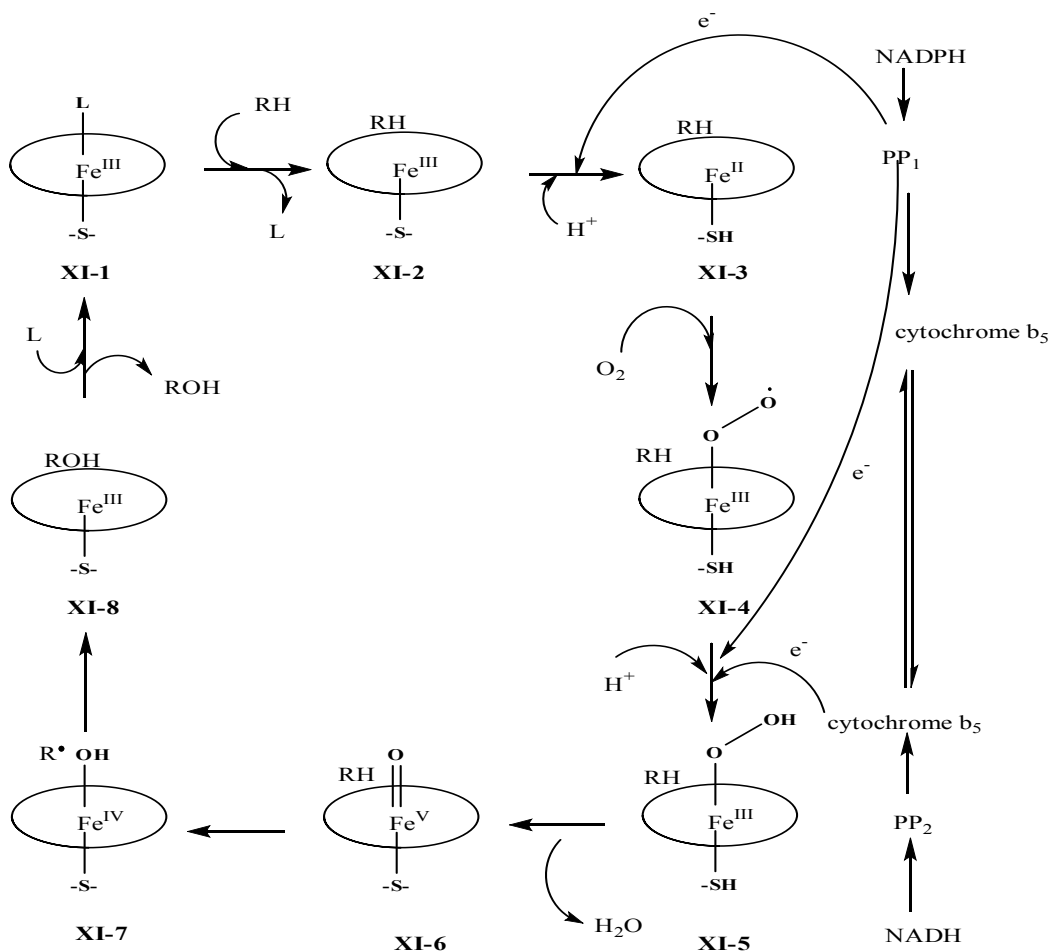


Figure 1.9: Structure of cytochrome P450 showing the heme structure [6].

The structure of P450 consists of four coordination sites with iron involved in the active centre. The iron is coupled to nitrogen atoms from a porphyrin molecule and a sulfur atom in the fifth position from a cystein molecule. It can break down any natural organic compound including alkanes, which are relatively chemically inert. They can be degraded and used as a carbon source by bacteria and fungi [7, 9, 48].

The catalytic cycle proposed for alkane oxidation, which uses dioxygen in the presence of P450 consists of eight steps (see Scheme 1). The initial step involves the change of P450 from a low-spin form into a high spin form, which is followed by the second and third steps, the reduction steps where the dioxygen molecule is coupled to the Fe(II) ion. The fourth and fifth steps involve the coordination of hydrogen and elimination of water. In the sixth and seven steps, the cleavage of C-H bond in a substrate molecule and transfer of the second electron to oxycytochrome P450 forming $\text{Fe}^{2+} \text{O}^{2-}$ or $\text{Fe}^{3+} \text{O}^{2-}$ species occurs. The last step is the decomposition of these species into a superoxide and the rate constant for the formation of oxygenated products is 30 min^{-1} depending on the substrate and the nature of the enzymes [6, 7, 9].



Scheme 1.1: The catalytic cycle proposed for alkane oxidation by O₂ promoted by cytochrome P450 [6].

1.7 Heterogeneous catalysis in C-H Activation

In heterogeneous catalysis, the catalyst is usually present in a solid state and it catalyzes reactions in a liquid or gas phase. Since these catalysts are solids they are impenetrable and that results in reactions taking place on the surface of the catalyst. In most cases, these catalysts are supported on porous materials. Therefore, the particles present are in the nanometer size range. Heterogeneous catalysis is the backbone of many chemical industries, since approximately 85% of industry processes use these catalysts [5, 49-51]. Heterogeneous catalysts are essential in:

1. Bulk and fine chemical production
2. Minimization of waste products as they convert all the unwanted products into desirable products
3. Prevention of pollution since they convert all pollutants from car exhausts
4. Production of fuel for the motor industry

Heterogeneous catalysis is more popular than homogeneous catalysis, because it comparatively offers some key advantages. The catalysts are easily separated from the products, which make them favorable and important in large-scale industries. Since heterogeneous catalysts are usually solids they are usually thermally more stable than homogeneous catalysts. As a result, they give rise to higher reaction rates. Deactivation of these catalysts involves deposition of by-products onto the catalysts surface, however, regeneration can often be performed by burning off the deposited by-products. This is where the importance of thermally stable catalysts is important. This regeneration can also be done under *in situ* conditions, which is an advantage for large scale industries [1, 3, 52]. Examples of heterogeneous reactions are dehydrogenation, catalytic cracking, steam reforming, etc.

1.8 Homogenous catalysis

Homogeneous catalytic processes generally use soluble metal complexes of transition metals for the production of organic compounds. This is due to the solubility of these catalysts in the reaction medium, which allows them control in chemoselectivity, regioselectivity, as well as enantioselectivity [48]. Homogeneous catalysts have disadvantages which limits their industrial use because their reactions may involve side reactions, which tends to minimize the concentration of the main product. This can happen through the deactivation of the active species into inactive complexes. Another disadvantage of homogeneous catalysis is the difficulty often encountered in separation of the products and reactants. There are homogeneous catalysts that are commercialized, however, most of those give products with a low boiling point and therefore they are easily separable, or the organic ligands are not thermally sensitive. The reasons for choosing homogeneous catalysts over heterogeneous are based on their selectivity, activity, ease of study and ease of modification [48].

1.9 Methods of C-H bond activation using homogeneous catalysis

1.9.1 Oxidative addition of paraffins

Oxidative addition is a type of reaction that results in an increased coordination number as well as increased oxidation number of the metal atom. In this reaction the coordination number increases by two and the total electron count increases by two at the metal atom. Oxidative addition mostly occurs in d-group metals although sometimes it occurs with Grignard reagents. For oxidative addition to occur it requires a coordinative unsaturated metal centre and as a result these reactions are common with 16-electron square-planar metal complexes. The kind of molecules that can be added oxidatively to a metal atom are alkyl halides, aryl halides, dihydrogen and simple hydrocarbons [9, 17]. Oxidation in a presence of C-H bond occurs when a molecule such as an alkane adds to a metal atom by first cleavage of the C-H bond and forming a new M-H and M-C bond. The oxidative addition mechanisms are divided into:

- concerted fashion,
- S_N2 (Nucleophilic Substitution)
- radical oxidative addition.

I Concerted oxidative addition

When the substrate molecules coordinate to the metal centre, they are said to react in a concerted fashion. This means the molecule is coordinated to form a σ -bonded ligand. Due to back bonding from the metal, this double bond oxygen cleaves making the two incoming ligands *cis* to each other (figure 1.10) [52].

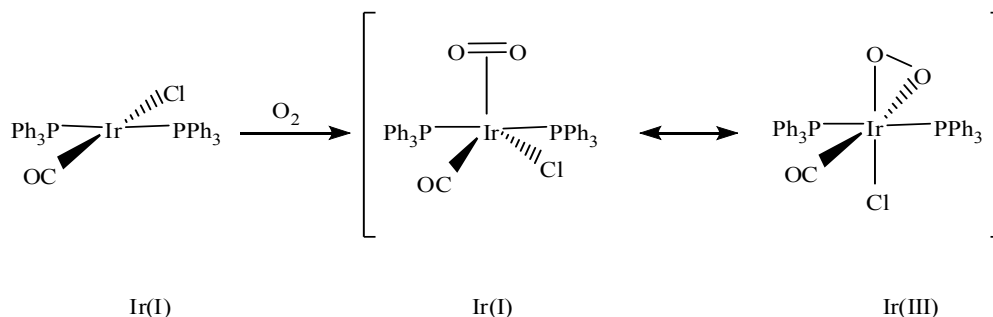


Figure 1.10: The concerted oxidative addition mechanism [52].

II S_N2 oxidative addition

In S_N2 oxidative addition (Figure 1.11), the two incoming ligands do not end up *cis* to each other and the chirality of the alkyl group is inverted. This type of oxidative addition is common for molecules such as alkyl halides. The lone pair of the metal attacks and cleaves the alkyl halide, which then coordinates, however, the coordination occurs via the S_N2 mechanism.

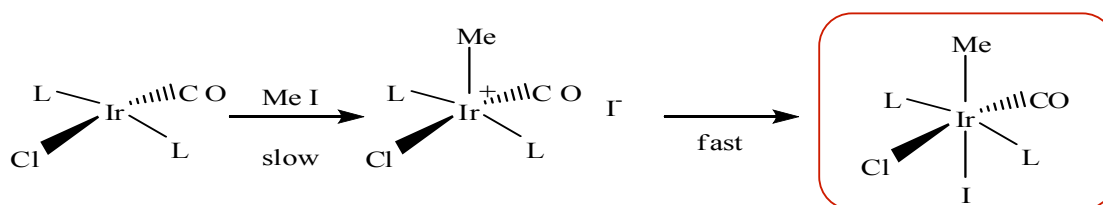


Figure 1.11: S_N2 oxidative addition mechanism [52].

III Radical oxidative addition

This oxidative type of reaction is divided into two types, the non-radical chain and radical chain reaction. In Figures 1.12 & 1.13, both types of reactions occur in the presence of alkyl halides. The only difference is that in the radical chain reaction a radical initiator is utilized, whereby in a non-radical chain it is the metal centre that cleaves the alkyl halide. The non-radical chain route involves the movement of electrons from the metal centre to the alkyl halide, which cleaves and forms a halide ion and a radical alkyl.

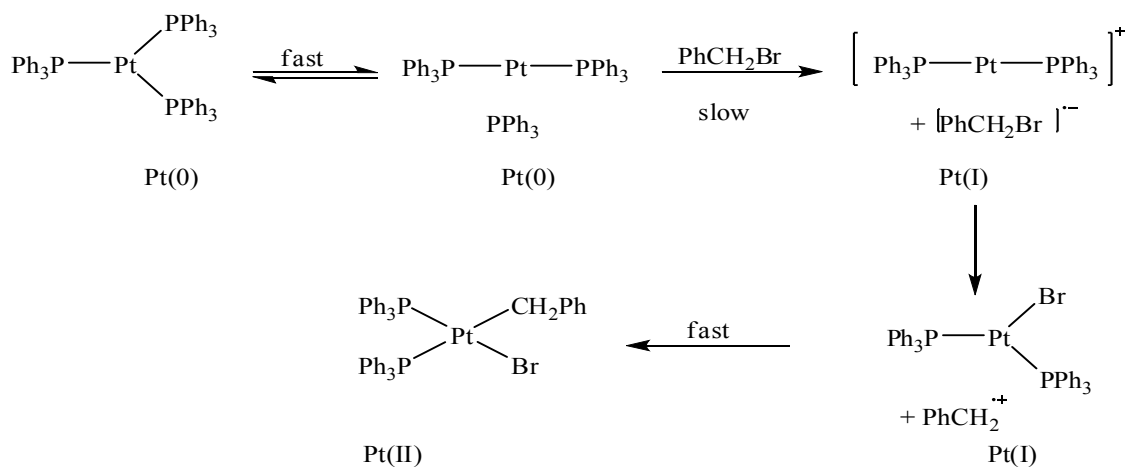


Figure 1.12: Non-radical chain oxidative addition mechanism [52].

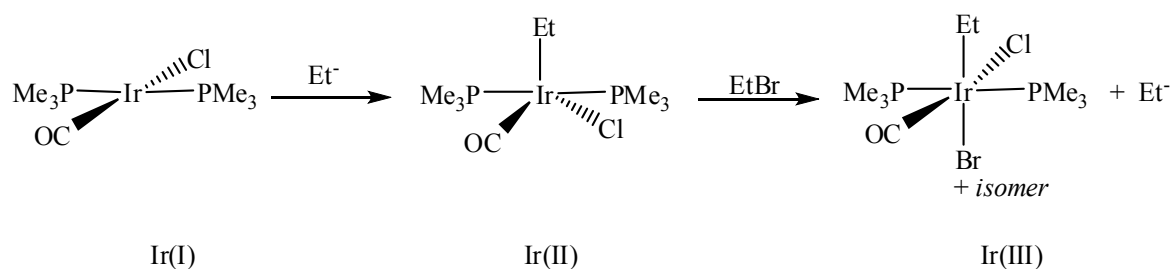


Figure 1.13: Radical chain oxidative addition mechanism [52].

1.9.2 Reductive elimination

Reductive elimination is the opposite of oxidative addition (Figure 1.14). This type of reaction is mostly seen in higher oxidation states whereby the formal oxidation states of metal is reduced by two units in a reaction. It occurs from the coordinatively saturated metal centre, where the two ligands in an 18-electron octahedral metal complex couple and eliminate from the metal centre. Oxidative addition and reductive elimination are reversible reactions. The formation of one is thermodynamically favoured [9, 52].

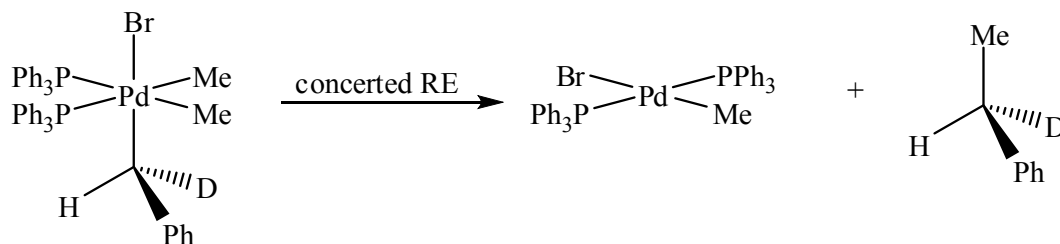


Figure 1.14: Reductive elimination mechanism [52].

1.10 Future use of Hydrocarbons in Catalysis

About 90% of all the products used will at one stage in their production require a catalyst [50]. Hence catalysis is very important in the industrial world. Catalysis has developed tremendously from humble beginnings in the 1880s both in diversity of application and applicable technology. Hydrogen production has a major impact in the industrial sector, since it is a promising energy carrier offering high-energy yields and limits secondary reactions. The major source of hydrogen is gaseous and liquid hydrocarbons and this is due to their abundance. Hydrogen is produced by the catalytic decomposition of liquid hydrocarbons via metal catalysis or a plasma approach with a decomposer, which consists of a catalytic bed of transition metals or carbon-based catalysts. This is the basis of fuel cell technology, which may be used in electricity production [50, 53].

1.11 The project aims and goal

The main challenge in homogeneous catalysis is to produce stable, highly selective and highly active catalysts. The key factor in designing such catalysts is based on the right choice of ligands. A lot of interesting work has been done on diphosphine ligands with xanthene-based backbones and they have been utilized in homogeneous catalysis due to their large bite angle. Notable findings include the work by van Leeuwen and co-workers where xanthene-based ligands were applied in hydroformylation, hydrocyanation and hydrogenation as they showed high activity and selectivity [1, 20, 27, 39, 44]. No application of xanthene-based complexes has been observed in the C-H activation of *n*-octane.

Therefore, alkanes will be the main focus on this study. They are very abundant molecules as they are produced from natural gas and oil. Production of linear alcohols is important in industry

as these are used as intermediates for the production of other chemicals. They are used as feedstock in chemical production as they are cheaper than their derivatives. Transformation of these hydrocarbons such as methane to methanol is important in energy production. In industry, there should be no waste because what is considered as waste should always be transformed into products of value. As a result there are always new methods that are being developed into changing by-products such as hydrocarbons into valuable products. The development of these new routes has increased the demand for the use of linear alkanes since they are selective and efficient.

1-octanol is another important intermediate product in the production of α -olefins such as 1-octene, which are used in chemical industry. There is a high demand of 1-octene since it is one of the key products in the production of LLDPE (Linear Low Density PolyEthylene), which is a polymer used as a film in packaging. Therefore, companies like SASOL have built a new plant in Secunda which was completed in 2007 only for production of 1-octenes. 1-octanol is converted into 1-octene by a dehydration process [54].

In this study, the aim is to:

- Use xanthene-based complexes in the C-H activation of *n*-octane into products of value, which can find use e.g. in solvents, detergent and LLDPE production [55].
- Design and synthesize xanthene-based ligands, Figure 1.7(b), focusing on two primary parameters:
 - ❖ **ligand backbone:** By introducing small variations in the backbone this will affect the bite angle and have influence on catalytic activity [22, 29]. Therefore to substitute this Y-position in Figure 1.7(b) by an aliphatic chain
 - ❖ **bite angle:**
 - a) Two substituents will be used, electron withdrawing (phenyl ring) and electron donating (*p*-tolyl ring).
 - b) The X-position will be exchanged with sulphur, a methyl group, as well as an isopropyl group.

- Attempt to chelate synthesized ligands onto metals such as cobalt and nickel, since very few complexes of these metals are known for xanthene-based ligands. These metals were used in this study because they are abundant and cheap.
- Investigate the chelate effect on the activity of these catalysts, as it is known that highly stable complexes tend to be inactive, due to strong chelation between ligand and metal.
- Investigate the effects of oxidants, *tert*-butyl hydroperoxide, hydrogen peroxide and *meta*-chloroperbenzoic acid, on the catalytic behavior of catalysts
- Investigate the effects of temperature on activity: RT (room temperature), 50 °C and 60 °C.

1.12 References

- [1] P.W.N. van Leeuwen, *Homogeneous Catalysis Understanding the Art*, Kluwer Academic Publishers, 2004.
- [2] S. Ahrland, J. Chatt and N.R. Davies, *Quarterly Reviews*, 12 (1958) 265.
- [3] C. Masters, *Homogeneous Transition-metal Catalysis: A Gentle Art*, Chapman & Hall, Routledge, 1981.
- [4] M.M. Ramirez-Corredores, *Applied Catalysis A: General*, 197 (2000) 3.
- [5] B. Cornils and W.A. Herrmann, *Journal of Catalysis*, 216 (2003) 23.
- [6] A.E. Shilov and G.B. Shul'pin, *Activation and Catalytic Reactions of Saturated Hydrocarbons in the Presence of Metal Complexes*, in B.R. James (Editor), Vol. 21, Kluwer Academic Publishers, Dordrecht, 2002, p. 550.
- [7] G.B. Shul'pin, *Journal of Molecular Catalysis A: Chemical*, 189 (2002) 39.
- [8] A. Sivaramakrishna, P. Suman, E.V. Goud, S. Janardan, C. Sravani, T. Sandeep, K. Vijayakrishna and H.S. Clayton, *Journal of Coordination Chemistry*, 12 (2013) 2091.
- [9] A.E. Shilov and G.B. Shul'pin, *Processes of C-H Bond Activation, Activation and Catalytic Reactions of Saturated Hydrocarbons in the Presence of Metal Complexes*, Kluwer Academic Publishers, Dordrecht, Netherlands, 2000.
- [10] S.S. Stahl, A.J. Labinger and J.E. Bercaw, *Angewandte Chemie-International Edition*, 37 (1998) 2180.
- [11] T.C.O. Mac Leod, M.V. Kirillova, A.J.L. Pombeiro, M.A. Schiavon and M.D. Assis, *Applied Catalysis A: General*, 372 (2010) 191.
- [12] A.J. Labinger and J.E. Bercaw, *Nature*, 417 (2002) 507.
- [13] R.I. McNeil, *Energy & Fuels*, 10 (1996) 60.
- [14] J. Walendziewski, *Fuel Processing Technology*, 86 (2005) 1265.
- [15] J. Walendziewski and M. Steininger, *Catalysis Today*, 65 (2001) 323.
- [16] R.G. Bergman, *Nature*, 446 (2007) 391.
- [17] B. Rybtchinski, A. Vigalok, Y. Ben-David and D. Milstein, *Journal of American Chemical Society*, 118 (1996) 12406.
- [18] P.C.J. Kamer, P.W.N. van Leeuwen, E. Zuidema and J.A. Gillespie, *Phosphorus (III) Ligands in Homogeneous Catalysis: Design and Synthesis*, John Wiley & Sons, Ltd, 2012.

- [19] V.F. Slagt, P. van Leeuwen and J.N.H. Reek, *Chemical Communications*, (2003) 2474.
- [20] M. Kranenburg, Y.E.M. Vanderburgt, P.C.J. Kamer, P. Vanleeuwen, K. Goubitz and J. Fraanje, *Organometallics*, 14 (1995) 3081.
- [21] P.C.J. Kamer, P.W.N. van Leeuwen and J.N.H. Reek, *Accounts of Chemical Research*, 34 (2001) 895.
- [22] P.W.N. van Leeuwen and P. Dierkes, *Journal of the Chemical Society, Dalton Transactions*, (1999) 1519.
- [23] T. Marimuthu, M.D. Bala and H.B. Friedrich, *Journal of Chemical Crystallography*, 42 (2012) 251.
- [24] L.A. van der Veen, P.H. Keeven, G.C. Schoemaker, J.N.H. Reek, P.C.J. Kamer, P.W.N. van Leeuwen, M. Lutz and A.L. Spek, *Organometallics*, 19 (2000) 872.
- [25] G. Mora, B. Deschamps, S. van Zutphen, X.F. Le Goff, L. Ricard and P. Le Floch, *Organometallics*, 26 (2007) 1846.
- [26] T. Appleby and J.D. Woolins, *Coordination Chemistry Reviews*, 235 (2002) 121.
- [27] P.W.N. van Leeuwen, P.C.J. Kamer, J.N.H. Reek and P. Dierkes, *Chemical Reviews*, 100 (2000) 2741.
- [28] J.T. Singleton, *Tetrahedron*, 59 (2003) 1837.
- [29] A. Romerosa, C. Saraiba-Bello, M. Serrano-Ruiz, A. Caneschi, V. McKee, M. Peruzzini, L. Sorace and F. Zanobini, *Dalton Transactions*, (2003) 3233.
- [30] B. Vidjayacoumar, S. Ilango, M.J. Ray, T. Chu, K.B. Kolpin, N.R. Andreychuk, C.A. Cruz, D.J.H. Emslie, H.A. Jenkins and J.F. Britten, *Dalton Transactions*, 41 (2012) 8175.
- [31] S. Kundu, W.W. Brennessel and W.D. Jones, *Inorganic Chemistry*, 50 (2011) 9443.
- [32] J.-L. Niu, X.-Q. Hao, J.-F. Gong and M.-P. Song, *Dalton Transactions*, 40 (2011) 5135.
- [33] M. Peruzzini and L. Gonsalvi, *Phosphorus Compounds: Advanced Tools in Catalysis and Material Sciences (Catalysis by Metal Complexes)* M. Peruzzini and L. Gonsalvi (Editors), Vol. 37, Springer, 2011.
- [34] E. Zuidema, P.E. Goudriaan, B.H.G. Swennenhuis, P.C.J. Kamer, P.W.N. van Leeuwen, M. Lutz and A.L. Spek, *Organometallics*, 29 (2010) 1210.
- [35] A.R. Carlson, *Design and Synthesis of Early Transition Metal Trianionic Pincer Ligands* Masters of Science, University of Florida, 2007.

- [36] P.C.J. Kamer and P.W.N. van Leeuwen, *Phosphorus(III) Ligands in Homogeneous Catalysis: Design and Synthesis*, first edition ed., John Wiley & Sons, 2012.
- [37] C.A. Tolman, *Chemical Reviews*, 77 (1977) 313.
- [38] M.N. Birkholz (nee' Gensow), Z. Freixa and P.W.N.M. Van Leeuwen, *Chemical Society Review*, 38 (2009) 1099.
- [39] M. Kranenburg, P.C.J. Kamer and P.W.N. van Leeuwen, *European Journal of Inorganic Chemistry*, (1998) 25.
- [40] L.A. van der Veen, P.K. Keeven, P.C.J. Kamer and P.W.N. van Leeuwen, *Journal of the Chemical Society, Dalton Transactions*, (2000) 2105.
- [41] N.J. DeStefano, D.K. Johnson and L.M. Venanzi, *Angewandte Chemie-International Edition*, 86 (1974) 133.
- [42] L.A. van der Veen, P.C.J. Kamer and P.W.N. van Leeuwen, *Angewandte Chemie-International Edition*, 38 (1999) 336.
- [43] W. Goertz, P.C.J. Kamer, P.W.N. van Leeuwen and D. Vogt, *Chemical Communications*, (1997) 1521.
- [44] P. van Leeuwen, P.C.J. Kamer and J.N.H. Reek, *Pure and Applied Chemistry*, 71 (1999) 1443.
- [45] A. Pintado-Alba, H. de la Riva, M. Nieuwhuyzen, D. Bautista, P.R. Raithby, H.A. Sparkes, S.J. Teat, J.M. Lopez-de-Luzuriaga and M.C. Lagunas, *Dalton Transactions*, (2004) 3459.
- [46] I.G. Denisov, T.M. Makris, S.G. Sligar and I. Schlichting, *Chemical Reviews*, 105 (2005) 2253.
- [47] A.J. Labinger, *Journal of Molecular Catalysis A: Chemical*, 220 (2004) 27.
- [48] D.J. Cole-Hamilton, *Science*, 299 (2003) 1702.
- [49] I. Chorkendorff and J.W. Niemantsverdriet, *Concepts of Modern Catalysis and Kinetics*, WILEY-VCH Verlag GmbH &Co. KGaA, Weinheim, 2003.
- [50] C. Marcilly, *Journal of Catalysis*, 216 (2003) 47.
- [51] J.N. Armor, *Catalysis Today*, 163 (2011) 3.
- [52] G.L. Miessler and D.A. Tarr, *Inorganic Chemistry*, Pearson Prentice Hall, New Jersey, 2004.
- [53] A.E. Comyns, *Focus on Catalysts*, 2009 (2009) 1.

- [54] P.W.N. van Leeuwen, N.D. Clement and M.J.L. Tschan, *Coordination Chemistry Reviews*, 255 (2011) 1499.
- [55] M. Claeys, *Background to the DST-NRF Centre of Excellence in Catalysis, The Paraffin Activation Programme University of Cape Town, Capetown, 2004*, p. 5.

Chapter 2

Experimental

2.1 General

All reactions were performed using Schlenk techniques under an atmosphere of UHP grade argon. All the solvents used were dried according to standard procedures and all catalytic reactions were performed under inert conditions with the solvents of analytical grade. Tetrahydrofuran (THF), diethyl ether, toluene and hexane were dried over sodium wire with benzophenone as the indicator. Methanol and ethanol were dried over magnesium turnings and iodine. Dichloromethane (DCM) was dried over phosphorus pentoxide.

All chemicals, 9,9-dimethyl xanthene (**2.1**), hexanoyl chloride, aluminium chloride (AlCl_3), magnesium sulphate anhydrous (MgSO_4), magnesium turnings, triethylene glycol, sodium hydroxide (NaOH), bromopropane, xanthone, ammonium chloride, hydrochloric acid (HCl), sodium wire, benzophenone, potassium hydroxide (KOH), hydrazine monohydrate, silica gel, thin layer chromatography (TLC) plates, tetramethylethylenediamine (TMEDA), 1.6 M solution in hexane of *n*-BuLi, chlorodiphenylphosphine, chlorodi(*p*-tolyl)phosphine, $\text{CoCl}_2 \cdot x\text{H}_2\text{O}$ and $\text{NiCl}_2 \cdot x\text{H}_2\text{O}$ were purchased from Merck, Sigma Aldrich, and DLD Scientific and used as supplied.

The reagents used in catalysis, oxidants and standards were: *n*-octane (99%), 1-octanol (99%), 2-octanol (97%), 3-octanol (98%), 4-octanol (98%), 2-octanone (98%), 3-octanone (97%), 4-octanone (99%), octanal (99%), octanoic acid (99%), pentanoic acid (98%), H_2O_2 (30%) and TBHP (70%) and were purchased from Sigma Aldrich, Merck or DLD Scientific.

TMEDA was distilled and stored in a refrigerator. Chlorodiphenylphosphine and chlorodi(*p*-tolyl)phosphine were used as received. 2,8-dimethylphenoxathiin (**2.7**) was synthesized by Thashree Marimuthu [1]

Purification of ligands was done using column chromatography over silica and alumina. Purification of the metal complexes was conducted via recrystallization from suitable solvents.

2.1.1 Instrumentation

Structural elucidation was conducted using NMR, IR spectroscopy and Liquid Chromatography Mass Spectroscopy (LC-MS). Melting point and elemental analysis were used to determine purity. Lastly, single crystal *X*-Ray diffraction was undertaken for structure determination.

All NMR spectra were recorded on a Bruker Avance III 400 MHz spectrometer at ambient temperature. The ¹H-NMR spectra were reported as chemical shifts in parts per million (ppm) and referenced to CDCl₃ with the solvent peak (7.24). Multiplicity, number of protons and coupling constants are reported. ¹³C-NMR was reported as chemical shifts in ppm and referenced to the CDCl₃ peak ($\delta = 77.0$), multiplicity due to (C-P) coupling, coupling constant and number of carbons. Melting points were recorded using a Bibby Stuart Scientific.

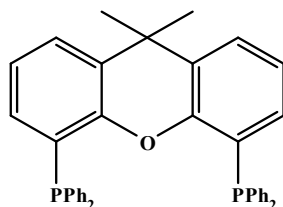
Significant band modes for structure elucidation were recorded using a Perkin Elmer FTIR spectrophotometer with an Attenuated Total Reflectance (ATR) kit. LC-MS was recorded with an Agilent Technologies 1200 Series Quaternary.

2.1.2 Experimental Methods

2.1.2.1 4,5-bis(diphenylphosphino)-9,9-dimethyl xanthene (2.2)

Ligand **2.2** was prepared according to the literature method [1-5]. A Schlenk tube saturated with argon and filled with a solution of compound **2.1** (1 g, 1.72 mmol) and TMEDA (0.70 ml, 4.47 mmol) in THF was cooled to 0 °C. *n*-BuLi (2.79 ml, 4.47 mmol) was then added to the chilled mixture. The reaction was allowed to warm up to room temperature and left to stir for 16 h. Thereafter the resulting dark red solution was cooled to 0 °C and chlorodiphenylphosphine (0.80 ml, 4.47 mmol) was added dropwise and the reaction was left to stir for another 16 h at room temperature. It was then hydrolysed with 10% HCl, brine and extracted with DCM (3 x 20 ml) under inert conditions. The organic fractions were dried with MgSO₄ and the solvent was removed under reduced pressure, resulting in an oil. The oil was triturated with diethyl ether and

evaporated to offer an off-white powder. It was further washed with hexane (3 x 10 ml) and left to dry overnight *in vacuo*.



2.2

Yield: 55%, 0.54 g (white powder)

MP: 219-222 °C (lit. value 221-222 °C)

^1H NMR (400 MHz, CDCl_3, δ): 7.37 (dd, $J = 7.4, 1.4$ Hz, 2H), 7.22 – 7.14 (arom, 20H),
6.95 (t, $J = 7.6$ Hz, 2H), 6.54 (dd, $J = 7.4, 1.4$ Hz, 2H),
1.62 (s, 6H).

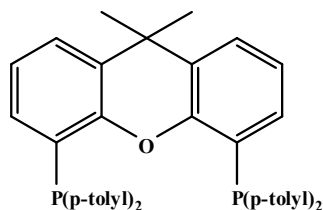
^{13}C NMR (101 MHz, CDCl_3, δ): 150.26 (t, CO), 138.60 – 134.22 (m, C), 133.80 (t, CH),
132.02 (CH), 128.12 (CH), 128.02 (d, CH),
126.30 (CH), 126.21 – 125.70 (m, CP), 123.10 (CH),
34.40 (C), 31.84 (CH_3).

^{31}P NMR (162 MHz, CDCl_3, δ): -17.9 ppm

IR: 1398(s), 1432(w), 1560 (w), 1458 (w), 3056 (w),
2951 (w), 2974(w), 1098 (s), 1231 (m), 688 (s)

2.1.2.2 4,5-bis(di-*p*-tolylphosphino)-9,9-dimethyl xanthene (2.3)

This compound was prepared analogous to compound **2.2** using chlorodi(*p*-tolyl)phosphine (1.92 ml, 9.0 mmol), TMEDA (1.34 ml, 9.0 mmol), *n*-BuLi (5.6 ml, 9.0 mmol) and compound **2.1** (2 g, 3.5 mmol).



2.3

Yield: 64%, 3.85 g (off-white powder)

MP: 259-261 °C

¹H NMR (400 MHz, CDCl₃, δ): 7.35 (dd, J = 7.7, 1.1 Hz, 2H), 7.04 – 6.97 (arom., 20H),
6.93 (t, J = 7.6 Hz, 2H), 6.54 (dd, J = 7.5, 1.6 Hz, 2H),
2.28 (s, 12H), 1.61 (s, 6H).

¹³C NMR (101 MHz, CDCl₃, δ): 152.71 – 152.52 (t, CO), 137.79 (C), 133.98 – 133.77 (t, C),
132 (s, CH), 129.89 (s, CH), 128.92 – 128.85 (t, C),
126.07 (s, CH), 123.20 (s, CH), 34.44 (s, CH₂),
31.74 (s, CH₂), 21.34 (s, CH₃).

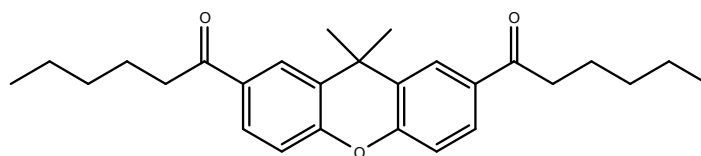
³¹P NMR (162 MHz, CDCl₃, δ): -19.6 ppm

IR: 1405 (s), 1440 (w), 1495 (w), 1563 (w), 3012 (w),
2864 (w), 2967 (w), 1091 (s), 1239 (m), 625 (s)

2.1.2.3 (2,7-di-n-hexanoyl-9,9-dimethyl xanthene) (2.4)

This synthetic method was adapted from literature [1, 6]. To an argon saturated Schlenk tube, 25 ml of DCM was purged with argon. Then a solution of compound **2.1** (1.8 ml, 11.4 mmol) and hexanoyl chloride (3.2 ml, 23.5 mmol) were added and cooled to 0 °C. To the chilled reaction mixture, AlCl₃ (3 g, 22.5 mmol) was added slowly, the reaction was allowed to then warm to room temperature and left stirring for 5 h. After stirring for 5 h it was poured into chilled water

and extracted with (3 x 20 ml) DCM. Organic fractions were combined and dried with MgSO₄. The solvent was removed under reduced pressure to give a crude pale yellow powder. The solid was washed with pentane several times to remove the unreacted starting material. It was transferred into a round bottom flask fitted with a tap and dried overnight.



2.4

Yield: 81%, 3.73 g (yellow powder)

MP: 70 – 72 °C

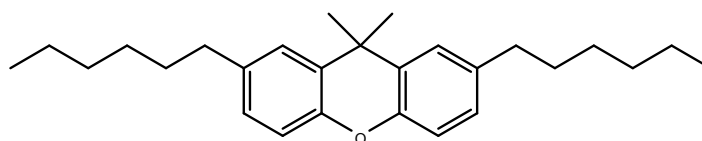
¹H NMR (400 MHz, CDCl₃, δ): 8.11 (s, 2H), 7.84 – 7.82 (d, J = 8.50, 1.94 Hz, 2H),
7.11 (d, J = 8.52 Hz, 2H), 2.96 (t, J = 7.40 Hz, 4H),
1.70 (s, 6H), 1.40 – 1.36 (m, J = 10.44 Hz, 8H),
0.94 – 0.90 (m, J = 13.96 Hz, 6H).

¹³C NMR (101 MHz, CDCl₃, δ): 199.17 (C=O), 153.17 (CO), 133.01 (C), 129.88 (C)
128.17 (CH), 127.12 (CH), 116.57 (CH), 38.39 (C)
34.16 (CH₂), 32.85 (CH₂), 31.59 (CH₃), 24.23 (CH₂),
22.54 (CH₂), 13.96 (CH₃).

2.1.2.4 2,7-di-n-hexyl-9,9-dimethyl xanthene (2.5)

This was prepared according to literature [1, 6]. To a flame dried Schlenk tube fitted with a condenser, triethylene glycol 15 ml and compound **2.4** (1 g, 2.5 mmol) was added. To this stirred mixture NaOH pellets (0.6 g, 15 mmol) and hydrazine monohydrate (0.98 ml, 31.2 mmol) was added. The reaction mixture was refluxed for 1 h at temperature between 110 – 115 °C. Compound **2.4** was then dissolved at 110 °C and thereafter, the condenser was removed and the

temperature was raised to 195 °C. The condenser was reattached and the reaction was refluxed for another 3 h at 220 °C. After 3 h the reaction mixture had turned yellow. It was cooled to room temperature then diluted with DCM 20 ml and hydrolyzed with 10% aqueous HCl (3 x 10 ml). The organic fractions were combined and the solvent was removed under reduced pressure to get a crude yellow powder. The crude product was chromatographed on a silica gel with 100% hexane elution to afford a colourless oil.



2.5

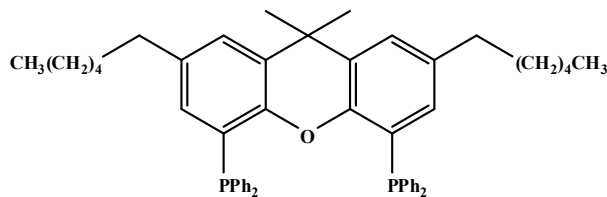
Yield: 37%, 0.35 g (colourless oil)

^1H NMR (400 MHz, CDCl_3 , δ): 7.16 (d, $J = 1.84$ Hz, 2H), 6.98 (d, $J = 1.92$ Hz, 2H),
6.96 (d, $J = 1.92$ Hz, 2H), 2.57 (t, $J = 7.76$ Hz, 4H),
1.60 (s, 6H), 1.31-1.28 (m, $J = 5.16$ Hz, 12H),
0.88 (s, 6H).

^{13}C NMR (101 MHz, CDCl_3 , δ): 162.67 (CO), 151.25 (C), 133.02 (C), 129.76 (C),
126.32(CH), 125.26 (CH), 116.30 (CH), 61.79 (CH_2),
34.24 (CH_2), 32.76 (C), 32.56 (CH_2), 32.22 (CH_3),
31.72 (CH_2), 28.98 (CH_2), 22.39 (CH_2), 13.98 (CH_3).

2.1.2.5 4,5-bis(diphenylphosphino)-2,7-dihexyl-9,9-dimethyl xanthene (2.6)

This compound was prepared analogous to compound **2.2** using chlorodiphenylphosphine (0.43 ml, 2.4 mmol), TMEDA (0.36 ml, 2.4 mmol), *n*-BuLi (1.5 ml, 2.4 mmol) and compound **2.5** (0.35 g, 0.92 mmol).



2.6

Yield: 47%, 0.32 g (white powder)

MP: 152 – 154 °C

^1H NMR (400 MHz, CDCl_3 , δ): 7.21 (d, 2H), 7.19 – 7.13 (arom, 20H), 6.3 (d, 2H),
2.38 (t, $J = 6.98$ Hz, 4H), 1.60 (s, 6H), 1.30 – 1.15
(m, 16 H), 0.84 (t, $J = 6.92$ Hz, 6H).

^{13}C NMR (101 MHz, CDCl_3 , δ): 150.89 (s, CO), 137.75 – 137.62 (t, C), 137.12 (s, C),
133.98 – 133.78 (t, CH), 131.88 (s, CH), 129.54 (s, C),
128.06 -127.98 (t, CH), 126.20 (s, CH_2),
35.31 (s, CH_3), 34.50 (s, CH_2), 31.86 – 30.97 (q, CH_2),
28.61 (s, CH_2), 22.57 (s, CH_2), 14.07 (s, CH_3).

^{31}P NMR (162 MHz, CDCl_3 , δ): -17.8 ppm

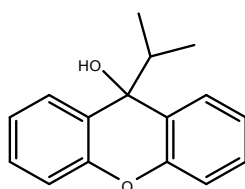
IR: 1418 (s), 1432 (w), 3054 (w), 2955 (w), 2921 (w),
2851 (w), 1091 (s), 1239 (m), 691 (s)

MS: Calc. of $\text{C}_{51}\text{H}_{56}\text{OP}_2$, 746.38, found 769.38 $[\text{M} + \text{Na}]^+$

2.1.2.6 9-isopropyl-9H-xanthen-9-ol (2.8)

The preparation of this compound involves a Grignard reaction. The synthesis was taken from literature [7]. A Schlenk tube flushed with argon was filled with 20 ml of dry ether and 2-bromopropane (8.5 ml, 89.2 mmol) which was then stirred at 0 °C. This was followed by the

addition of fresh magnesium turnings (2.2 g, 89.2 mmol) which was added slowly and continued stirring at 0 °C. After 2 h, the reaction mixture had turned murky white with all the magnesium reacted. A solution of xanthone (3.5 g, 17.8 mmol) in 10 ml of dry diethyl ether was added to the chilled Grignard reaction. The reaction mixture was then allowed to warm up to room temperature and refluxed for 1 h. It was then cooled to room temperature and diluted with diethyl ether (20 ml). Thereafter, the reaction was cooled to 0 °C and quenched using ammonium chloride solution which was added drop wise. The reaction mixture was filtered and the organic layer extracted twice with diethyl ether. The fractions were combined and dried over anhydrous MgSO₄. The solvent was removed under vacuum to give a yellow viscous oil which was passed through a silica column (hexane 90/ diethyl ether 10 solvent elution). The product was dried to get a white powder.



2.8

Yield: 54%, 2.3 g (white powder)

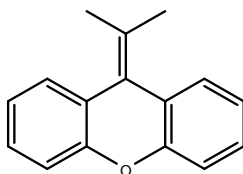
MP: 69 – 70 °C

¹H NMR (400 MHz, CDCl₃, δ): 7.66 (dd, J = 7.8, 1.6 Hz, 2H), 7.29 (dd, J = 7.3, 1.7 Hz, 2H), 7.18 -7.07 (m, 4H), 2.22 (s, 1H, OH), 2.10 (m, 1H), 0.71 (d, J = 6.8 Hz, 6H).

¹³C NMR (101 MHz, CDCl₃, δ): 152.01 (CO), 128.60 (C), 127.10 (CH), 126.90 (CH), 123.02 (CH), 116.12 (CH), 72.14 (C), 42.62 (CH), 16.80 (CH₃).

2.1.2.7 10-isopropylidene xanthene (2.9)

In a Schlenk tube flushed with argon, 20 ml of DCM was degassed with argon. Thereafter, compound **2.8** (1g, 4.2 mmol) was dissolved followed by the addition of *p*-toluene sulfonic acid monohydrate (1.6 g, 8.4 mmol). The reaction was refluxed for 2 h and monitored with TLC. The reaction was allowed to cool to room temperature, followed by the slow addition of 10 ml of deionized water and 15 ml of 10% sodium hydroxide. The organic layer was extracted with DCM twice and dried over anhydrous MgSO₄. It was filtered and dried under vacuum to give a solid which was purified through a silica column with 100% hexane. The solvent was evaporated to give a yellow solid.



2.9

Yield: 60%, 0.56 g (yellow solid)

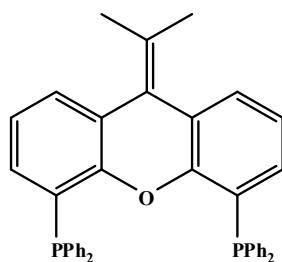
MP: 79 – 80 °C

¹H NMR (400 MHz, CDCl₃, δ): 7.38 (dd, J = 7.6, 1.3 Hz, 2H), 7.17 (m, 4H),
7.09 (m, 2H), 2.09 (s, 6H).

¹³C NMR (101 MHz, CDCl₃, δ): 152.21 (CO), 130.60 (C), 129.40 (CH), 128.03 (CH),
126.95 (C), 122.42 (CH₂), 120.20 (CH), 116.19 (CH),
23.20 (CH₃).

2.1.2.8 4, 5-bis(diphenylphosphino) 10-isopropylidene xanthene (2.10)

Ligand **2.10** was prepared similarly to ligand **2.2** using compound **2.9** (0.3 g, 1.35 mmol), TMEDA (0.53 ml, 3.51 mmol), 1.6 M *n*-BuLi (2.2 ml, 3.51 mmol) and PPh₂Cl (0.63 ml, 3.51 mmol) in 10 ml of dry hexane.



2.10

Yield: 63%, 0.5 g

MP: 212-214 °C

¹H NMR (400 MHz, CDCl₃, δ): 7.36 (dd, J = 7.6, 1.4 Hz, 2H), 7.23 – 7.22 (arom, 20H),
7.01 (t, J = 7.6 Hz, 2H), 6.56 (dd, J = 7.6, 1.7 Hz, 2H),
2.10 (s, 6H).

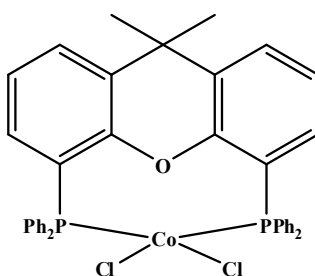
¹³C NMR (101 MHz, CDCl₃, δ): 151.30 (t, CO), 137.22 (s, C), 134.14 – 133.94 (t, CH),
131.47 (s, CH), 131.31 (s, C), 128.97 (s, CH),
128.25 – 128.14 (q, CH), 126.34 (s, CH),
122.85 (s, C), 122.66 (s, CH), 23.28 (s, CH₃).

³¹P NMR (162 MHz, CDCl₃, δ): -17.9 ppm

IR: 1393 (s), 1417 (w), 1433 (w), 3057 (w), 2932 (w),
1068 (s), 1220 (m), 692 (s)

2.1.2.9 Co(4,5-bis(diphenylphosphino)-9,9-dimethyl xanthene)Cl₂ (2.11)

This method was adapted from literature [8]. To a solution of anhydrous cobalt(II) chloride (0.24 g, 1.0 mmol) and compound **2.2** (0.54 g, 0.93 mmol) in THF (10 ml) was refluxed at 80 °C for 3 h. Thereafter the solution was cooled to room temperature and diethyl ether was added. The volume of solvent was reduced *in vacuo* to yield a blue solid which was filtered and dried *in vacuo*.



2.11

Yield: 83%, 0.55 g (blue powder)

MP: 387-390 °C

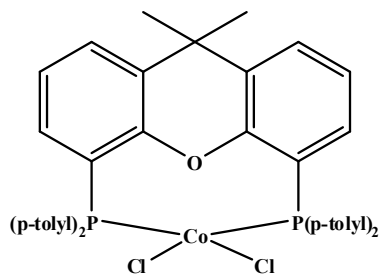
IR: 1409 (*s*), 1436 (*w*), 3061 (*w*), 2975 (*w*), 1100 (*s*),
1243 (*m*), 690 (*s*)

EA of C₃₉H₃₂OP₂CoCl₂: %C - 66.64 (66.22).

%H - 4.30 (4.55)

2.1.2.10 Co(4,5-bis(di-*p*-tolylphosphino)-9,9-dimethyl xanthene)Cl₂ (2.12)

This compound was prepared analogous to compound **2.11** by using compound **2.12** (0.30 g, 0.47 mmol) and anhydrous cobalt(II) chloride (0.14 g, 0.59 mmol).



2.12

Yield: 83%, 0.30 g (indigo blue powder)

MP: 448-450 °C

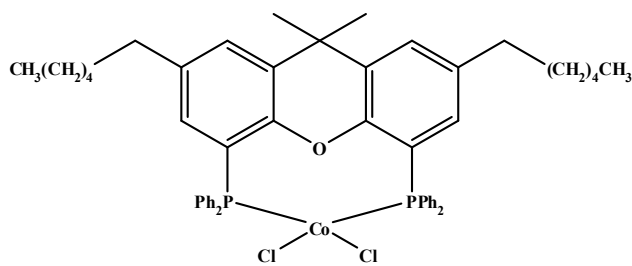
IR: 1411 (*s*), 1435 (*w*), 3052 (*w*), 2957 (*w*), 2975 (*w*),
1098 (*s*), 1246 (*m*), 621 (*s*)

EA of C₄₃H₄₀OP₂CoCl₂: %C 67.90 (67.55)

%H 5.06, (5.27)

2.1.2.11 Co(4,5-bis(diphenylphosphino)-2,7-dihexyl-9,9-dimethyl xanthene)Cl₂ (2.13)

This compound was prepared analogous to compound **2.11** by using anhydrous cobalt(II) chloride (0.09 g, 0.38 mmol) and ligand **2.6** (0.24 g, 0.32 mmol).



2.13

Yield: 42%, 0.12 g (blue powder)

MP: 250-251 °C

IR: 1422 (*s*), 3049 (*w*), 2924 (*w*), 2954 (*w*), 2855 (*w*),

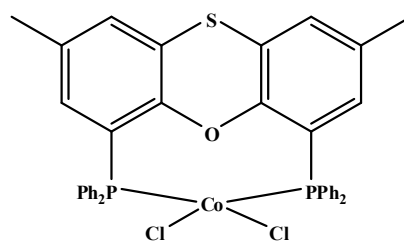
1099 (*s*), 1239 (*m*), 691 (*s*)

EA of C₅₁H₅₆OP₂CoCl₂: %C 70.42 (69.95)

%H 6.27 (6.44)

2.1.2.12 Co(Thixantphos)Cl₂ (2.14)

This compound was prepared analogous to compound **2.11** by using the thixantphos ligand (0.15 g, 0.26 mmol) and anhydrous cobalt(II) chloride (0.06 g, 0.25 mmol).



2.14

Yield: 66%, 0.12 g (pale blue powder)

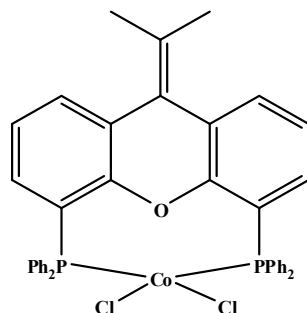
MP: 379-382 °C (decomposed)

IR: 1410 (*s*), 1435 (*m*), 1480 (*w*), 3046 (*w*), 2865 (*w*),

1094 (*s*), 1207 (*m*), 1243 (*m*), 694 (*s*)

2.1.2.13 Co(4,5-bis(diphenylphosphino) 10-isopropylidene xanthene)Cl₂ (2.15)

This compound was prepared analogous to compound **2.11** by using ligand **2.10** (0.15 g, 0.25 mmol) and anhydrous cobalt(II) chloride (0.055 g, 0.23 mmol).



2.15

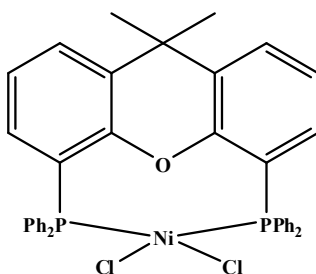
Yield: 82%, 0.14 g (blue powder)

MP: 398-401 °C (decomposed)

IR: 1402 (*s*), 1436 (*m*), 1482 (*w*), 3074 (*w*), 2960 (*w*),
2861 (*w*), 1101 (*s*), 1227 (*m*), 692 (*s*)

2.1.2.14 Ni(4, 5-bis(diphenylphosphino)-9,9-dimethyl xanthene)Cl₂ (2.16)

This method was adapted from literature [9, 10]. Two Schlenk tubes were used. One was filled with a solution of NiCl₂ hydrate (0.06 g, 0.25 mmol) in 5 ml of methanol and the other with a solution of compound **2.2** (0.15 g, 0.26 mmol) in 5 ml of DCM. The solution containing compound **2.2** in DCM was added dropwise by cannula into the solution of NiCl₂ under argon atmosphere. The reaction mixture was then heated to 50°C and stirred for 2 h. After 2 h, a green precipitate was observed and the reaction mixture was cooled to room temperature and filtered. The green powder obtained was washed several times with hexane and dried over night under high vacuum.



2.16

Yield: 50%, 0.09 g (green powder)

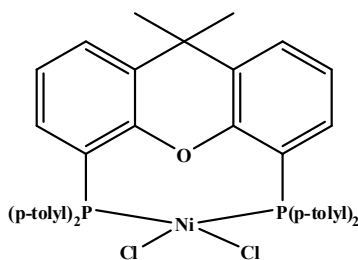
MP: > 350 °C (decomposed)

IR: 1411 (*s*), 1435 (*w*), 3052 (*w*), 2957 (*w*), 2975 (*w*),
1098 (*s*), 1246 (*m*), 689 (*s*)

EA of C₃₉H₃₂OP₂NiCl₂: %C 63.53 (63.16)
%H 6.91 (6.51)

2.1.2.15 Ni(4, 5-bis(di-*p*-tolylphosphino)-9,9-dimethyl xanthene)Cl₂ (2.17)

This complex was prepared analogous to complex **2.16** using ligand **2.3** (0.054 g, 0.085 mmol) and NiCl₂ hydrate (0.03 g, 0.13 mmol).



2.17

Yield: 49%, 32 mg (olive green)

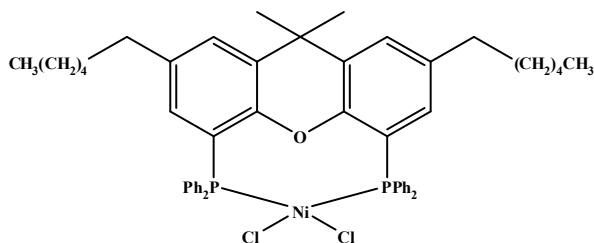
MP: > 350 °C (decomposed)

IR: 1425 (*s*), 3052 (*w*), 2953 (*w*), 2925 (*w*), 2855 (*w*),
1099 (*s*), 1239 (*m*), 620 (*s*)

EA of C₄₃H₄₀OP₂NiCl₂: %C 67.39 (67.57)
%H 5.05 (5.27)

2.1.2.16 Ni(4, 5-bis(diphenylphosphino)-2,7-dihexyl-9,9-dimethyl xanthene)Cl₂ (2.18)

Complex **2.18** was prepared analogous to complex **2.16** using compound **2.6** (0.2 g, 0.27 mmol) and NiCl₂ hydrate (0.093 g, 0.39 mmol).



Yield: 45%, 0.11 g (dark green)

MP: 258–260 °C

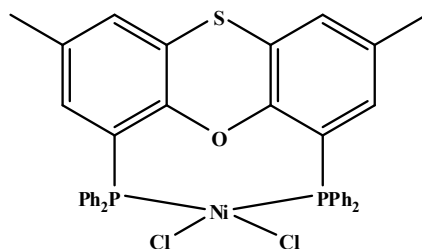
IR: 1425 (*s*), 3052 (*w*), 2525 (*m*), 2953 (*m*), 2855 (*w*),
1099 (*s*), 1239 (*m*), 691 (*s*)

EA of C₅₁H₅₆OP₂NiCl₂: %C 69.72 (69.88)

%H 6.38 (6.44)

2.1.2.17 Ni(thixantphos)Cl₂ (2.19)

This complex was prepared analogous to complex **2.16** using thixantphos ligand (0.15 g, 0.26 mmol) and NiCl₂ hydrate (0.05 g, 0.21 mmol).

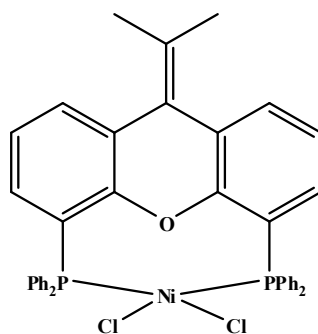


Yield: 80%, 0.12 g (olive green)

MP: 366-370 °C
IR: 1412 (*s*), 1434 (*m*), 1480 (*w*), 3051 (*w*), 2865 (*w*),
1094 (*s*), 1207 (*w*), 1243 (*m*), 693 (*s*)

2.1.2.18 Ni(4,5-bis(diphenylphosphino) 10-isopropylidene xanthene)Cl₂ (2.20)

This complex was prepared analogous to complex **2.16** using ligand **2.10** (0.15 g, 0.25 mmol) and NiCl₂ hydrate (0.055 g, 0.23 mmol).



2.20

Yield: 82%, 0.14 g (dark green)
MP: 387-390 °C
IR: 1404 (*s*), 1435 (*m*), 1481 (*w*), 3050 (*w*), 2865 (*w*),
1101 (*s*), 1229 (*m*), 691(*s*)

2.2 References

- [1] T. Marimuthu, The Preparation and Novel Application of Diphosphorous Xanthenes Family Ligands in Homogenous Catalysis, PhD Thesis, University of KwaZulu Natal, 2011, p. 74.
- [2] L.A. van der Veen, P.H. Keeven, G.C. Schoemaker, J.N.H. Reek, P.C.J. Kamer, P.W.N. van Leeuwen, M. Lutz and A.L. Spek, *Organometallics*, 19 (2000) 872.
- [3] M. Kranenburg, Y.E.M. Vanderburgt, P.C.J. Kamer, P. Vanleeuwen, K. Goubitz and J. Fraanje, *Organometallics*, 14 (1995) 3081.
- [4] J.M. Mallan and R.L. Bebb, *Chemical Reviews*, 69 (1969) 693.
- [5] V.H. Gessner, C. Daschlein and C. Strohmann, *Chemistry: A European Journal* 15 (2009) 3320.
- [6] R.P.J. Bronger, J.P. Bermon, J. Herwig, P.C.J. Kamer and P.W.N.M. van leeuwen, *Advanced Synthesis & Catalysis*, 346 (2004) 789.
- [7] I.T. Badejo, R. Karaman and J.L. Fry, *Journal of Organic Chemistry*, 54 (1989) 4591.
- [8] M.M.P. Grutters, C. Muller and D. Vogt, *Journal of the American Chemical Society*, 128 (2006) 7414.
- [9] J.A.S. Bomfim, F.P. de Souza, C.A.L. Filgueiras, A.G. de Sousa and M.T.P. Gambardella, *Polyhedron*, 22 (2003) 1567.
- [10] S. Kundu, W.W. Brennessel and W.D. Jones, *Inorganic Chemistry*, 50 (2011) 9443.

Chapter 3

Results & Discussion

3.1 Introduction

3.1.1 Preparation of Ligands

All the ligands prepared in this study are built around the general xantphos structure depicted in Figure 3.1. At position X, different donors were introduced which contribute to the electronic variability of the backbone without affecting the electronic environment around the phosphorus donors. Hence, to get the thio-derivative, the carbon atom was replaced by the more electron withdrawing heteroatom sulphur at position X. For other ligands, the carbon atom was maintained, only the functionality on the carbon was varied with a methyl group and then an isopropyl group. The substitution at position Y with an aliphatic chain was done to change the solubility of the ligand in organic solvents. The substituents of the phosphorus donor atoms were varied to study their effect on the reactivity of the catalyst. Phenyl substituents were replaced with more electron donating *p*-tolyl ones in order to induce positive electronic effects around the environment of the phosphorus donor atom [1].

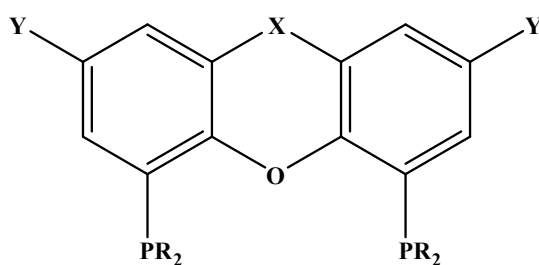
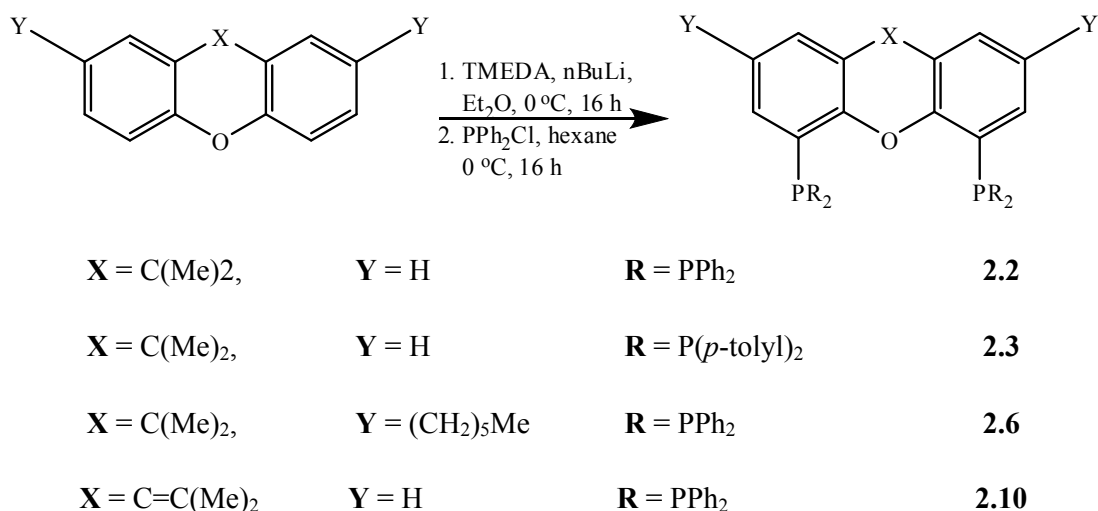


Figure 3.1: General structure of the ligands studied in this project.

The preparation of these ligands involved the abstraction of the acidic proton from the respective backbone, followed by lithiation, which is a critical step as it requires very-dry reagents. Therefore, the Lewis base (TMEDA) used was distilled to remove any moisture and the whole

process was conducted using Schlenk techniques under an atmosphere of argon gas. The solvents used were dry and the *n*-BuLi was added via a syringe flushed with argon. To couple the phosphorus to the respective backbones, electrophilic PR₂Cl was used and this required moisture and oxygen free conditions, since PR₂Cl oxidizes easily. Synthesis was continued using Schlenk techniques under argon gas to eliminate any oxygen [1-4].

In this work, four ligands were synthesized and one was purchased. Of the four that were synthesized, one (ligand **2.3**) is new. For the complexes, all five ligands were complexed to cobalt and then to nickel. To our knowledge, eight of the complexes are novel. Scheme 1 shows the general procedure for the preparation of ligands (**2.2-2.10**). Tables 3.1, 3.2, 3.3 and 3.4 respectively show percentage yields of the synthesized precursors, ligands and the complexes.



Scheme 3.1: General procedure for the synthesis of ligands (**2.2, 2.3, 2.6 & 2.10**).

3.1.2 NMR Analysis

NMR spectroscopy is the dominant characterization technique most suited to the elucidation of ligand structures. Hence, in this study, ¹H, ¹³C and ³¹P NMR were employed.

The most significant peaks for xanthene-based ligands appear in the aromatic and aliphatic regions. Xanthene-backbones are symmetric in nature with a C₂ plane passing through the X

and oxygen atoms (Table 3.1). ^1H -NMR spectra of ligands **2.2**, **2.3**, **2.6** and **2.10** are represented in Figures 3.2-3.5 with the assignment of important peak positions summarized in Table 3.5.

Table 3.1: Precursors and their percentage yields.

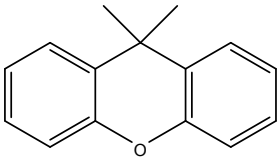
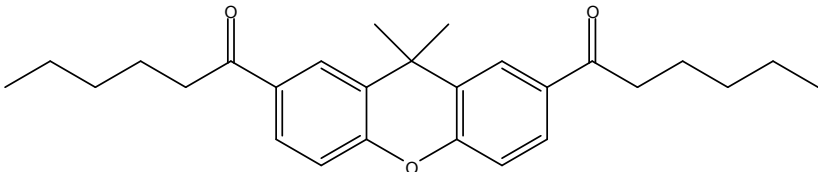
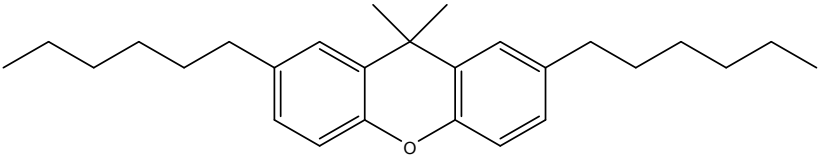
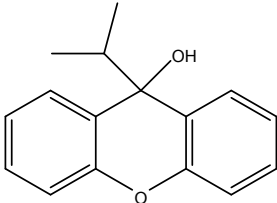
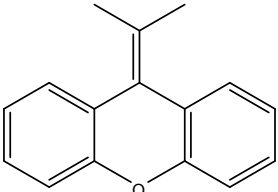
Name	Precursor	Yield%
2.1		purchased
2.4		81
2.5		37
2.8		54
2.9		60

Table 3.2: Ligand structures and their percentage yields.

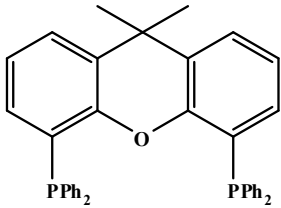
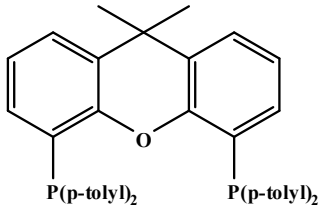
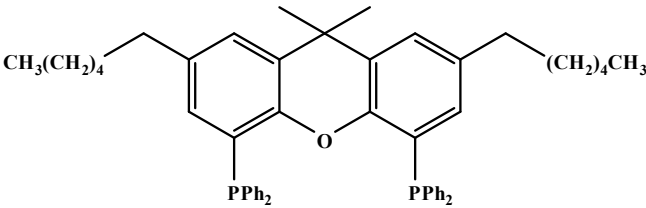
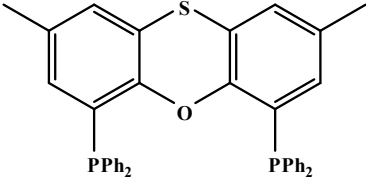
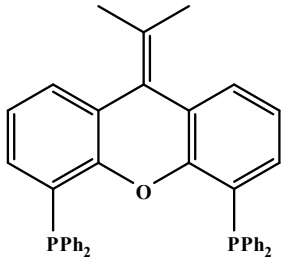
Name	Ligand	Yield %
2.2		55
2.3		64
2.6		47
2.7		previously synthesized (reference 17)
2.10		63

Table 3.3: Cobalt complexes and their percentage yields.

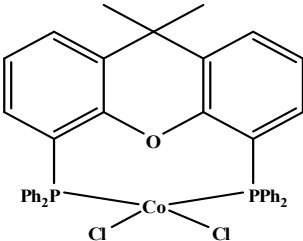
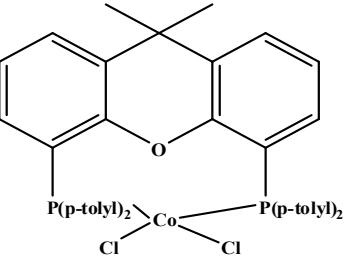
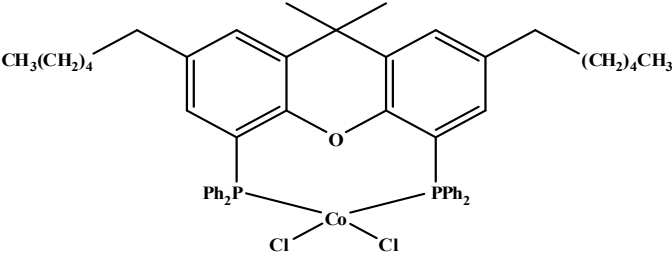
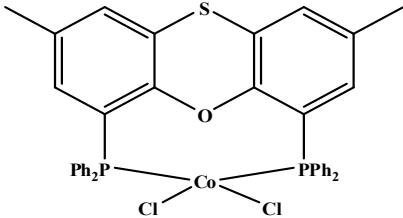
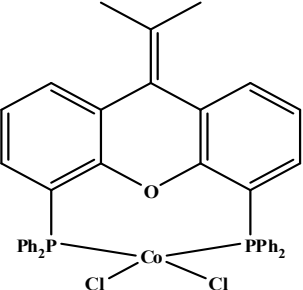
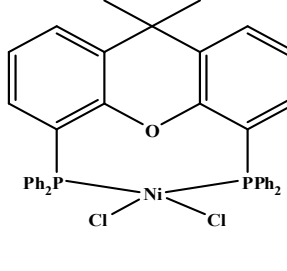
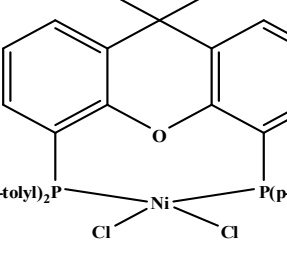
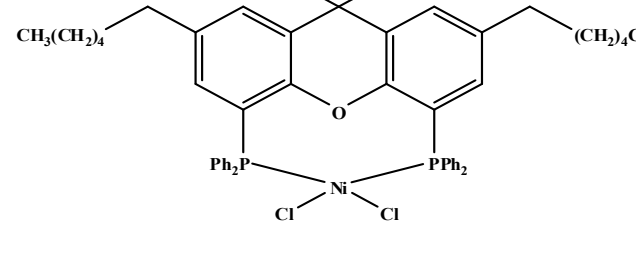
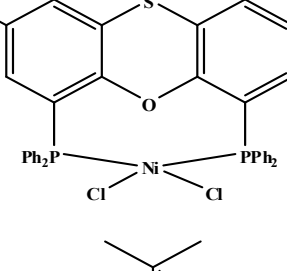
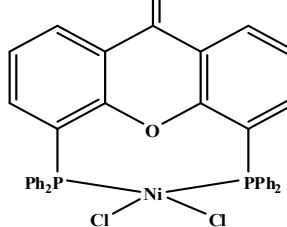
Name	Complex	Yield %
2.11		83
2.12		83
2.13		42
2.14		66
2.15		82

Table 3.4: Nickel complexes and their percentage yields.

Name	Complex	Yield %
2.16		50
2.17		49
2.18		45
2.19		80
2.20		82

In ligand **2.2** (Figure 3.2), position 1 represents the two shielded methyl groups which gave rise to a singlet at 1.62 ppm. They appear as a singlet because they are in equivalent chemical environments due to the symmetric backbone. Protons on position 2 of the phenyl rings appear as a doublet of doublets at 6.54 ppm and those on position 3 as a triplet at 6.95 ppm. The multiplicity is due to the neighbouring protons that couple with them. Position 4, which is a doublet of doublets, resonates at 7.37 ppm. It is more deshielded when compared to other protons in the ring due to the negative inductive effect of the neighbouring oxygen atom, which pulls electron density from position 4 leaving it deshielded. The rest of the protons are aromatic protons from the phenyl rings which appear, as expected, between 7.22 – 7.14 ppm.

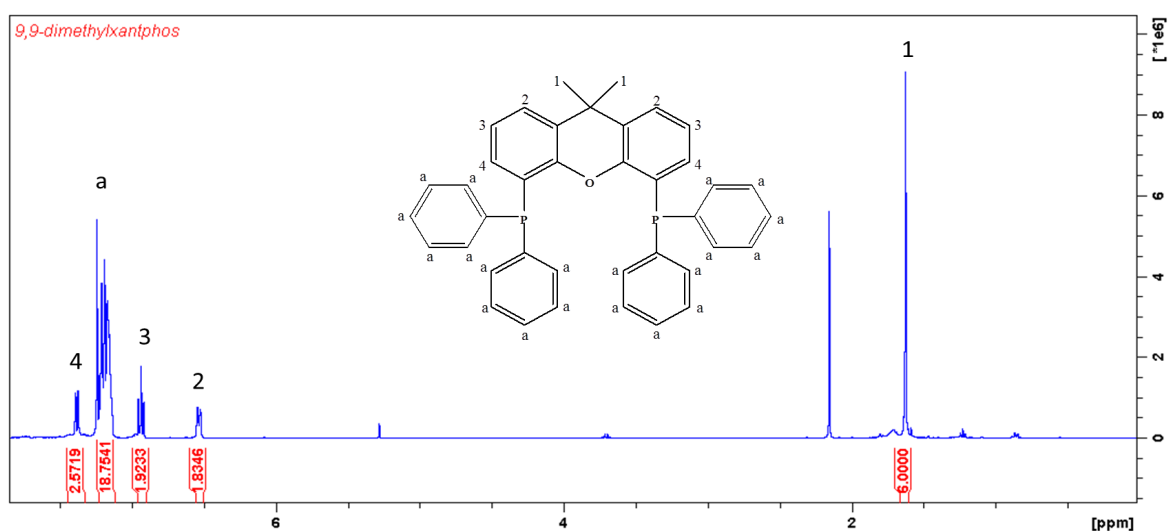


Figure 3.2: ^1H NMR of ligands 4,5-bis(diphenylphosphino)-9,9-dimethyl xanthene (**2.2**).

Ligand **2.3** (Figure 3.3) differs from ligand **2.2** due to the methyl groups on the phenyl rings at the *para*-position to the donor P atom. Protons **b** of the methyl groups appear as a singlet at 2.28 ppm and integrate to 12 units.

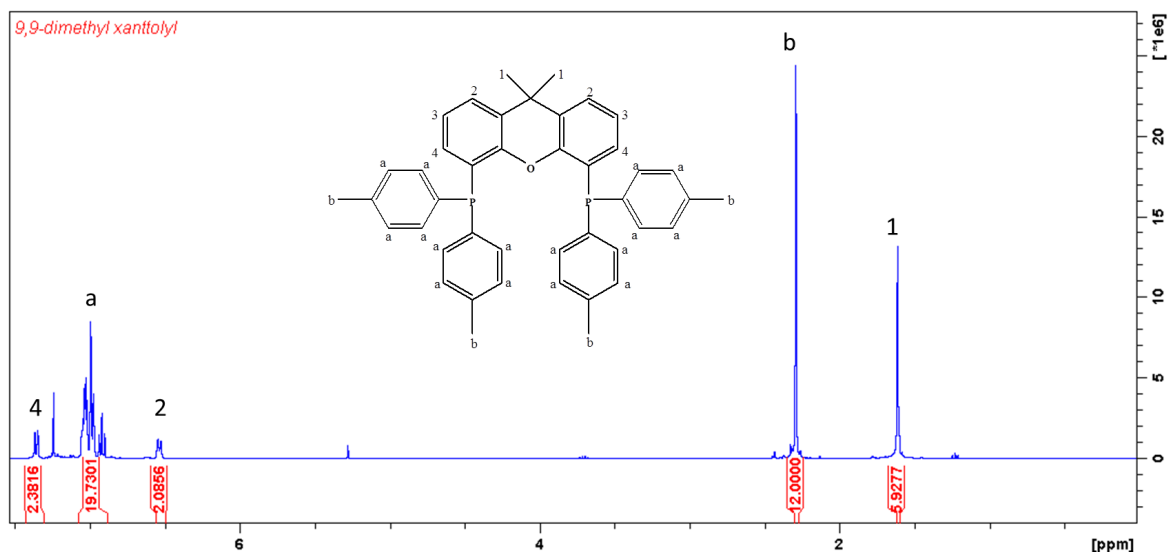


Figure 3.3: ^1H NMR of ligand 4,5-bis(di-*p*-tolylphosphino)-9,9-dimethyl xanthene (**2.3**).

The difference between ligand **2.6** (Figure 3.4) and ligand **2.2** is the aliphatic chain labelled 4-7 on the structure of ligand **2.6**. The methylene protons (position 4) appear as a triplet at 2.38 ppm due to their proximity to the benzene ring, deshielding the protons and shifting their resonance downfield. The methylene protons at position 6 appear as a multiplet between 1.30 – 1.15 ppm. The methyl group (position 7) appear as a triplet at 0.84 ppm. The multiplicity is explained by the coupling effect which is brought about by the neighbouring protons.

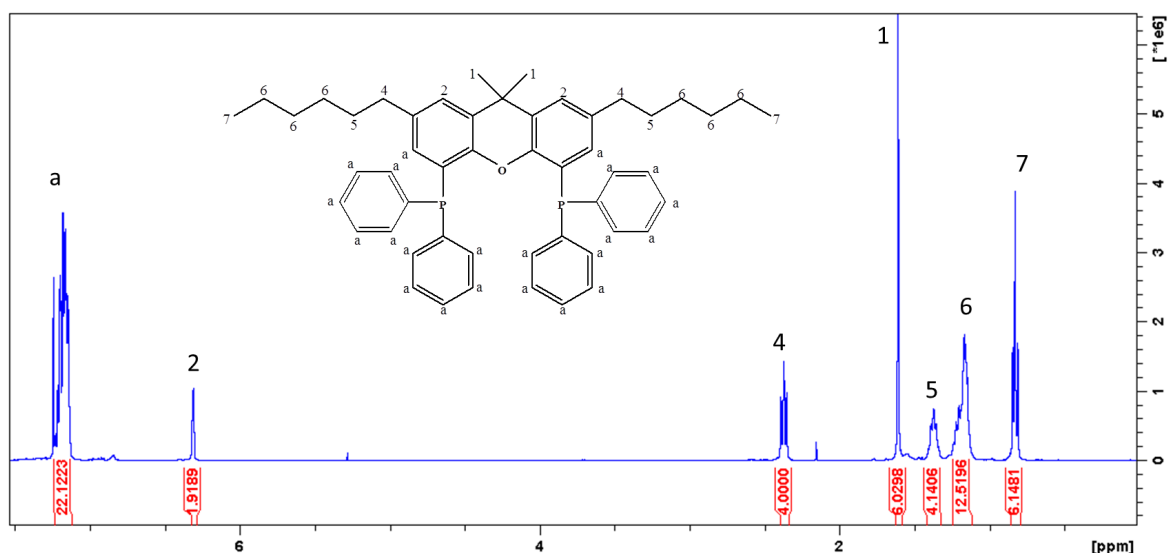


Figure 3.4: ^1H NMR of ligand 2,7-di-*n*-hexyl-9,9-dimethyl xanthene (**2.6**).

Finally, ligand **2.10** (Figure 3.5) is also similar to ligand **2.2**, with the only difference being an *isopropyl* group instead of the two methyl groups at the central carbon. The two protons in position 1 are equivalent to each other and appear as a singlet at 2.10 ppm. The methyl groups, which normally appear at 0.9 ppm, are deshielded with their resonance shifted slightly downfield due to the effect of the C=C which withdraws electron density away from the methyl protons [5].

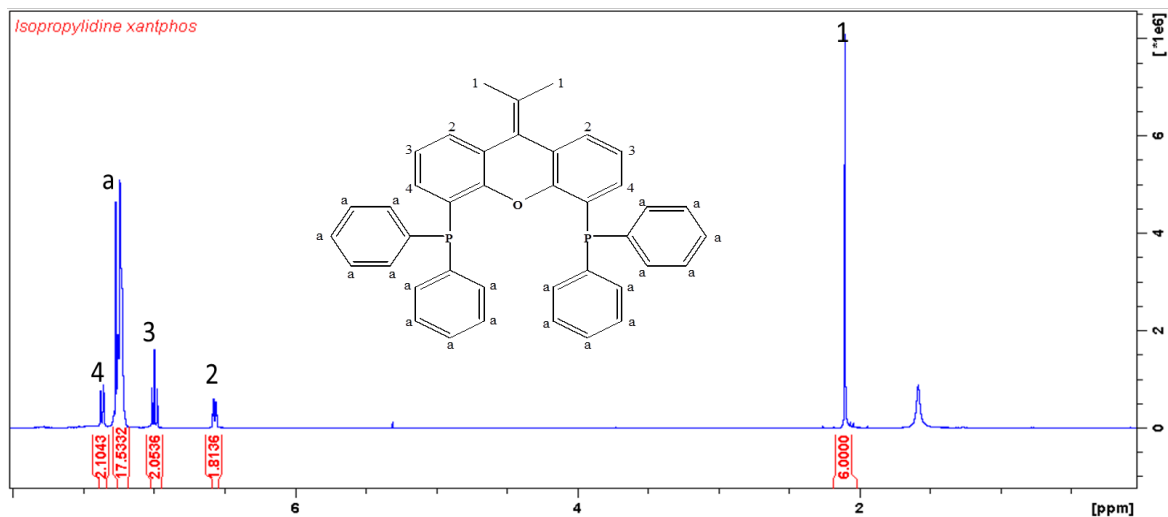


Figure 3.5: ¹H NMR of ligand 4,5-bis(diphenylphosphino)-10-*isopropylidene* xanthene (**2.10**).

Table 3.5: ¹H NMR peaks of representative ligands and their integration.

Ligand	Position of Proton	H-NMR peak (CDCl ₃)/ ppm	Proton integration
2.2	1	1.62(s)	6H
	2	6.54(dd)(J = 7.4, 1.4 Hz)	2H
	3	6.95(t) (J = 7.6 Hz)	2H
	4	7.37(dd) (J = 7.4, 1.4 Hz)	2H
	a	7.22-7.14	20H
2.3	1	1.61 (s)	6H
	2	6.54 (dd) (J = 7.5, 1.6 Hz)	2H
	3	6.93 (t) (J = 7.6 Hz)	2H
	4	7.35 (dd) (J = 7.7, 1.1 Hz)	2H
	a	7.04 - 6.97 (arom)	20H
	b	2.28 (s)	12H
2.6	1	1.60 (s)	6H
	2	6.3 (d)	2H
	3	7.21 (d)	2H
	4	2.38 (t) (J = 6.98 Hz)	4H
	5	1.30 (t)	4H
	6	1.30-1.15 (m)	12H
	7	0.84 (t) (J = 6.92 Hz)	6H
	a	7.19 - 7.13 (arom)	20H
2.10	1	2.10 (s)	6H
	2	6.56 (dd) (J = 7.6, 1.7 Hz)	2H
	3	7.01 (t) (J = 7.6 Hz)	2H
	4	7.36 (dd) (J = 7.6, 1.4 Hz)	2H
	a	7.23 – 7.22 (arom)	20H

Table 3.6 shows a summary of the ³¹P-NMR data of the ligands. When compared to those of related known compounds in literature, the values confirm that the ligands have been successfully synthesized [2, 3, 6]. The ³¹P NMR peak of diphenylphosphine appeared at -41 ppm which was deshielded when hydrogen is replaced by a more electron withdrawing group, such as chlorine. Therefore, the ³¹P NMR peak of chlorodiphenylphosphine appeared downfield

at 81 ppm. If the chloride from chlorodiphenylphosphine was replaced by a less electron withdrawing atom an upfield shift was observed. However, this means that the sp hybridized carbon from the xanthene backbone creates a more electron rich environment, resulting in a shielding effect which shifts the phosphorus resonance peak upfield [7, 8]. Hence, it appeared around -17.8 ppm for ligands **2.2**, **2.6** and **2.10**.

Another observation to take note of is the ^{31}P chemical shift of ligand **2.3**, when compared to ligands **2.2**, **2.6** and **2.10**. The phosphorus peak of **2.3** has shifted upfield to -19 ppm, while the other ligands have peaks at -17.8 ppm. This shows the effect of the methyl groups on the phosphorus peak shift. Since the methyl groups are electron donating they increase the electron density slightly, causing a shielding effect, thereby shifting the phosphorus peak upfield [5].

Table 3.6: ^{31}P NMR data of ligands **2.2**, **2.3**, **2.6** and **2.10**.

Ligand	^{31}P -NMR peak shifts (CDCl_3)/ ppm	
	Experimental	Literature
2.2	-17.9	-17.5
2.3	-19.6	N/A
2.6	-17.8	-17.8
2.10	-17.9	-17.9

3.1.3 IR Analysis

IR was used to compare changes in bond vibration frequencies between the metal complexes and the respective uncoordinated ligands, as shown in Table 3.7.

The aromatic C-H stretch which appears in the $3100 - 3000 \text{ cm}^{-1}$ region was detected in all ligands and complexes [9]. This confirms the presence of the xanthene backbone. Another observation is the absorption at 690 cm^{-1} for the Ar-H bend. The methylene C-H stretch, which appears between $3000-2900 \text{ cm}^{-1}$, was common for all ligands and complexes as well [9, 10]. This is the characteristic band of methyl groups and indicates the presence of an aliphatic chain if the intensity is strong. The presence of methyl and methylene C-H bends at $1400-1435 \text{ cm}^{-1}$ showed the presence of methyl groups in the ligands and complexes. For ligands **2.2**, **2.7** and **2.10** an absorption at 2950 cm^{-1} was also observed for the methyl groups. In the case of ligand

2.3, a medium absorption at 2967 cm^{-1} indicated the presence of the methyl group at position 9 of the xanthene backbone and methyl groups on the phenyl rings at the *para*-position. Ligand **2.6** showed strong intensity bands at 2921 cm^{-1} and 2851 cm^{-1} indicating the presence of the aliphatic chain. The absorption at 722 cm^{-1} , representing a C-H bend, is also an indication of the presence of the aliphatic chain. It is important to note the strong intensity of the band at 2921 cm^{-1} . The intensity of the absorption depends on the number of C-H bonds present, as well as the dipole moment of the bond, therefore, for an aliphatic chain a relatively strong intensity is expected due a combination of the methyl, methylene and methyne groups present [11, 12].

The aryl or alkyl ether group (C-O-C) shows strong bands between $1275\text{-}1200\text{ cm}^{-1}$ due to a large dipole moment in the C-O bond. This stretch appears for all ligands and complexes, mainly because of the C-O-C linkage of the xanthene backbone [9]. An aryl thioether C-S stretch is visible in the range of $800\text{-}600\text{ cm}^{-1}$, which was only observed for ligand **2.7** and complexes **2.14** and **2.19** indicating the presence of sulphur between the carbons [6, 13-17].

A trend of peak shifts from lower to higher frequencies was observed when comparing uncoordinated ligands with corresponding complexes. Bands such as those of the aryl ethers (C-O-C stretch), C-H aromatic stretch, CH_3 and CH_2 stretches, methyl and methylene C-H bends were observed to have shifted to higher frequencies upon coordination. The shift to higher frequency is explained by the nature of the substituents on the phenyl groups. Phosphorus substituents have strong electron accepting properties. Therefore, a transfer of electron density from metal to the ligand increases the electron density in the ligand causing the energy of vibrations (C-O-C, CH_3 and CH_2 stretch, aromatic C-H stretch and CH_3 and CH_2 bend) to increase, giving rise to signals at higher frequencies [18].

Table 3.7: IR data of ligands and corresponding complexes.

Ligand/ Complex	CH ₃ , CH ₂ bend v/cm⁻¹	C-H aromatic, CH ₃ , CH ₂ (stretch) v/cm⁻¹	Aryl ethers C-O-C (stretch) v/cm⁻¹	C-S stretch v/cm⁻¹	Ar-H bend v/cm⁻¹
2.2	1398, 1432	3056, 2974, 2951	1231	-	688
2.11	1409, 1436	3061, 2975	1243	-	690
2.16	1411, 1435	3052, 2975, 2957	1246	-	689
2.3	1405, 1440	3012, 2967	1239	-	625
2.12	1441, 1498	3019, 2953	1253	-	621
2.17	1415, 1498	3018, 2951	1254	-	620
2.6	1418, 1432	3054, 2955, 2921	1239	-	691
2.13	1422, 1481	3049, 2954, 2924	1239	-	691
2.18	1425, 1481	3052, 2953, 2925	1239	-	691
2.7	1403, 1432, 1476	3050, 2951	1200, 1221, 1238	741	692
2.14	1410, 1435, 1480,	3046	1207, 1243	749	694
2.19	1412, 1434, 1480	3051	1207, 1243	748	693
2.10	1393, 1417, 1433	3057, 2932	1220	-	692
2.15	1402, 1436, 1482	3074, 2960	1227	-	692
2.20	1404, 1435, 1481	3050	1229	-	691

3.1.4 Melting points

Impurities are associated with a widening of the melting range and lowering of the melting points of pure compounds. The melting points for the ligands were sharp, implying high purity (Table 3.8). Also noted was that all ligands first changed from powder to crystalline form, followed by melting. Most of the complexes decomposed at temperatures above 350 °C [19]. The melting points of the ligands **2.2**, **2.3**, **2.7** and **2.10** were comparable, while that of ligand **2.6**

was totally different, as it was found to be between 152-154°C, which is lower than those of the other ligands. This may be due to the aliphatic chain at positions 2 and 7 which has many conformations about the C-C bonds and restricts orderly packing of the molecule, thereby lowering the melting point [3, 4].

Table 3.8: Melting point of ligands and their complexes.

Ligand/Complex	Melting point/ °C
2.2	219-221
2.11	387-390
2.16	>350 (decomposed)
2.3	259-261
2.12	448-450
2.17	>350 (decomposed)
2.6	152-154
2.13	250-251
2.18	258-260
2.14	379-382 (decomposed)
2.19	366-370
2.10	212-213
2.15	398-401 (decomposed)
2.20	387-390

3.2 Complexes

Two metals, nickel and cobalt, were used for complexation with the synthesized ligands. These transition metals are abundant in nature, relatively cheap and readily available. Many characterization techniques were used to confirm complexation such as melting point, IR, colour change from ligands to complexes, as well as single crystal XRD. All the complexes are high spin and paramagnetic, hence NMR and MS characterization were not employed.

All the complexes of nickel and cobalt were found to be stable in air, the metals are in the +2 oxidation state.

3.2.1 Elemental Analysis

Elemental analysis for carbon and hydrogen is important and is used to confirm the elemental composition and bulk purity of the compounds. The obtained elemental analyses data are within the acceptable range of 0.5 % of theoretically calculated values. This not only confirms that complexation had taken place, but also that the complexes were pure. Table 3.9 shows the results obtained for each complexes.

Table 3.9: Elemental analysis data for complexes **2.11-2.20**.

Complexes	%C	%H
2.11	66.64 (66.22)	4.30 (4.55)
2.16	63.53 (63.16)	6.91 (6.51)
2.12	67.90 (67.55)	5.06 (5.27)
2.17	67.39 (67.57)	5.05 (5.27)
2.13	70.42 (69.95)	6.27 (6.44)
2.18	69.72 (69.88)	6.38 (6.44)
2.19	62.62 (62.84)	4.55 (4.16)
2.20	66.73 (66.70)	4.83 (4.48)

(calculated values are shown in paranthesis).

3.2.2 XRD

Single crystal X-ray diffraction determines the structure of molecules by employing electron density maps. A crystal is bombarded with X-rays producing diffraction patterns. The diffraction patterns reflect an electron density which is used in elucidating the structure of the crystalline compound. This type of technique shows the connectivity of the atoms in space so that the stereochemistry can be determined. It also gives bond distances between atoms as well as bond angles [20, 21].

Crystals that were analyzed were grown by two methods, slow vapour diffusion of diethyl ether into saturated dichloromethane and by slow evaporation [22].

3.2.2.1 Crystal Structures

The data was collected on a Bruker Smart APEXII diffractometer with Mo k α radiation ($\lambda = 0.71073 \text{ \AA}$). Reflections were successfully indexed by an automated indexing routine built in the APEXII programme suite (Bruker, 2008). The data collection method involved ω scans of width 0.5° . Data reduction was carried out using the programme SAINT + (Bruker, 2008). The structure was solved by direct methods using SHELXS (Sheldrick, 2008) and refined (Bruker, 2008). All hydrogen atoms were positioned geometrically and were refined isotropically.

X-ray quality crystals were grown of ligand **2.3**, complexes **2.12** and **2.17**. Ligand **2.3** is an analogue of **2.2** with the only difference being the methyl group on the phenyl rings at the para-position. The crystal data and structure refinement is shown in Table 3.10.

Table 3.10: Crystallographic and structure refinement data for ligand **2.3**, complexes **2.12** and **2.17**.

	Ligand 2.3	Complex 2.12	Complex 2.17
Empirical formula	C ₄₃ H ₄₀ OP ₂	C ₄₃ H ₄₀ Cl ₂ CoOP ₂	C ₄₃ H ₄₀ Cl ₂ NiOP ₂
Formula weight	634.69	764.52	764.30
Temperature	173(2)K	173(2)K	173(2)K
Wavelength	0.71073 Å	0.71073 Å	0.71073 Å
Crystal system	Triclinic	Triclinic	Triclinic
Space group	P-1	P-1	P-1
Unit cell dimensions	a = 9.8811(6) Å,	a = 10.2166(3) Å	a = 10.2501(3) Å
	b = 9.9770(6) Å	b = 11.0261(3) Å	b = 11.1611(3) Å
	c = 18.3504(11) Å	c = 17.6982(5) Å	c = 17.7687(5) Å
	α = 97.650(3) Å	α = 74.7610(10) Å	α = 73.9650(10) Å
	β = 96.262(2) Å	β = 86.7170(10) Å	β = 86.322(2) Å
	γ = 94.637(2) Å	γ = 83.0110(10) Å	γ = 83.512(2) Å
Volume	1773.88(19) Å ³	1908.63(9) Å ³	1940.03(10) Å ³
Z	2	2	2
Density (calculated)	1.188 Mg/m ³	1.330 Mg/m ³	1.308 Mg/m ³
Absorption coefficient	0.155mm ⁻¹	0.706 mm ⁻¹	0.752 mm ⁻¹
F(000)	672	794	796
Crystal size	0.48 x 0.23 x 0.13 mm ³	0.25 x 0.24 x 0.12 mm ³	0.586 x 0.529 x 0.382 mm ³
The range for data collection	2.07 to 25.00°	1.19 to 28.00°	1.193 to 28.393°
Index ranges	-11 ≤ h ≤ 11,	-13 ≤ h ≤ 13	-13 ≤ h ≤ 12,
	-11 ≤ k ≤ 11	-14 ≤ k ≤ 14	-14 ≤ k ≤ 14,
	-21 ≤ l ≤ 21	-23 ≤ l ≤ 23	-23 ≤ l ≤ 23
Reflections collected	25830	54347	58526
Completeness to theta = 25.242	96.8%	98.2%	100.0%

Final R indices	R1 = 0.0349, wR2 =	R1 = 0.0488, wR2 =	R1 = 0.0327, wR2 =
[I>2sigma(I)]	0.0904	0.1178	0.0786
R indices (all data)	R1 = 0.0398, wR2 =	R1 = 0.0563, wR2 =	R1 = 0.0512, wR2 =
	0.0938	0.1225	0.0878

An ORTEP representation of ligand **2.3** is shown in Figure 3.6. The colourless single crystal of ligand **2.3** crystalized in the triclinic crystal system. Ligand **2.3** is symmetric in structure just like its analogue **2.2**. It has a twofold rotation axis dissecting the structure through the dimethyl bearing carbon (C21) and the oxygen atom (O1) into half. It shows the two phosphorus donor atoms as well as the oxygen atom. The orientation of the ORTEP diagram of the ligand shows that the backbone of the ligand **2.3** is not planar due to the stacking interaction between the phenyl rings of the diphenylphosphine which makes it dihedral angle between the two phenyl rings to be 166.12 °. This effect is also observed on the analogue **2.2** where its xanthene backbone is also not planar with a dihedral angle of 166 °. Xanthene backbone that are planar like that of xantham (4,5-(bis-(di(4-diethylaminomethylphenyl)phosphino)-9,9-dimethylxanthene) have a dihedral angle of 175.6 °. The bond lengths P1-C1, P1-C8, P2-C37 and P2-C30, which holds the tolyl groups are all at similar distance of about 1.84 Å to that of its analogue **2.2** which is 1.83 Å. The angles between the sets of phenyl rings are very close showing that the ligand is symmetric in its structure with C8—P1—C1 101.56 ° and C37—P2—C30 101.09 ° matching those of its analogue **2.2** which were 101.2 °. Addition of the methyl groups to the phenyl rings was seen to have minor effect, as the bond lengths changed slightly in comparison to its analogue ligand **2.2**. Table 3.11 shows selected bond lengths as well as the bond angles of ligand **2.3**.

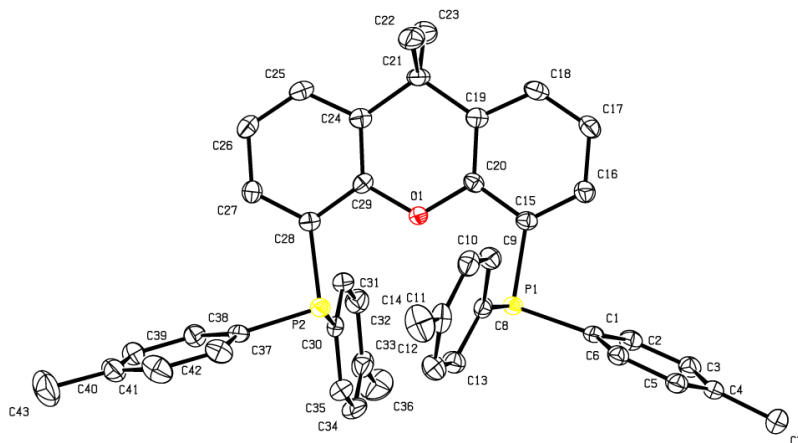


Figure 3.6: ORTEP diagram of ligand **2.3** showing the atom numbering scheme. Thermal ellipsoids are represented at the 50% probability levels.

Table 3.11: Selected bond lengths and bond angles of ligand **2.3**.

Bond Lengths	[Å and °]
P1—C1	1.8413(16)
P1—C8	1.8395(16)
P2—C37	1.8351(16)
P2—C30	1.8390(17)
P2—C28	1.8464(16)
P1—C15	1.8402(16)
P1—P2	4.168
Bond Angles	
C8—P1—C1	101.56(7)

The ORTEP diagram of the crystal structure of a blue crystal of complex **2.12** grown by slow diffusion is shown in Figure 3.7. Table 3.12 shows the selected bond lengths and bond angles of complex **2.12** and **2.17**. Complex **2.12** crystallized in a triclinic crystal system and collected at 173 K. The structure of **2.12** shows a tetrahedral geometry around the Co ion in a highly symmetrical molecular unit. The structure of ligand **2.3** shows that only little adjustment is required to form a chelate. The P-P distance in the free ligand **2.3** is 4.168 Å, while in a chelation with a P-Co-P (**2.12**) it P-P distance is 3.973 Å. The P atoms are brought together by means of a decrease of the angle between the phenyl planes in the backbone of the ligand **2.3** from 4.168 to 3.973 Å. The angles between the two sets of phenyl rings (C37—P1—C30) and (C16—P2—C23) are found to be similar with an angle of 105.94°. The P1—Co—P2 angle is found to be 111.76°. To complete the tetrahedral geometry, the other two sites are occupied by two chlorides with a Cl—Co—Cl angle of 117.98°. These show some distortion, as the angle is greater than 109° for a perfect tetrahedron, however, this is due to the lone-pair repulsion between the chlorine atoms [23]. The molecular structure also shows that the xanthene-based ligand is bound to the cobalt in a bidentate fashion via the phosphorus donor atoms. An analogue of this ligand, xantphos **2.2**, has showed that these xanthene – based ligands can be pincers by using the central oxygen to also bind to a metal [3]. This is explained by the flexibility range which is calculated to be between 97 and 133°. A number of studies have reported xanthene-based ligands of the xantphos type to behave as pincer ligands. The natural bite angle of xantphos has been determined as 111° [3]. There are other factors that also contribute towards the geometry of the **2.2** ligand, bearing in mind a knowledge that the bite angle preferred by the metal, is as a result of electronic effects. Therefore, parameters such as the type of ligands surrounding the metal complex, the charge and the type of metal play a role in determining whether the ligand will act as a bidentate or a pincer type ligand [24, 25]. An example, where **2.2** was reported as a pincer ligand, is the complex [Rh(xantphos)(COMe)I₂] [26].

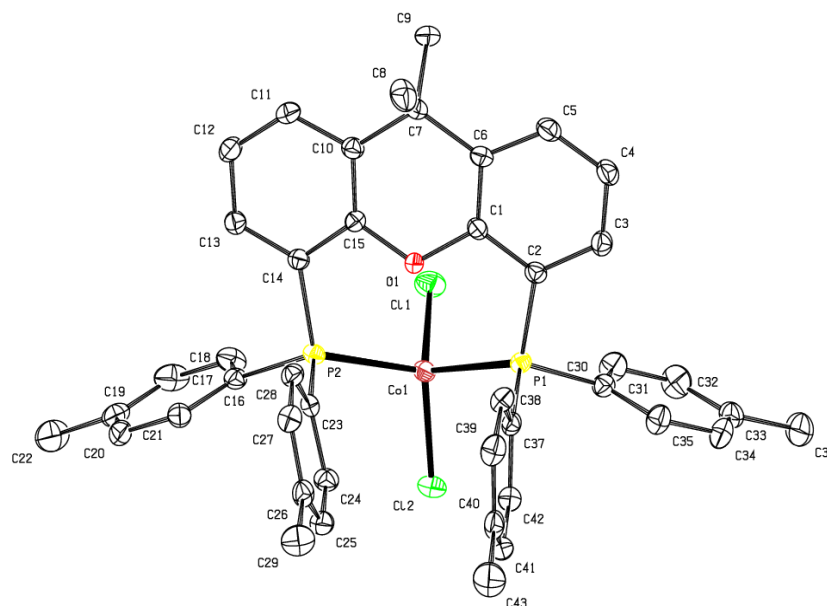


Figure 3.7: ORTEP diagram of complex **2.12** showing the atom numbering scheme. Thermal ellipsoids are represented at the 50% probability levels.

An ORTEP diagram of the emerald green complex **2.17** is shown in Figure 3.8. The complex crystallized in a triclinic crystal system. The data was collected at 173 K. Tetrahedral geometry around Ni ion is observed with a highly symmetrical molecular unit. Bond lengths P1-C30, P1-C37, P2-C16, P2-C23 and P2-C9, which holds the tolyl groups remained the same at about 1.81 Å even after complexation had taken place. The bite angle, which is represented by P(1)—Ni—P(2), was found to be 108.40 ° and to complete the tetrahedral geometry the other two sites are occupied by the two chloride ions with a Cl-Ni-Cl angle of 128.87 °. It was observed that the chlorides are distorted due to the lone pair repulsion between the two chlorine atoms. The structure also shows that the xanthene-based ligand is coordinated to the nickel in a bidentate fashion via the two phosphorus donor atoms [26].

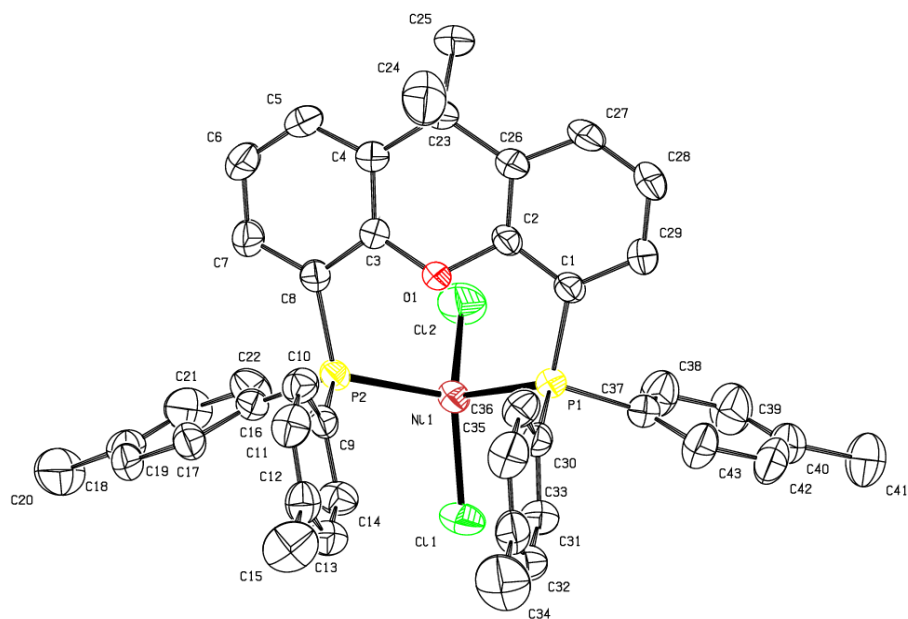


Figure 3.8: ORTEP diagram of complex **2.17** showing the atom numbering scheme. Thermal ellipsoids are represented at the 50% probability levels.

Table 3.12: Selected bond lengths and bond angles for complex **2.12** and **2.17**.

Bond lengths	Complex 2.12/ [Å and °]	Complex 2.17/ [Å and °]
P1-C30	1.813(3)	1.8109(18)
P1-C37	1.805(3)	1.8191(18)
P2-C16	1.816(3)	1.8193(17)
P2-C23 / C9	1.808(3)	1.8091(18)
P1—Ni / Co	2.3940(7)	2.3398(5)
P2—Ni / Co	2.4050(8)	2.3469(5)
Cl(1)—Ni / Co	2.2213(8)	2.2048(5)
Cl(2)—Ni / Co	2.2248(7)	2.1964(6)
Bond Angles		
Cl(2)—Ni/Co—Cl(1)	117.98(3)	128.87(3)
P(1)—Ni/Co—P(2)	111.76(3)	108.403(18)
Cl(2)—Ni/Co—P(1)	101.69(3)	108.62(2)
Cl(1)—Ni/Co—P(1)	110.89(3)	99.58(2)
Cl(2)—Ni/Co—P(2)	108.75(3)	102.95(2)
Cl(1)—Ni/Co—P(2)	105.87(3)	107.39(2)

3.3 Summary

The preparation of five cobalt and five nickel complexes with xanthene-based ligands was achieved. Due to their paramagnetic nature, NMR was found to be unsuitable for structural characterization. However, they were characterized by elemental analysis, IR, melting point and single crystal X-ray diffraction.

3.4 References

- [1] S. Hillebrand, B. Bartkowska, J. Bruckmann, C. Kruger and M.W. Haenel, *Tetrahedron Letters*, 39 (1998) 813.
- [2] T. Marimuthu, M.D. Bala and H.B. Friedrich, *Journal of Chemical Crystallography*, 42 (2012) 251.
- [3] M. Kranenburg, Y.E.M. Vanderburgt, P.C.J. Kamer, P. Vanleeuwen, K. Goubitz and J. Fraanje, *Organometallics*, 14 (1995) 3081.
- [4] R.P.J. Bronger, J.P. Bermon, J. Herwig, P.C.J. Kamer and P.W.N.M. van leeuwen, *Advanced Synthesis & Catalysis*, 346 (2004) 789.
- [5] J. Clayden, N. Greeves, S. Warren and P. Wothers, *Organic Chemistry*, Oxford University Press, USA, 2001.
- [6] T. Marimuthu, *The Preparation and Novel Application of Diphosphorous Xanthenes Family Ligands in Homogenous Catalysis*, Vol. PhD Thesis, University of KwaZulu Natal, 2011, p. 74.
- [7] I.S. Koo, D. Ali, K. Yang, Y. Park, D.M. Wardlaw and E. Buncell, *Bulletin of the Korean Chemical Society*, 29 (2008) 2252.
- [8] L.D. Quin and A.J. Williams, *Practical Interpretation of 31P-NMR Spectra and Computer Assisted Structure Verification*, Advanced Chemistry Development Toronto, Canada, 2004.
- [9] J. Coates, *Interpretation of Infrared Spectra, A Practical Approach* in R.A. Meyers (Editor), *Encyclopedia of Analytical Chemistry*, John Wiley and Sons Ltd, Chichester, 2000, p. 10815
- [10] K. Nakamoto, *Infrared and Raman Spectra of Inorganic and Coordination Compounds*, 4th Edition, A Wiley - Interscience publication, Canada, 1986.
- [11] K. Nakanishi and P.H. Solomon, *Infrared Absorption Spectroscopy*, 2nd Edition, Holden-Day, San Francisco, 1977.
- [12] M.S.C. Flett, *Characteristic Frequencies of Chemical Groups in the Infra-Red*, Elsevier Publishing Company, Amsterdam/ London/ New York, 1963.
- [13] M.A. Esteruelas, M. Oliván and A. Velez, *Inorganic Chemistry*, (2013) A.
- [14] J.A.S. Bomfim, F.P. de Souza, C.A.L. Filgueiras, A.G. de Sousa and M.T.P. Gambardella, *Polyhedron*, 22 (2003) 1567.

- [15] M.A. Kirillova, M.V. Kirillova, L.S. Shul'pina, P.J. Figiel, K.R. Gruenwald, M.F.C.G. da Silva, M. Haukka, A.J.L. Pombeiro and G.B. Shul'pin, *Journal of Molecular Catalysis A: Chemical*, 350 (2011) 26.
- [16] C. Ehrhardt, M. Gjikaj and W. Brockner, *Thermochimica Acta*, 432 (2005) 36.
- [17] Y. Mulyana, K.G. Alley, K.M. Davies, B.F. Abrahams, B. Moubaraki, K.S. Murray and C. Boskovic, *Dalton Transactions*, (2014).
- [18] J. Atkins, T. Overton, J. Rourke, M. Weller and F. Armstrong, *Shriver & Atkins Inorganic Chemistry*, Oxford University Press, USA & Canada, 2006.
- [19] A.R. Katritzky, R. Jain, A. Lomaka, R. Petrukhin, U. Maran and M. Karelson, *Perspective on the Relationship Between Melting Points and Chemical Structure*, University of Florida 2001.
- [20] J.P. Glusker, *Accounts of Chemical Research*, 15 (1982) 231.
- [21] R.J. Read, *Overview of Macromolecular X-Ray Crystallography*, 22 April 2008 ed., University of Cambridge, 2008.
- [22] D.V. Partyka, J.B. Updegraff III, M. Zeller, A.D. Hunter and T.G. Gray, *Dalton Transactions*, 39 (2010) 5388.
- [23] W. Goertz, W. Keim, D. Vogt, U. Englert, M.D.K. Boele, L.A. van der Veen, P.C.J. Kamer and P.W.N.M. van Leeuwen, *Dalton Transactions*, (1998) 2981.
- [24] A.E.W. Ledger, *Chelating Phosphine Complexes of Ruthenium for the Coordination and Activation of Small Molecules*, PhD Thesis, University of Bath, 2011.
- [25] P.C.J. Kamer, P.W.N. van Leeuwen and J.N.H. Reek, *Accounts of Chemical Research*, 34 (2001) 895.
- [26] G.L. Williams, C.M. Parks, C.R. Smith, H. Adams, A. Haynes, A.J.H.M. Meijer, G.J. Sunley and S. Gaemers, *Organometallics*, 30 (2011) 6166.

Chapter 4

Oxidation of Alkanes

4.1 Introduction

The rapid development of the synthetic chemistry of metal-complexes serve to initiate the catalysis of saturated hydrocarbons [1]. A proper selection of metal-complexes, oxidants and reaction conditions can lead to the efficient oxidative transformation of alkanes [2-4]. The activation of C-H bonds by metal complexes is divided into three different types, based on the reaction mechanism. This classification of reaction mechanism is premised on the way in which the substrate (alkane) interacts with a metal complex [4]. The three types of processes are:

1. "True" organometallic activation.

It is referred to as a first type process and it involves a contact between the metal ion and the C-H bond. A C-H compound enters the coordination sphere of the metal complex in the form of an organyl σ -ligand. This is referred to as the preactivation of the compound's C-H bond [4, 5].

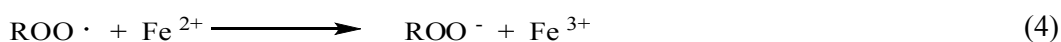
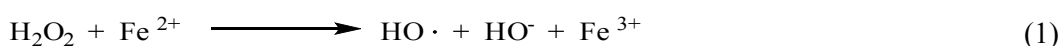
2. Interaction of a complex with a C-H bond via the ligand only.

This type of reaction has an interaction between a metal complex and a C-H bond through a complex ligand via the process called C-H bond cleavage. In this case a σ -C-M interaction does not occur. The function of the metal complex is to abstract an electron or hydrogen from the hydrocarbon, RH. The abstraction of the hydrogen or electron results in the formation of a radical ion or radicals which then interact with any species in solution such as molecular oxygen. Ligands of the metal complexes can serve as the species that abstract electrons or hydrogen from the hydrocarbons. In the following example, an oxo complex of a high valent metal is responsible for abstraction of the hydrogen or electron of the hydrocarbon [4].

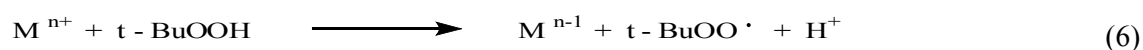


3. A metal complex generates an independent reactive species which then attacks the C-H bond.

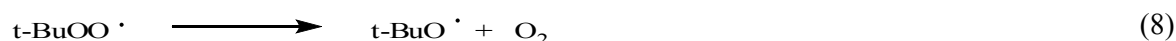
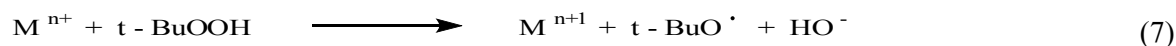
In the third type process, a metal complex activates reactants such as oxidants which form reactive species, such as hydroxyl radicals, which then attack the hydrocarbons. Oxidation of alkanes by Fenton's reagent is a good example of this mechanistic pathway (1-5) [6]:



In a case where TBHP is used as the oxidant, two radicals are formed, $t\text{-BuOO}\cdot$ and $t\text{-BuO}\cdot$. Whereas the former does not have sufficient strength to abstract a hydrogen atom from a hydrocarbon, the latter does have. Therefore, the first step involves the reduction of the metal by TBHP forming a $t\text{-BuOO}\cdot$ radical as shown in the following equation 6 [7]:



Oxidation of alkanes by TBHP occurs by the participation of the $t\text{-BuO}\cdot$ radical and proceeds as shown in equations 2-5. The reactive radical $t\text{-BuO}\cdot$ is formed when the low valent metal reacts with the second molecule of TBHP, (equation 7) or when it decomposes as in equation 8 [7, 8].



The substrate of choice in this study is *n*-octane since it serves as a model of medium chain length alkanes. Three oxidants were used, *tert*-butyl hydroperoxide (TBHP), hydrogen peroxide (H_2O_2) and *meta*-chloroperbenzoic acid.

4.2 Instrumentation

Analysis of catalytic reactions was done using a Perkin-Elmer Auto System gas chromatograph fitted with a Flame Ionization Detector (FID). GC parameters and column specifications are depicted in Table 4.1. Each GC run was conducted over a duration of 43 minutes excluding the oven cooling time. The GC was calibrated with the multicomponent standards (Appendix B, Table 2) of the expected products and the respective RF values were calculated.

Table 4.1: GC parameters and column specifications.

Column	Pona x 50 m x 0.20 mm x 0.5 μ m
Injector temperature	240 °C
Detector temperature	260 °C
Split	On flow rate: 123 ml/min
Attenuation	1
Range	1
Oven Programme	
Initial temperature	50 °C
Ramp 1	1 °/min
Temperature 2	80 °C
Ramp 2	15 °/min
Temperature 3	200 °C

4.3 General Procedure

Synthesis of ligands **2.2**, **2.3**, **2.6**, **2.9** and complexes **2.11** – **2.20** was discussed in detail in Chapter 2. All catalytic testing was done under inert atmosphere in a presence of argon in a 50 ml pear shape flask that had a condenser attached and a tap mounted with an argon balloon. In the pear shape flask the reaction mixture contained 10 ml of degassed THF, the respective oxidant, *n*-octane and 3 mg of the respective catalyst. The reaction mixture was stirred in an oil bath at the respective temperature and after 48 h an aliquot was taken using a glass pasteur pipette. A volume of 0.5 μ l was then injected into a GC using a GC syringe for analysis and quantification.

4.4 Optimization

The oxidation studies of *n*-octane were carried out using tetrahydrofuran (THF) as the solvent, since it was the only solvent that all complexes were soluble in. To choose the optimum conditions for our catalysis part a study was conducted using THF as the solvent at different temperatures (RT, 40, 50 and 60 °C). The oxidants used were TBHP, *m*-CPBA and H₂O₂ with pentanoic acid as the internal standard and *n*-octane as the substrate. The substrate to oxidant ratio was varied (1:2.5, 1:5, 1:7.5 and 1:10) to obtain the optimum ratio for conversion and selectivity. Catalyst to substrate ratio was kept at constant at 1:100. The catalyst used for optimization was the most stable and abundant no specific criteria was used. Each temperature (RT, 40, 50 and 60 °C) was tested on different oxidants (TBHP, *m*-CPBA and H₂O₂) different ratios (1:2.5, 1:5, 1:7.5 and 1:10) with pentanoic acid as the internal standard and *n*-octane as the substrate. At room temperature (RT) and 40 °C no activity was observed even after using different oxidants at different ratios for 48 h. Activity started to appear at 50 and 60 °C, TBHP was the only active oxidant at the ratios of 1:7.5 and 1:10.

Three blanks were run. The first blank contained all the other reagents (*n*-octane, pentanoic acid, TBHP, and THF) and no catalyst. This blank was run to check if no catalyst was present, would there be any other reagents that can activate the reaction. The second blank contained everything except TBHP. This was done to check if the catalyst has the strength to activate the reaction in the absence of the oxidant. The third blank contained everything except *n*-octane. Lastly this blank was run to check if there are any other reagents that can resemble the substrate. After running these blanks no activity was observed on all of them. This therefore showed that for a catalyst to be able to activate some reaction it required some oxidant to kick start the reaction as well as some heat. The activity started to appear from 50 and 60 °C.

4.4.1 Optimization results for cobalt and nickel catalysts

The 1:10 substrate to oxidant ratio gave the highest conversion of 8% conversion after 48 h with a 100% selectivity to 2-octanone. A substrate to oxidant ratio of 1:7.5 gave a conversion of 6% with also 100% selectivity to 2-octanone. The results on activity and selectivity at different substrate to oxidant ratios are shown in Figures 4.1 and 4.2. It was noted that there was no trace of 2-octanol for both ratios, but instead the product formed was 2-octanone, which is the product

of the over-oxidation of 2-octanol. The 2-octanol is more reactive than the substrate (octane) and over-oxidation is more prevalent, hence the formation of 2-octanone [3, 4, 6, 9].

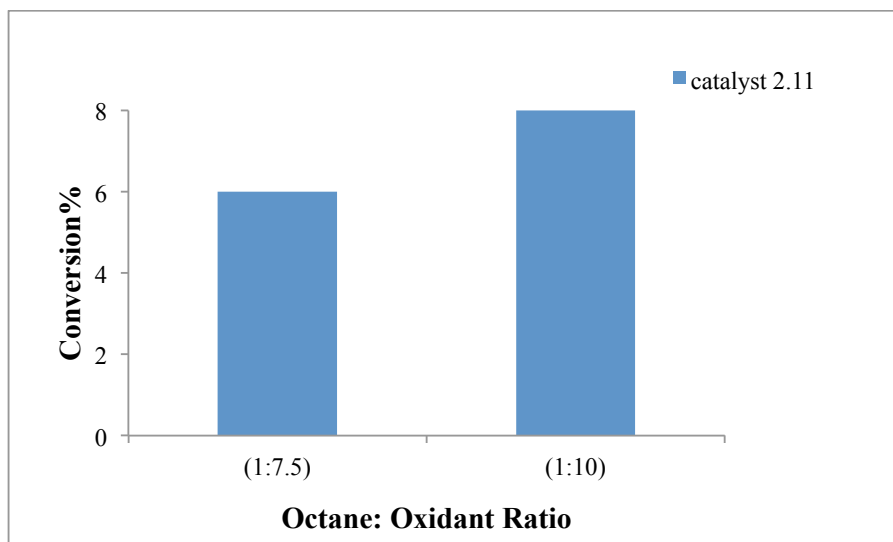


Figure 4.1: Conversion on *n*-octane over the blank reaction and over the catalysts at different substrate to oxidant ratios.

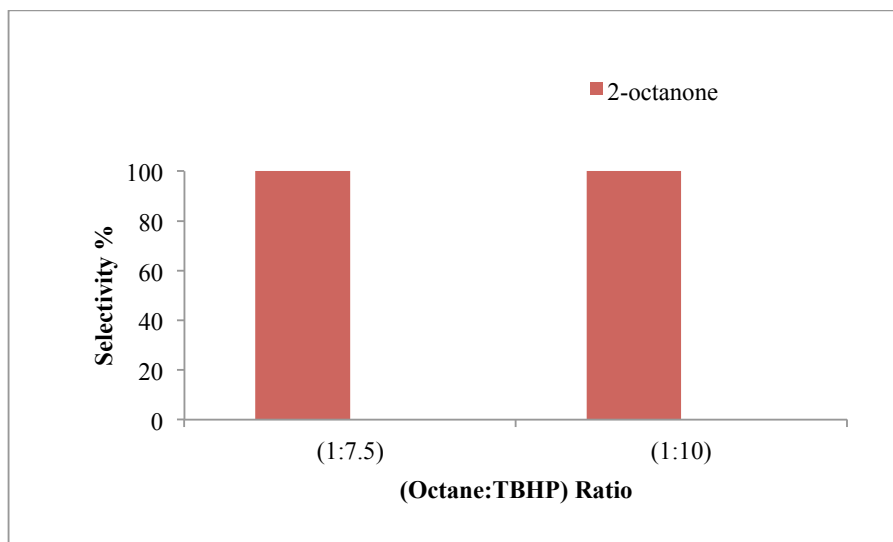


Figure 4.2: Selectivities at two substrate to oxidant ratios over catalyst **2.11**.

To establish optimum conditions for nickel based catalysts, catalyst **2.16** was used for 48 h at substrate to oxidant ratios (1:7.5 & 1:10) at 50 °C. The optimization study using catalyst **2.16** showed that the 1:10 ratio gave a conversion of 6% and it was decided to work with this ratio as this was used for the cobalt catalysts.

4.4.2 Oxidation of *n*-octane in the presence of H₂O₂ as the oxidant

In further study of *n*-octane activation, hydrogen peroxide was used as an oxidant, since it is the most widely used oxidant in hydrocarbon activation. This is due to its accessibility and the fact that it produces water as the by-product, means it is environmentally friendly [10].

Blank reactions (no catalyst) were carried out at 50 °C in THF as the solvent. No conversion was observed at the following substrate to oxidant ratios (1:7.5 and 1:10). Using the cobalt and nickel catalysts, only trace amounts of oxidized products were observed showing that the cobalt and nickel catalysts were inactive with H₂O₂ as the oxidant.

4.4.3 Oxidation of *n*-octane in the presence of *m*-CPBA as the oxidant

meta-chloroperbenzoic acid (*m*-CPBA) is a strong oxidizing agent, normally used in the oxidation of epoxides, hence it was also investigated as a potential oxidant for *n*-octane activation. An optimization study was carried out at 50 °C to determine if any thermal initiated oxidation may occur. Using the substrate to oxidant ratios of 1:7.5 and 1:10 no activity was observed with either the Co or Ni based systems.

4.5 Results & Discussion

4.5.1 Efficiency of the cobalt based catalyst using TBHP as oxidant at 50 °C

Table 4.2: Optimization conditions used for catalysis.

Solvent	THF
Temperature/ °C	50/ 60
Substrate	<i>n</i> -octane
Oxidant	TBHP
Internal standard	Pentanoic acid
Substrate to oxidant ratio	1:10
Catalyst to substrate	1:100
Reaction duration	48 h
Replication	triplicate

The blank reaction (no catalyst) gave no conversion but, all catalysts were active except for catalyst **2.14** as observed (Figure 4.3), which showed no activity and this can only be attributed to the sulphur atom in its ligand structure . Looking at the conversions, all the other catalysts behaved similarly, catalyst **2.11** gave a conversion of 8%, **2.12** - 9%, **2.13** - 7% and **2.15** - 8%. This activity trend can be expected as their structure differs only slightly, therefore one expects minor changes in their activity or no change in activity at all. Therefore, as much as their bite angle size changed, this had a minor impact on activity.

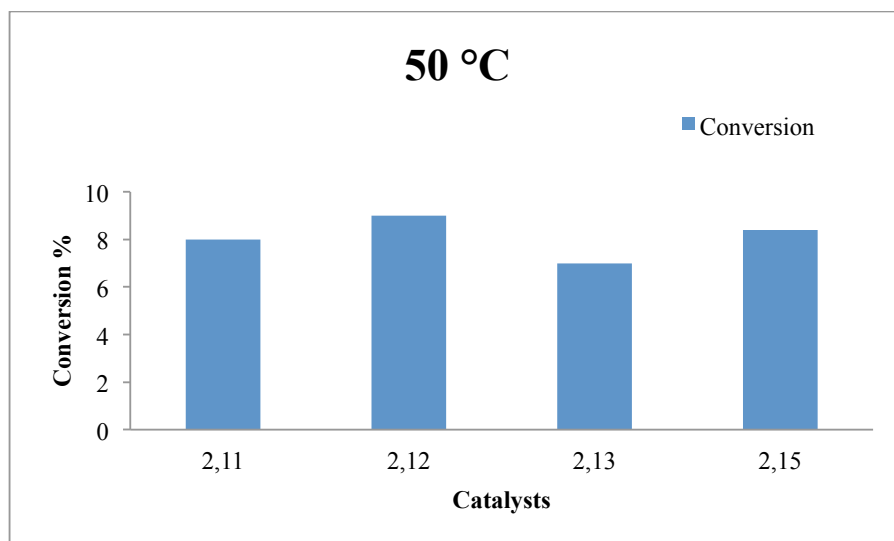
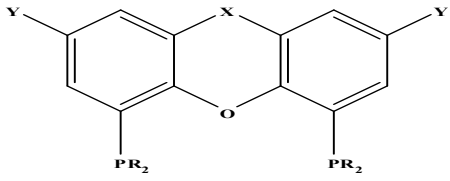


Figure 4.3: Conversion of *n*-octane over the cobalt catalysts at 50 °C.

All catalysts structure are based on the same structure. This structure comprises of various groups at position X (see Table 4.3) with changes made to this position expected to affect their activity as these have an impact on their bite angles [11-13]. Even catalyst **2.14** which has a strong donor atom, sulphur, gave no conversion.

It has been noted that through the changes in electronic effects due to changes at position X of the ligand backbone, small variations to the bite angle occur which normally have an effect on the activity of the catalyst as seen in hydroformylation and hydrocyanation reactions. In this study at RT the change of bite angle did not have any effect on activity [12, 14-16]. Table 4.3 shows the different bite angles of the ligands.

Table 4.3: Natural bite angle of ligands [10, 16]

				
Ligand	X	Y	R	Bite angle [β n]
2.2	C(Me) ₂	H	Ph	111.4
2.3	C(Me) ₂	H	p-tolyl	111.7
2.6	C(Me) ₂	(CH ₂) ₅ Me	Ph	116.0
2.7	S	CH ₃	Ph	109.6
2.10	C=C(Me) ₂	H	Ph	113.2

Ligands **2.2**, **2.7** and **2.10** are similar with the only difference being the group at position X, and they have different bite angles. Substitution of the phenyl substituent by a tolyl group, which is another electron donating group, on catalyst **2.12** also gave no activity at RT. This shows that the structure of the complexes played no part at this temperature, rather that activation energy was required for the reaction to proceed.

Since there was no activity with TBHP at RT, another oxidant was investigated, namely *m*-CPBA, but it also gave no substantial conversion. Thus, while at RT no activity was observed for all catalysts, when the temperature was increased some activity was observed, which clearly points out the importance of activation energy.

Figure 4.4 reveals that catalysts show high selectivity to the formation of 2-octanone. At this temperature one starts to see the formation of 4-octanol as well. Higher temperature means higher activation energy, and therefore the reactive 2-octanol reacts further forming products of over-oxidation. At this temperature one also starts to see the activation of C-4, as catalyst **2.15** forms 4-octanol.

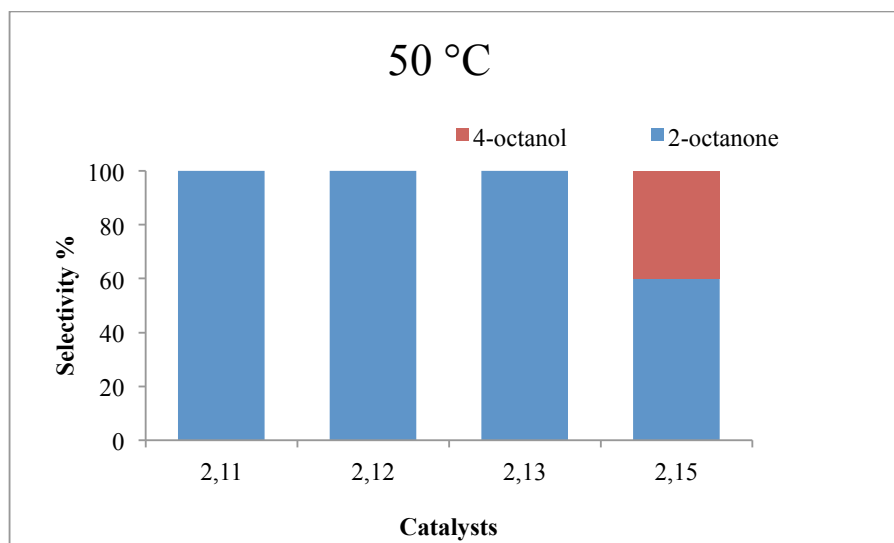


Figure 4.4: Selectivity to products over the cobalt catalysts at 50 °C.

The regioselectivity on Table 4.4 shows that all catalysts were selective to the ketone at position C-2. Catalyst **2.15** shows the activation of C-4 by forming an alcohol.

Table 4.4: Regioselectivity of cobalt catalysts (**2.11-2.15**)^a at 50 °C.

Catalysts	Alcohols ^b	Ketones ^b	Total ^c
	C3: C4	C2: C3: C4	C2: C3: C4
2.11	0	1: 0: 0	1: 0: 0
2.12	0	1: 0: 0	1: 0: 0
2.13	0	1: 0: 0	1: 0: 0
2.15	0: 1	1: 0: 0	2: 0: 1

^a Regioselectivity Parameter C2: C3: C4 is the relative reactivities of hydrogen atoms at carbon 2, 3 and 4 of the *n*-octane chain.

^b The calculated reactivities from % selectivity are normalized, this takes into account the number of hydrogen atoms at each carbon (Appendix B).

^c The % selectivity of all products were taken into account i.e. alcohols, ketones.

4.5.2 Catalyst efficiency at 60 °C

At 60 °C the conversion of most catalysts dropped and some were not active at all. Catalysts **2.11**, **2.13** and **2.14** were not active (Figure 4.5). Therefore, at 60 °C the drop in activity of the catalysts could be ascribed to the decomposition of the catalyst at higher temperatures under an oxidizing environment. Another observation was the colour change of the reaction, which was initially pale blue but turned yellow after 48 h.

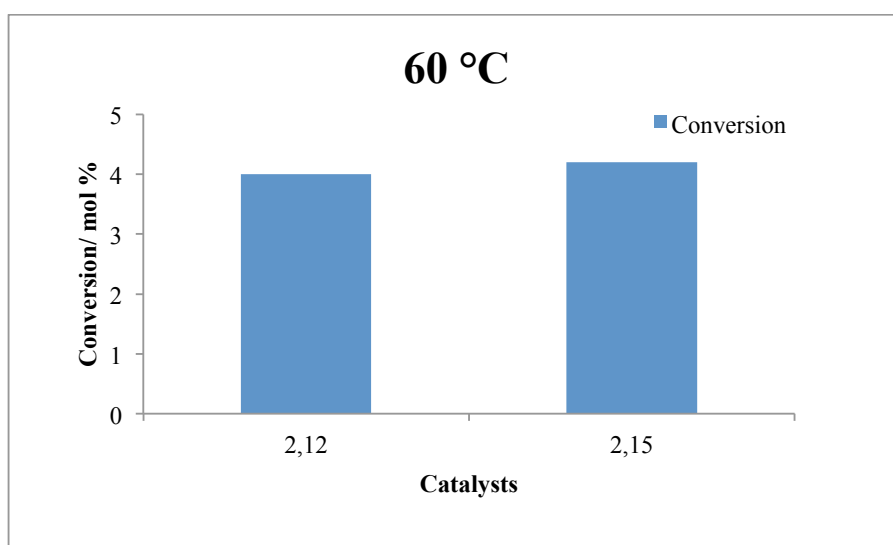


Figure 4.5: Conversion over the cobalt catalysts in the presence of TBHP at 60 °C.

For catalysts **2.12** and **2.15** at 60 °C, more products formed (Figure 4.6) although the conversion was lower, which shows that at higher temperature the formation of more products from C-2, C-3 and C-4 activation is favoured.

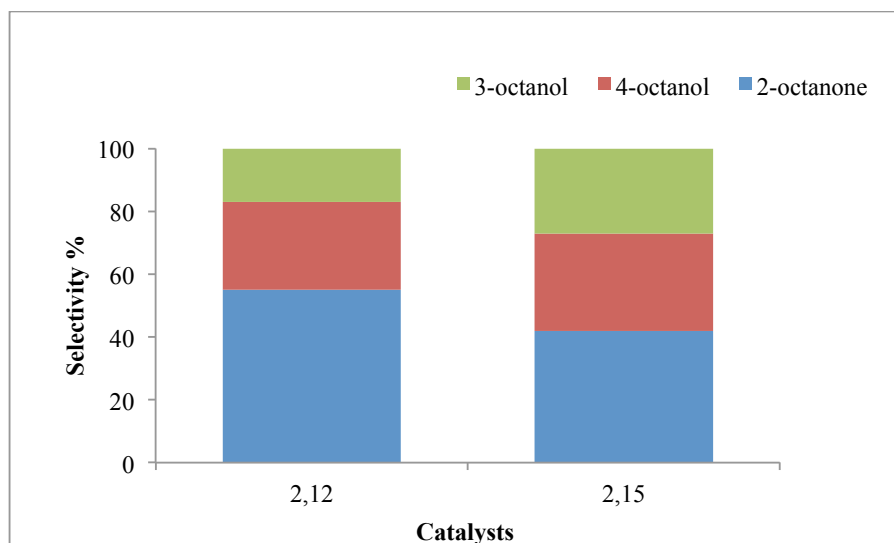


Figure 4.6: Selectivity over the cobalt catalysts in the presence of TBHP at 60 °C.

Table 4.5 Presents data on the regioselectivity parameter, to C-2, C-3 and C-4 at 60 °C.

Table 4.5: Regioselectivity of cobalt catalysts (**2.12**, **2.15**)^a at 60 °C.

Catalysts	Alcohols ^b	Ketones ^b	Total ^c
	C3: C4	C2: C3: C4	C2: C3: C4
2.12	1: 2	1: 0: 0	3: 1: 2
2.15	1: 1	1: 0: 0	2: 1: 1

^a Regioselectivity Parameters C2: C3: C4 are the relative reactivities of hydrogen atoms at carbons 2, 3 and 4 of the *n*-octane chain.

^b Calculated reactivities from % selectivity are normalized, this takes into account the number of hydrogen atoms at each *n*-octane carbon (Appendix B).

^c The % selectivity of all products were taken into account i.e. alcohols and ketones.

4.5.3 Efficiency of the nickel based catalysts using TBHP as the oxidant at 50 °C

The blank reaction (no catalyst) carried out at 50 °C showed no conversion, but most of the catalysts showed some level of activity at this temperature (Figure 4.7). Catalyst **2.19** with a heteroatom at position X, was the only one that showed no activity. Catalyst **2.16** showed a conversion of 6% and **2.18** showed 5% and they thus have similar activity. Catalyst **2.17** showed a higher conversion than all the other catalysts with a conversion of 9%. Comparatively, this was also the more active in the cobalt series, it showed the higher conversion of all the catalysts studied. Hence, from the ligand structure, it shows that substituting the phenyl substituent with a *p*-tolyl substituent had a positive effect. Therefore, the inductive effect brought in by the tolyl substituent had a positive effect on the activity.

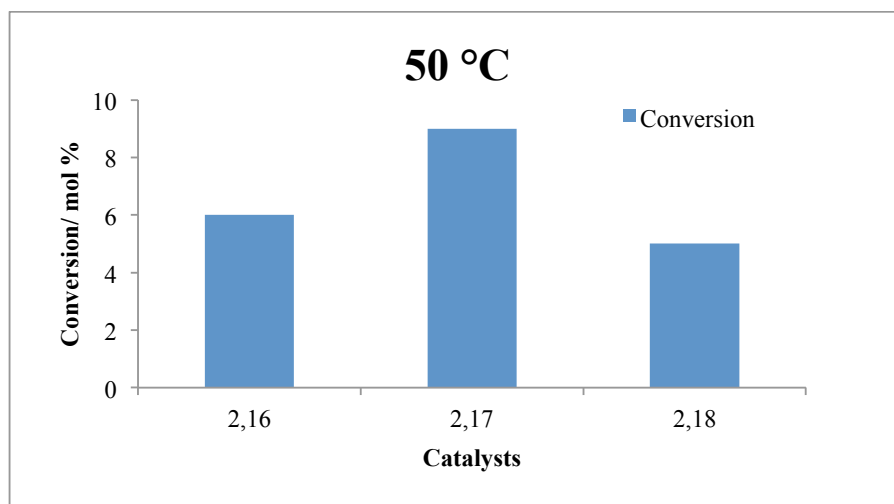


Figure 4.7: Nickel catalysts activity in the presence of TBHP as oxidant.

All catalysts showed C-2 position activation producing 2-octanone, with the most efficient being **2.17** and **2.18**, which gave 100% selectivity. Catalyst **2.16** also showed activation of the C-3 position (Figure 4.8).

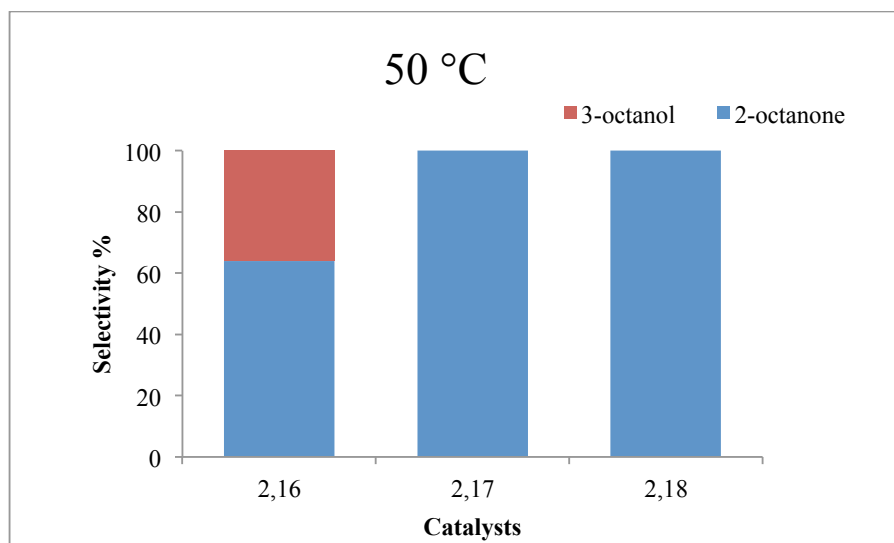


Figure 4.8: Selectivity over the nickel catalysts in the presence of TBHP as oxidant.

The selectivity was dominant to ketones and this may be due to the higher temperature.

Table 4.6: Selectivity parameters in *n*-octane activation by nickel catalysts (2.16-2.20)^a at 50 °C.

Catalysts	Alcohols ^b	Ketones ^b	Total ^c
	C3: C4	C2: C3: C4	C2: C3: C4
2.16	1: 0	1: 0: 0	2: 1: 0
2.17	0	1: 0: 0	1: 0: 0
2.18	0	1: 0: 0	1: 0: 0
2.19	0	0	0
2.20	0	0	0

^a Regioselectivity Parameter C2: C3: C4 is the relative reactivities of hydrogen atoms at carbon 2, 3 and 4 of the *n*-octane chain.

^b The calculated reactivities from % selectivity are normalized, this takes into account the number of hydrogen atoms at each carbon (Appendix B).

^c The % selectivity of all products were taken into account i.e. alcohols and ketones.

4.5.4 Catalyst efficiency at 60 °C

There was a major drop in the activity of all catalysts at 60 °C, with catalysts **2.18**, **2.19** and **2.20** being inactive (Figure 4.9). In terms of catalysts activity there is no particular trend to compare to the cobalt catalysts. With the cobalt series several catalysts were inactive as observed here with the nickel series but the related ones were **2.13**, **2.18** and **2.14**, **2.19** (similar ligand structure) exhibited similar trends. However, **2.16** and **2.17** showed low activities between 1-3% and as expected the blank reaction (no catalyst) gave no conversion.

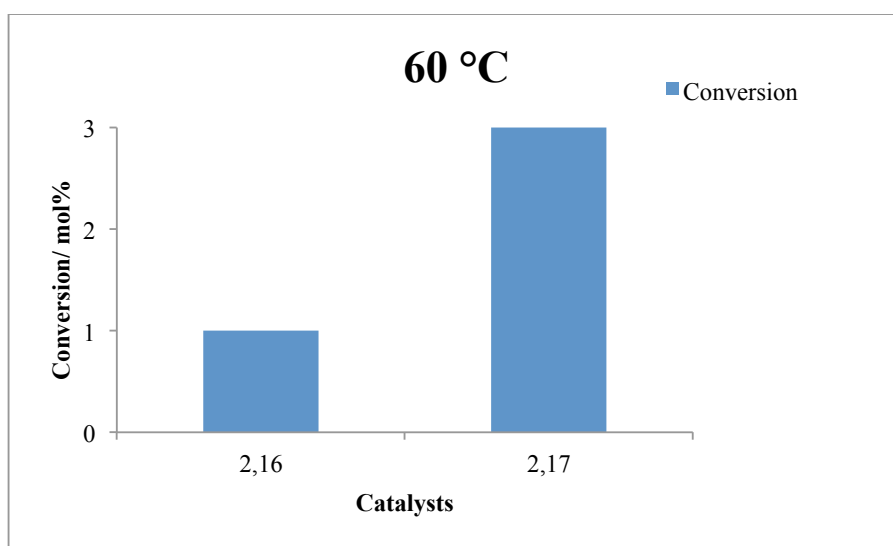


Figure 4.9: Conversion over the nickel catalysts in the presence of TBHP as oxidant.

Both cobalt and nickel catalyst series produced 2-octanone as the dominant product (Figure 4.10). Catalyst **2.19** was the only one that showed no activity at all temperatures. Formation of other products, such as 3-octanol and 4-octanol was observed with increased temperature (Figure 4.10). This trend was also observed with the cobalt catalysts. The regioselectivity observed for catalysts **2.16** and **2.17** is presented in Table 4.7. We can also conclude that sulphur at the X position deactivated the catalyst **2.14**.

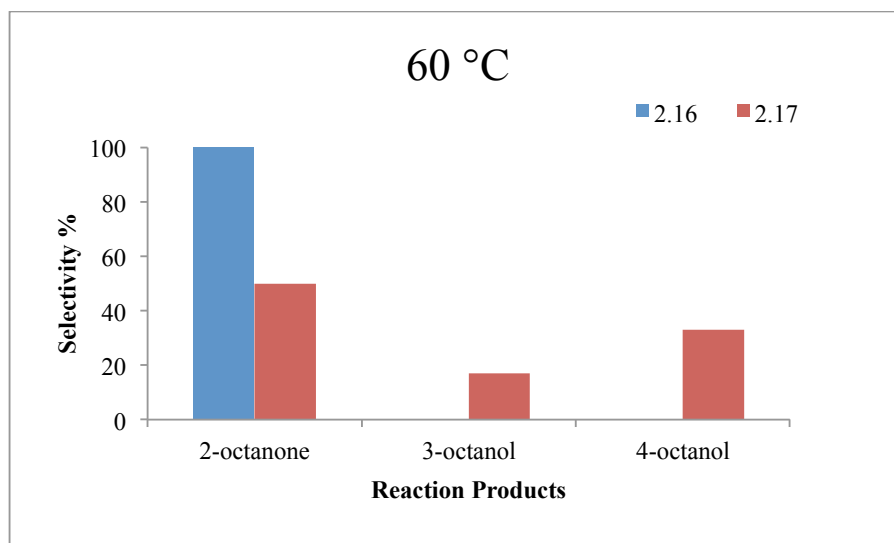


Figure 4.10: Selectivity of the nickel based catalysts in the presence of TBHP as oxidant.

Table 4.7: Selectivity parameters in *n*-octane activation by the nickel catalysts (2.16-2.20)^a at 60 °C.

Catalysts	Alcohols ^b	Ketones ^b	Total ^c
	C3: C4	C2: C3: C4	C2: C3: C4
2.16	0	1: 0: 0	1: 0: 0
2.17	1: 2	1: 0: 0	3: 1: 2
2.18	0	0	0
2.19	0	0	0
2.20	0	0	0

^a Parameters C2: C3: C4 are the relative reactivities of hydrogen atoms at carbons 2, 3 and 4 of the *n*-octane chain.

^b The calculated reactivities from % selectivity are normalized, this takes into account the number of hydrogen atoms at each carbon (Appendix B).

^c The % selectivity of all products were taken into account i.e. alcohols and ketones.

4.6 Effects of oxidant

A drastic change occurred in the conversion when the oxidant, TBHP, was added in smaller portions with catalysts **2.16**, **2.17** and **2.18**. The results obtained showed a major improvement in the conversions and the selectivity remained constant. This showed a vital role of oxidant in catalytic testing. The results are shown on Figure 4.11.

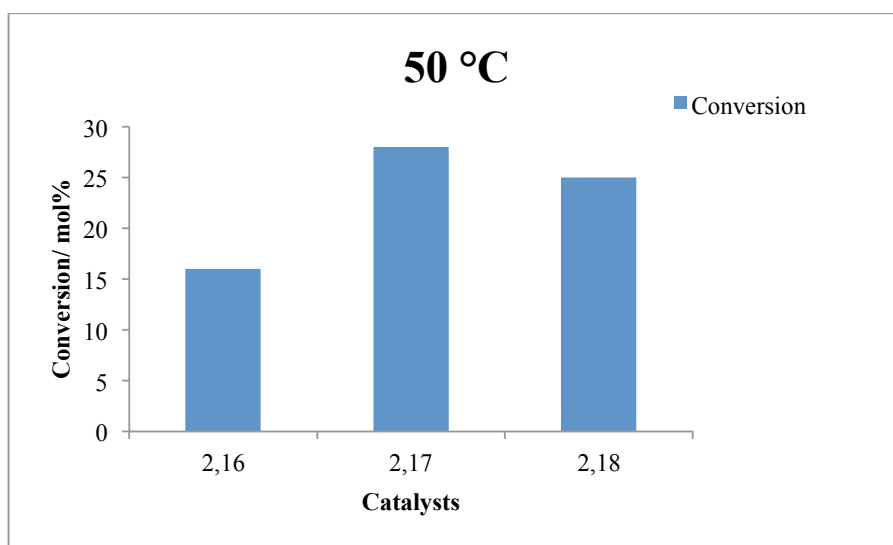


Figure 4.11: Conversion over the nickel catalysts (**2.16**, **2.17** and **2.18**) when TBHP was added slowly at the interval of 24 h.

It was also observed that TBHP is not a stable oxidant, as it was observed to break down into radicals at higher temperatures. This was seen when it was injected on a GC column, which showed many peaks. In the presence of a polar aprotic solvent, such as THF, the reactive radicals reacted with the solvent. Therefore this concludes that THF was not a good choice of solvent for this type of catalysis.

4.7 Catalyst Efficiency

Catalyst efficiency expressed in turn over numbers (TON) is presented in Table 4.8. At 50 °C using TBHP as an oxidant, the nickel catalysts were more efficient than the cobalt catalysts. This trend is at variance with that observed for cyclohexene oxidation using cobalt and nickel Schiff base complexes, where cobalt complexes showed a higher activity than nickel complexes

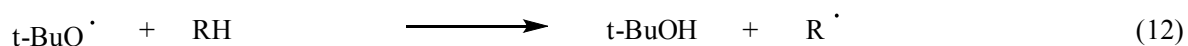
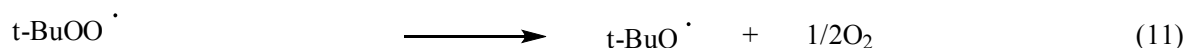
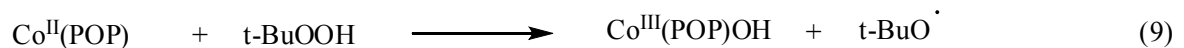
[17]. In a study by Nagataki et al. whereby Mn, Fe, Co, and Ni were used in the presence of *m*-CPBA as the oxidant on the hydroxylation of alkanes, it was discovered for the first time that nickel catalysts gave higher TON [18, 19]. Looking at the total efficiency of this study, both cobalt and nickel catalysts showed high selectivity towards 2-octanone.

Table 4.8: Turn over numbers of various catalysts at 50 and 60 °C.

Catalysts	TON ^a 50°C	TON ^a 60°C
2.11	4.2	0
2.12	5.1	3.3
2.13	4.0	0
2.15	4.7	4.8
2.16	5.3	0.8
2.17	7.2	1.7
2.18	4.6	0

^a TON = Moles of product (mol)/Moles of catalyst (mol).

The mechanism of the *n*-octane oxidation was considered in light of the high selectivity to C-2 and C-4. The lack of C-selectivity implies that the reaction proceeded through a free radical chain pathway as shown in Scheme 4.1. The reaction likely took place at the metal center, as Co^{II}(POP) was oxidized by *t*-BuOOH into Co^{III}(POP)OH and a *t*-BuO· radical (equation **9**). Then the Co^{III}(POP)(OH) reacted with another *t*-BuOOH to form a *t*-BuOO· radical, H₂O and Co^{II}(POP) (equation **10**). The *t*-BuOO· radical broke down into a *t*-BuO· radical and O₂, (equation **11**). The *t*-BuO· radical, which is more reactive, cleaved a hydrogen from the alkane forming *t*-BuOH and an R· radical (equation **12**). The R· radical combined with oxygen to form an ROO· radical (equation **13**). The ROO· radical can combine with a *t*-BuOO· radical forming the ketone (R=O) and *t*-BuOH (equation **14**). It can also abstract hydrogen from an alkane forming ROOH and an R· radical (equation **15**). The ROOH then reacts with Co^{II}(POP) to form an RO· radical and Co^{III}(POP) (equation **16**). Lastly the RO· radical can abstract a hydrogen from the alkane forming an alcohol and an R· radical (equation **17**) [9, 20, 21].



Scheme 4.1: Adapted mechanism for the oxidation of *n*-octane (RH) by cobalt and nickel complexes and TBHP as oxidant [9, 21].

4.8 Summary

The oxidation studies of *n*-octane activation using two sets of catalysts, namely cobalt and nickel complexes, were performed at room temperature, 50 and 60 °C. Oxidants H₂O₂, TBHP and *m*-CPBA were also investigated.

H₂O₂ and *m*-CPBA as oxidants were not active for the series of xanthene-based complexes investigated in this study, while TBHP was active. At RT all cobalt and nickel catalysts were inactive. At 50 °C all catalysts showed highest activity, except for catalyst **2.14** which was inactive. Of the nickel catalysts, only **2.19** was not active at 50 °C. Selectivity at 50 °C favoured the C-2 position of the carbon chain producing 2-octanone. At 60 °C all catalysts showed a major drop in activity. In terms of selectivity, higher temperature did not only decrease activity, but also favoured the formation of other products, such as 3-octanol and 4-octanol. Ketones (3-octanone and 4-octanone) were observed but in trace amounts. Alcohols were observed as the other products with all catalysts at the higher temperature. The terminal position showed no products of alkane oxygenation. Steric factors did not seem to have much effect on both selectivity and activity, but temperature seemed to have an effect in terms of both activity and

selectivity. Changes that were made at position X of the ligand backbone affected the bite angle, which resulted in minor changes in the activity of the catalysts. In comparison to other reactions such as hydroformylation and hydrocyanation the bite angle size had a minor effect on the oxidation of *n*-octane.

Therefore, the best temperature to work with when using xanthene-based complexes of cobalt and nickel is 50 °C as it was the temperature where most catalysts were active.

4.9 References

- [1] B. Rybtchinski, A. Vigalok, Y. Ben-David and D. Milstein, *Journal of American Chemical Society*, 118 (1996) 12406.
- [2] A. Sivaramakrishna, P. Suman, E.V. Goud, S. Janardan, C. Sravani, T. Sandeep, K. Vijayakrishna and H.S. Clayton, *Journal of Coordination Chemistry*, 12 (2013) 2091.
- [3] S.S. Stahl, A.J. Labinger and J.E. Bercaw, *Angewandte Chemie-International Edition*, 37 (1998) 2180.
- [4] A.E. Shilov and G.B. Shul'pin, *Activation and Catalytic Reactions of Saturated Hydrocarbons in the Presence of Metal Complexes*, in B.R. James (Editor), Vol. 21, Kluwer Academic Publishers, Dordrecht, 2002, p. 550.
- [5] G.B. Shul'pin, *Dalton Transactions*, 42 (2013) 12794.
- [6] G.B. Shul'pin, *Journal of Molecular Catalysis A: Chemical*, 189 (2002) 39.
- [7] M.A. Kirillova, M.V. Kirillova, L.S. Shul'pina, P.J. Figiel, K.R. Gruenwald, M.F.C.G. da Silva, M. Haukka, A.J.L. Pombeiro and G.B. Shul'pin, *Journal of Molecular Catalysis A: Chemical*, 350 (2011) 26.
- [8] P.A. MacFaul, I. Arends, K.U. Ingold and D.D.M. Wayner, *Journal of the Chemical Society-Perkin Transactions 2*, (1997) 135.
- [9] T.C.O. Mac Leod, M.V. Kirillova, A.J.L. Pombeiro, M.A. Schiavon and M.D. Assis, *Applied Catalysis A: General*, 372 (2010) 191.
- [10] U. Schuchardt, D. Cardoso, R. Sercheli, R. Pereira, R.S. de Cruz, M.C. Guerreiro, D. Mandelli, E.V. Spinace and E.L. Fires, *Applied Catalysis A: General*, 211 (2001) 1.
- [11] P.C.J. Kamer, P.W.N. van Leeuwen and J.N.H. Reek, *Accounts of Chemical Research*, 34 (2001) 895.
- [12] P.W.N. van Leeuwen, P.C.J. Kamer, J.N.H. Reek and P. Dierkes, *Chemical Reviews*, 100 (2000) 2741.
- [13] T. Appleby and J.D. Woolins, *Coordination Chemistry Reviews*, 235 (2002) 121.
- [14] L.A. van der Veen, P.H. Keeven, G.C. Schoemaker, J.N.H. Reek, P.C.J. Kamer, P.W.N. van Leeuwen, M. Lutz and A.L. Spek, *Organometallics*, 19 (2000) 872.
- [15] T. Marimuthu and H.B. Friedrich, *ChemCatChem*, 4 (2012) 2090.

- [16] T. Marimuthu, The Preparation and Novel Application of Diphosphorous Xanthenes Family Ligands in Homogenous Catalysis, PhD Thesis, University of KwaZulu Natal, 2011, p. 74.
- [17] M. Salavati-Niasari and S.H. Banitaba, *Journal of Molecular Catalysis A: Chemical*, 201 (2003) 43.
- [18] T. Nagataki, Y. Tachi and S. Itoh, *Chemical Communications*, (2006) 4016.
- [19] E. Tordin, M. List, U. Monkowius, S. Schindler and G. Knoer, *Inorganica Chimica Acta*, 402 (2013) 90.
- [20] B.R. Cook, T.J. Reinert and K.S. Suslick, *Journal of the American Chemical Society*, 108 (1986) 7281.
- [21] M.A. Kirillova, M.V. Kirillova, M.P. Reis, J.A.L. Silva, J.J.R.F. da Silva and A.J.L. Pombeiro, *Journal of Catalysis*, 248 (2007) 130.

Chapter 5

General Conclusion

Xanthene-based ligands were successfully synthesized and characterized by NMR, melting point, IR and LC-MS. Design of these ligands focused on different types of backbones with different bite angle size. Complexation of xanthene-based ligands to nickel and cobalt was a success. The prepared complexes were found to be NMR inactive due to their paramagnetic properties and they were then characterized by Mp, EA, IR and some by single crystal X-ray diffraction. Crystal structures of 4, 5-bis(di-*p*-tolylphosphino)-9,9-dimethyl xanthene, Co(4, 5-bis(di-*p*-tolylphosphino)-9,9-dimethyl xanthene)Cl₂, and Ni(4, 5-bis(di-*p*-tolylphosphino)-9,9-dimethyl xanthene)Cl₂ were obtained.

The prepared cobalt and nickel complexes were used in the activation of *n*-octane. The *n*-octane activation was done at different temperatures (RT, 50 °C, 60 °C) using three different types of oxidants (H₂O₂, TBHP, *m*-CPBA) in THF solvent. The use of H₂O₂ and *m*-CPBA as an oxidant on *n*-octane activation in the presence of xanthene-based complexes showed no conversion. TBHP as an oxidant gave activity at all temperatures and showed its best activity at 50 °C. Selectivity towards 2-octanone was high at 50 °C and 60 °C for both cobalt and nickel catalysts. At higher temperatures a major drop in conversion was observed and formation of other products such as 3-octanol, 4-octanol were observed. Alcohols were observed as other products at 50 °C and 60 °C temperatures. Other products such as ketones (3-octanone and 4-octanone) were observed in trace amounts. No products of alkane oxygenation were observed at the terminal position of *n*-octane.

All catalysts showed that the bite angle size has a minor effect on the catalytic activity. Temperature seemed to have a greater effect in activity as well as selectivity. Sulphur had a deactivating effect on both cobalt and nickel catalysts.

To conclude, the aim of the study was achieved as ligand synthesis and complexation to cobalt and nickel was a success. Small variations on the xanthene backbone brought changes to the bite angle size and resulted in minor changes in catalytic activity. TBHP was the most successful

oxidant used. The temperature effect was also investigated and one can conclude that when using xanthene-based catalysts the best temperature to work with is 50 °C.

List of Figure

Figure 2: ^1H NMR of ligand (4,5-bis(di- <i>p</i> -tolylphosphino)-9,9-dimethyl xanthene).....	1
Figure 1: ^{31}P NMR of ligand (4,5-bis(diphenylphosphino)-9,9-dimethyl xanthene).....	1
Figure 3: ^{13}C NMR of ligand (4,5-bis(di- <i>p</i> -tolylphosphino)-9,9-dimethyl xanthene).....	2
Figure 4: ^{31}P NMR of ligand (4,5-bis(di- <i>p</i> -tolylphosphino)-9,9-dimethyl xanthene)	2
Figure 6: ^{13}C NMR of precursor (2,7-(di- <i>n</i> -hexanoyl)-9,9-dimethyl xanthene).....	3
Figure 5: ^1H NMR of precursor (2,7-(di- <i>n</i> -hexanoyl)-9,9-dimethyl xanthene).....	3
Figure 8: ^{13}C NMR of precursor (2,7-(di- <i>n</i> -hexyl)-9,9-dimethyl xanthene)	4
Figure 7: ^1H NMR of precursor (2,7-(di- <i>n</i> -hexyl)-9,9-dimethyl xanthene).....	4
Figure 9: ^1H NMR of ligand (4,5-bis(diphenylphosphino)-2,7-di- <i>n</i> -hexyl-9,9-dimethyl xanthene).5	5
Figure 10: ^{13}C NMR of ligand (4,5-bis(diphenylphosphino)-2,7-di- <i>n</i> -hexyl-9,9-dimethyl xanthene)	5
Figure 11: ^{31}P NMR of ligand (4,5-bis(diphenylphosphino)-2,7-di- <i>n</i> -hexyl-9,9-dimethyl xanthene)	6
Figure 12: ^1H NMR of ligand (4,5-bis(diphenylphosphino) 10-isopropylidene xanthene).....	6
Figure 13: ^{13}C NMR of ligand (4,5-bis(diphenylphosphino) 10-isopropylidene xanthene).....	7
Figure 14: ^{31}P NMR of ligand (4,5-bis(diphenylphosphino) 10-isopropylidene xanthene)	7
Figure 15: ^1H NMR of ligand 2.7	8

List of Tables

Table 1: Standards used for GC calibration and the suppliers.....	8
Table 2: Mass of standards used in THF solvents and their respective RF values.....	9
Table 3: Quantities used in the blank runs for the optimization of the substrate to oxidant (TBHP) ratio.....	9
Table 4: Quantities used in the optimization of the substrate to oxidant (TBHP) ratio using catalyst	10
Table 5: Quantities used in the blank runs for the substrate to oxidant (<i>m</i> -CPBA) ratio	11
Table 6: Quantities used in the optimization of the substrate to oxidant (<i>m</i> -CPBA) ratio using catalyst	11
Table 7: Quantities used in the blank runs for the optimization of the substrate to oxidant (H ₂ O ₂) ratio.....	11
Table 8: Quantities used in the optimization of the substrate to oxidant (H ₂ O ₂) ratio using catalyst	12
Table 9: Mass and molar quantities used in the catalytic testing in THF with TBHP as the respective oxidant.....	12
Table 10: Calculated reactivities from the % selectivity of the alcohols and ketones for catalyst	13
Table 11: Crystal data and structure refinement for (4, 5-bis(di- <i>p</i> -tolylphosphino)-9,9-dimethyl xanthene)	14
Table 12: Atomic coordinates and isotropic displacement parameters for(4,5-bis(di- <i>p</i> -tolylphosphino)-9,9-dimethyl xanthene)	16
Table 13: Bond lengths [Å] and angles [°] for (4,5-bis(di- <i>p</i> -tolylphosphino)-9,9-dimethyl xanthene)	17
Table 14: Anisotropic displacement parameters for (4, 5-bis(di- <i>p</i> -tolylphosphino)-9,9-dimethyl xanthene)	24
Table 15: Hydrogen coordinates and isotropic displacement parameters for (4,5-bis(di- <i>p</i> -tolylphosphino)-9,9-dimethyl xanthene)	26
Table 16: Torsion angles for (4,5-bis(di- <i>p</i> -tolylphosphino) 9,9-dimethyl xanthene).....	27
Table 17: Hydrogen bonds for (4, 5-bis(di- <i>p</i> -tolylphosphino)-9,9-dimethyl xanthene).....	30

Table 18: Crystal data and structure refinement for (Co(4,5-bis(di- <i>p</i> -tolylphosphino)-9,9-dimethyl xanthene)Cl ₂).....	31
Table 19: Atomic coordinates and equivalent isotropic displacement parameters for (Co(4,5-bis(di- <i>p</i> -tolylphosphino)-9,9-dimethyl xanthene)Cl ₂)	32
Table 20: Bond lengths [Å] and angles [°] for (Co(4,5-bis(di- <i>p</i> -tolylphosphino)-9,9-dimethyl xanthene)Cl ₂)	34
Table 21: Anisotropic displacement parameters for (Co(4,5-bis(di- <i>p</i> -tolylphosphino)-9,9-dimethyl xanthene)Cl ₂).....	42
Table 22: Hydrogen coordinates and isotropic displacement parameters for (Co(4,5-bis(di- <i>p</i> -tolylphosphino)-9,9-dimethyl xanthene)Cl ₂).....	43
Table 23: Torsion angles for (Co(4,5-bis(di- <i>p</i> -tolylphosphino)-9,9-dimethyl xanthene)Cl ₂)	45
Table 24: Crystal data and structure refinement for (Ni(4,5-bis(di- <i>p</i> -tolylphosphino)-9,9-dimethyl xanthene)Cl ₂).....	49
Table 25: Atomic coordinates and equivalent isotropic displacement parameters for (Ni(4,5-bis(di- <i>p</i> -tolylphosphino)-9,9-dimethyl xanthene)Cl ₂)	50
Table 26: Bond lengths [Å] and angles [°] for (Ni(4,5-bis(di- <i>p</i> -tolylphosphino)-9,9-dimethyl xanthene)Cl ₂)	52
Table 27: Anisotropic displacement parameters for (Ni(4,5-bis(di- <i>p</i> -tolylphosphino)-9,9-dimethyl xanthene)Cl ₂).....	60
Table 28: Hydrogen coordinates and isotropic displacement parameters for (Ni((4,5-bis(di- <i>p</i> -tolylphosphino)-9,9-dimethyl xanthene)Cl ₂).....	61
Table 29: Torsion angles for (Ni((4,5-bis(di- <i>p</i> -tolylphosphino)-9,9-dimethyl xanthene)Cl ₂)	63
Table 30: Hydrogen bonds for (Ni((4,5-bis(di- <i>p</i> -tolylphosphino)-9,9-dimethyl xanthene)Cl ₂)...	66

Appendix A

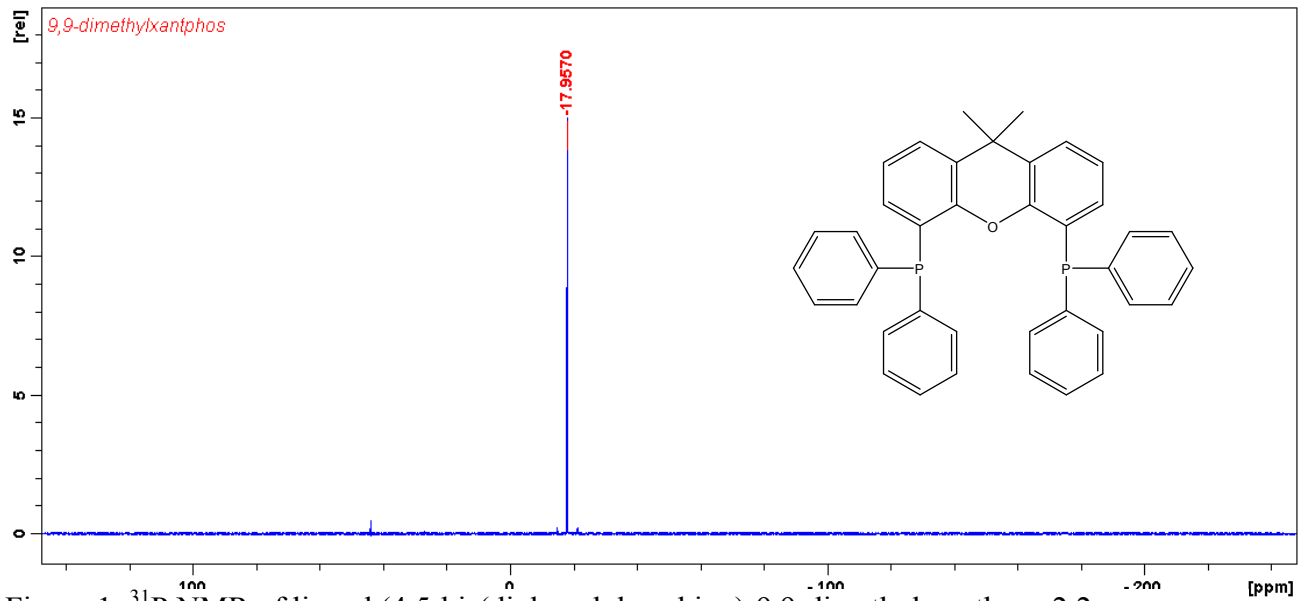


Figure 1: ^{31}P NMR of ligand (4,5-bis(diphenylphosphino)-9,9-dimethyl xanthene) 2.2

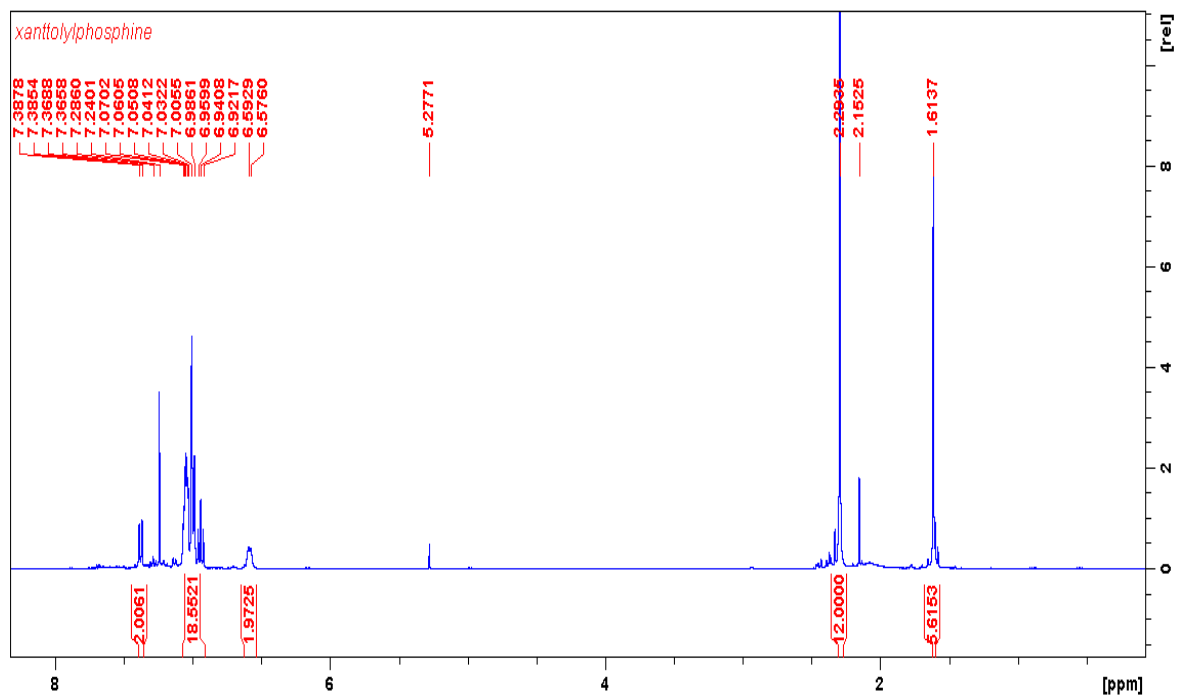


Figure 2: ^1H NMR of ligand (4,5-bis(di-*p*-tolylphosphino)-9,9-dimethyl xanthene) 2.3

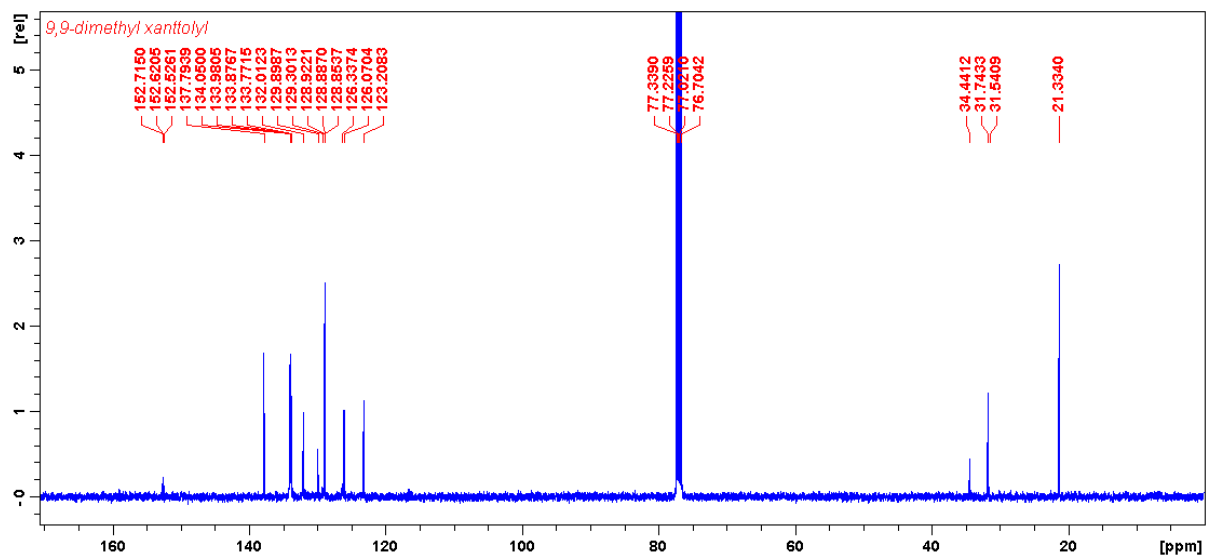


Figure 3: ^{13}C NMR of ligand (4,5-bis(di-*p*-tolylphosphino)-9,9-dimethyl xanthene) 2.3

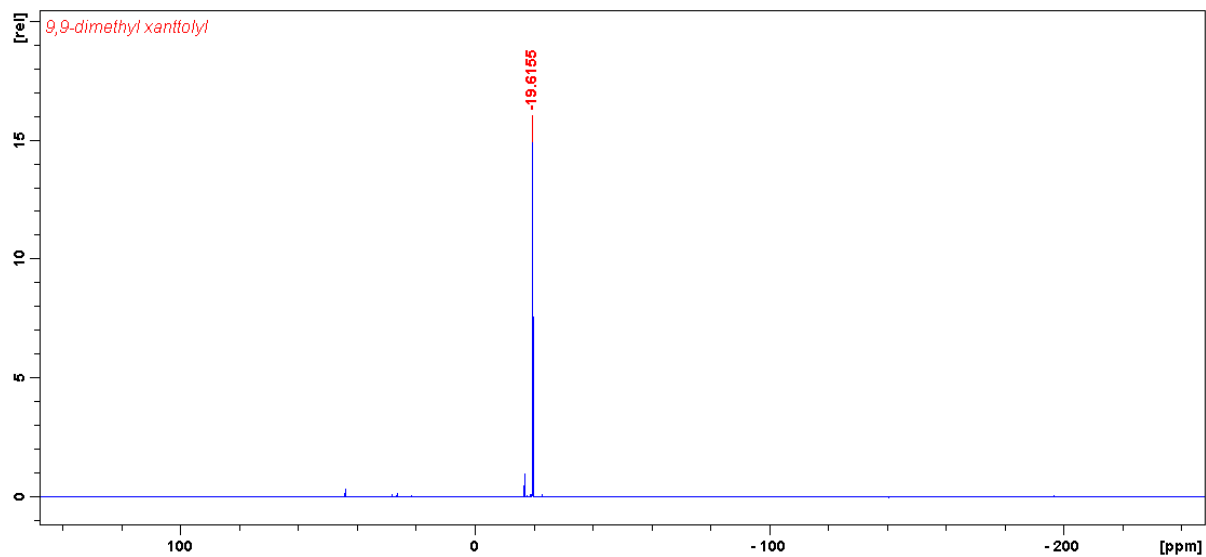


Figure 4: ^{31}P NMR of ligand (4,5-bis(di-*p*-tolylphosphino)-9,9-dimethyl xanthene) 2.3

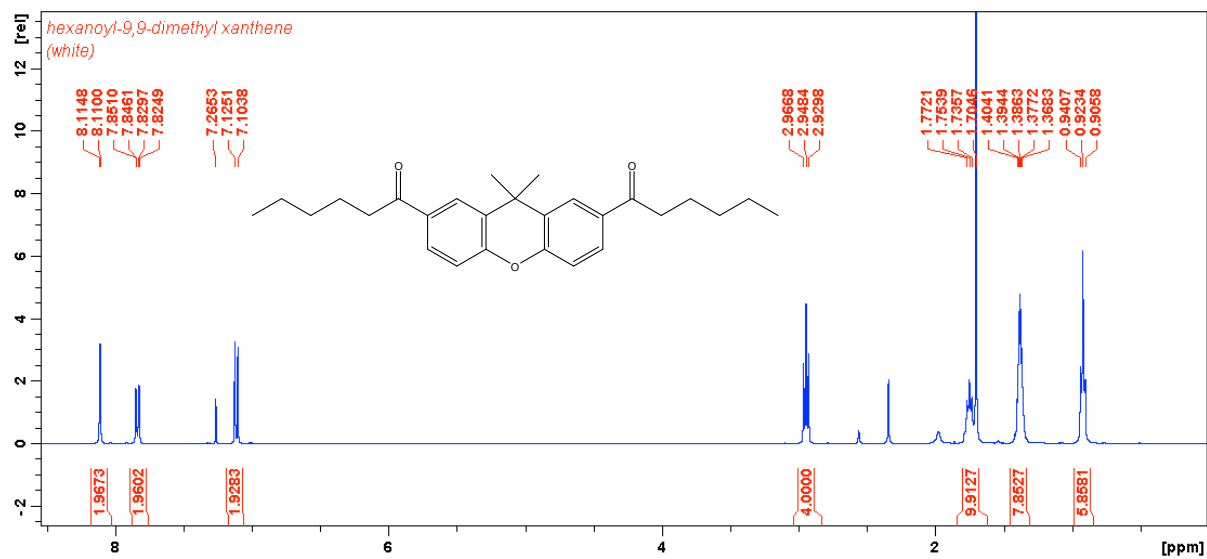


Figure 5: ^1H NMR of precursor (2,7-(di-n-hexanoyl)-9,9-dimethyl xanthene) 2.4

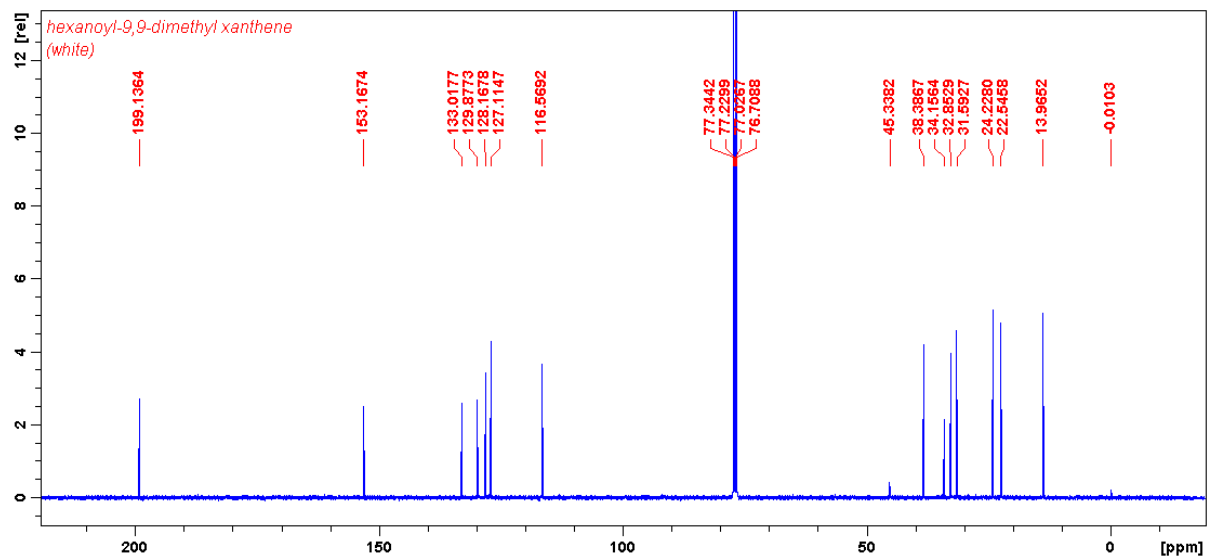


Figure 6: ^{13}C NMR of precursor (2,7-(di-n-hexanoyl)-9,9-dimethyl xanthene) 2.4

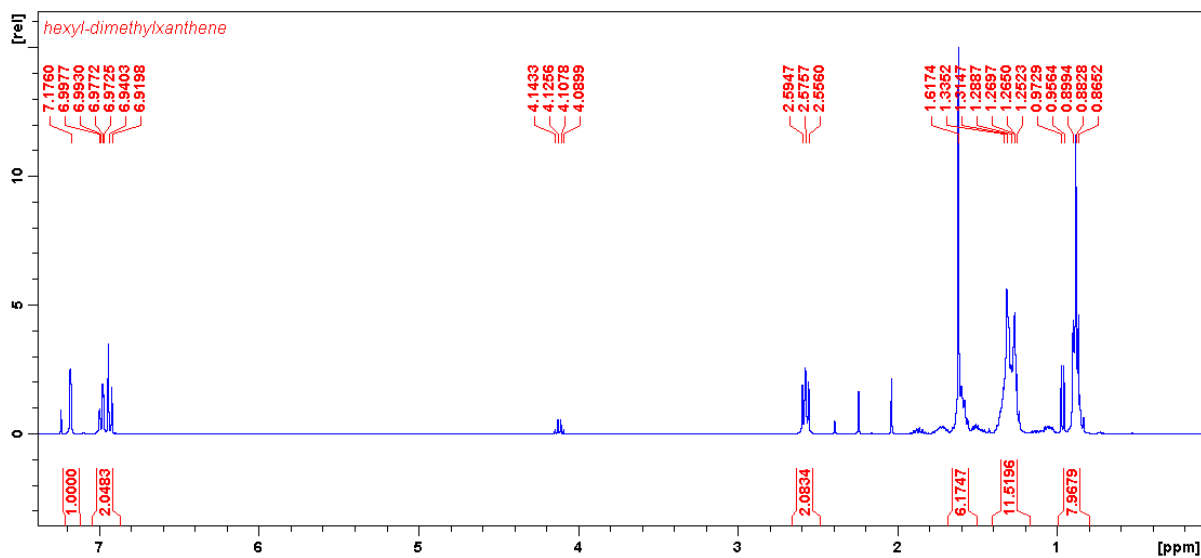


Figure 7: ¹H NMR of precursor (2,7-(di-n-hexyl)-9,9-dimethyl xanthene) 2.5

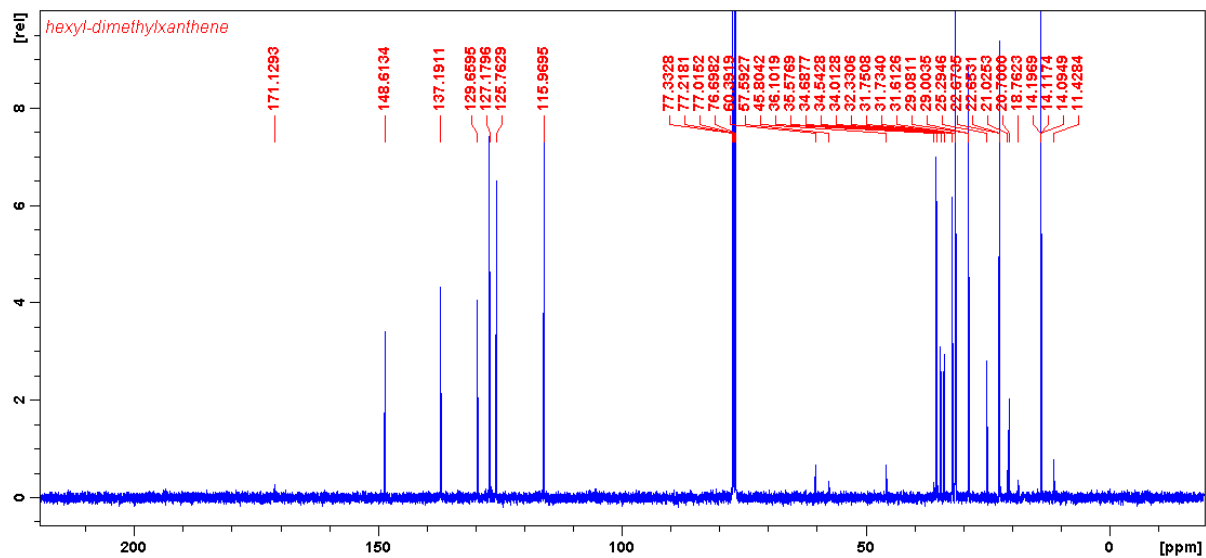


Figure 8: ¹³C NMR of precursor (2,7-(di-n-hexyl)-9,9-dimethyl xanthene) 2.5

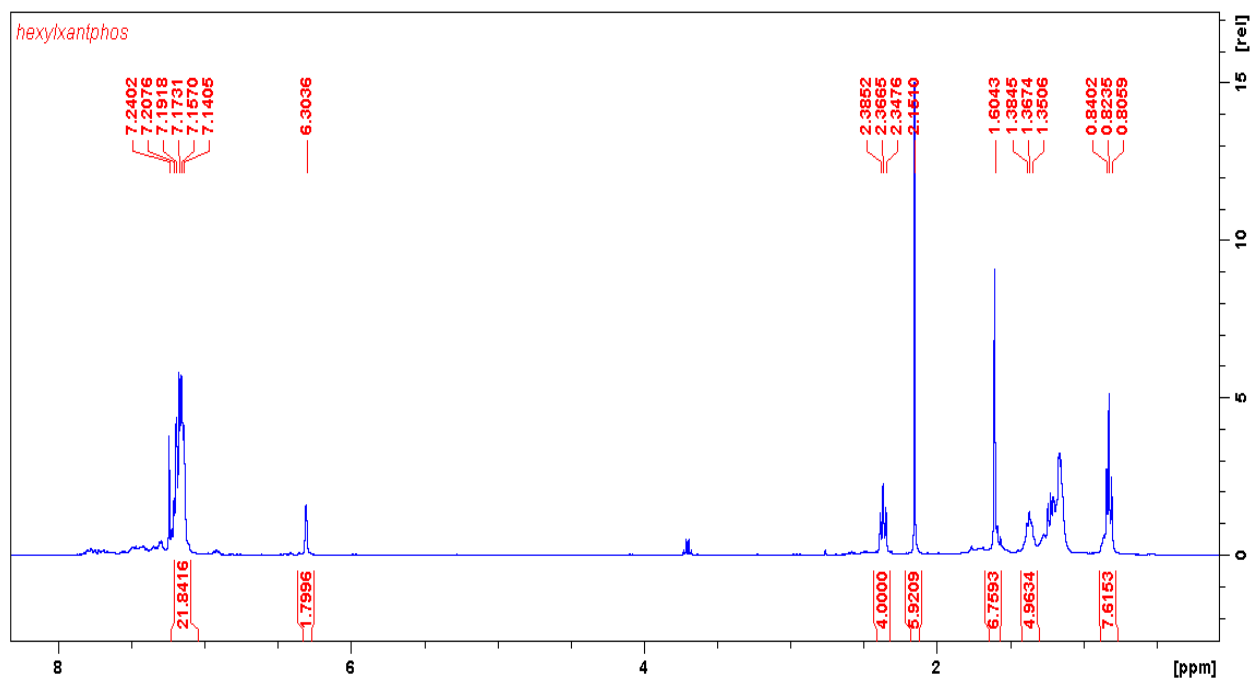


Figure 9: ^1H NMR of ligand (4,5-bis(diphenylphosphino)-2,7-di-n-hexyl-9,9-dimethyl xanthene) 2.6

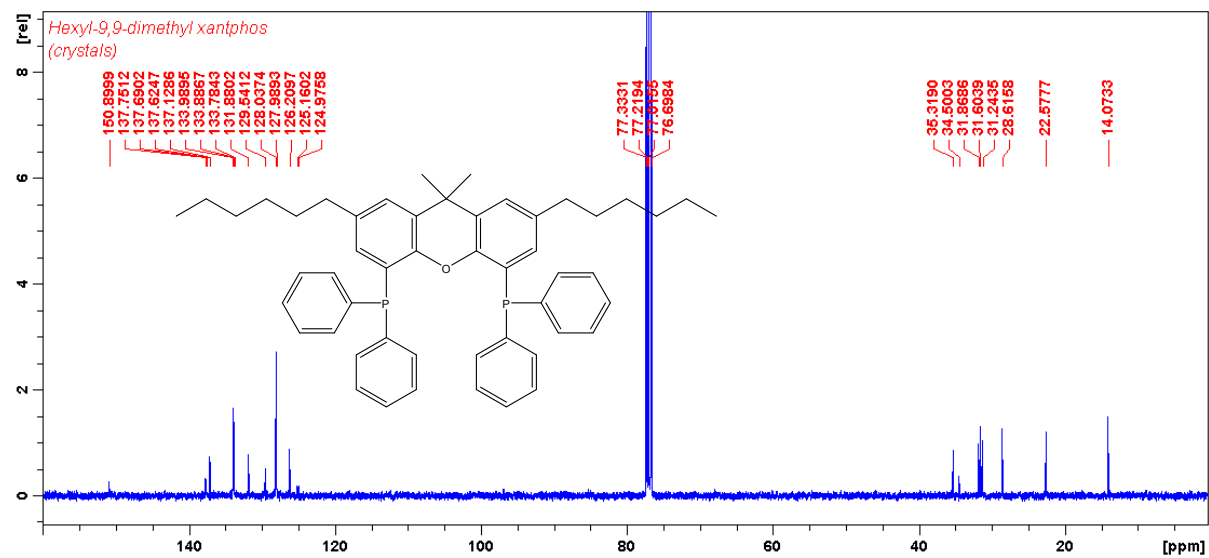


Figure 10: ^{13}C NMR of ligand (4,5-bis(diphenylphosphino)-2,7-di-n-hexyl-9,9-dimethyl xanthene) 2.6

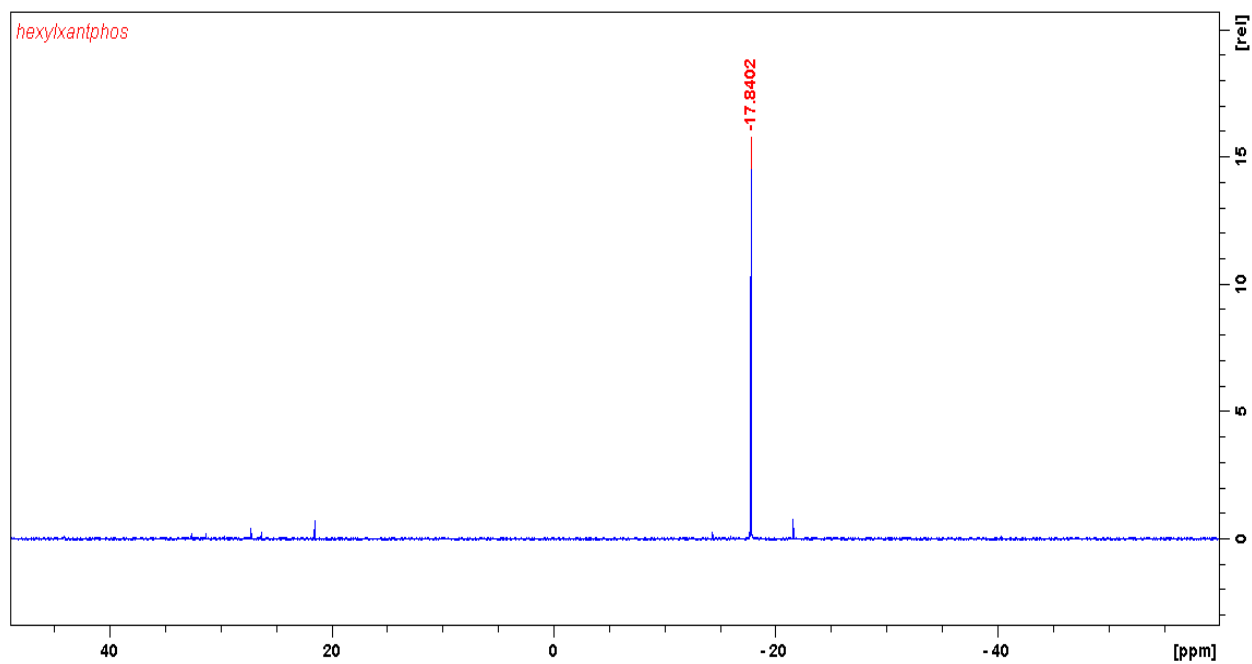


Figure 11: ^{31}P NMR of ligand (4,5-bis(diphenylphosphino)-2,7-di-n-hexyl-9,9-dimethyl xanthene) 2.6

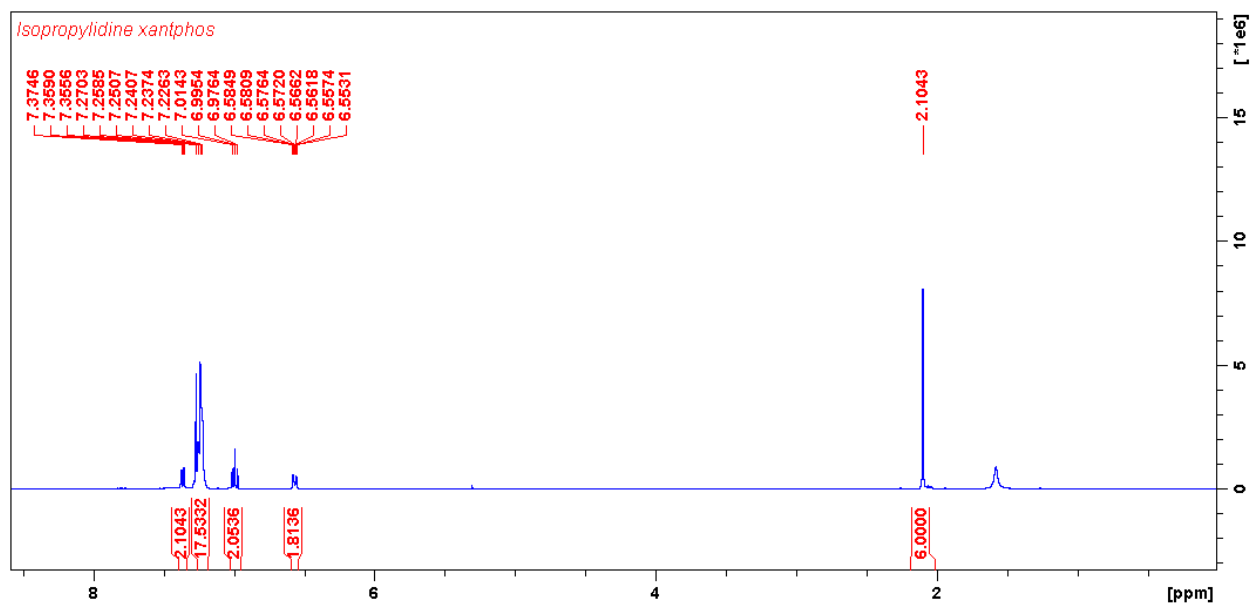


Figure 12: ^1H NMR of ligand (4,5-bis(diphenylphosphino) 10-isopropylidene xanthene) 2.10

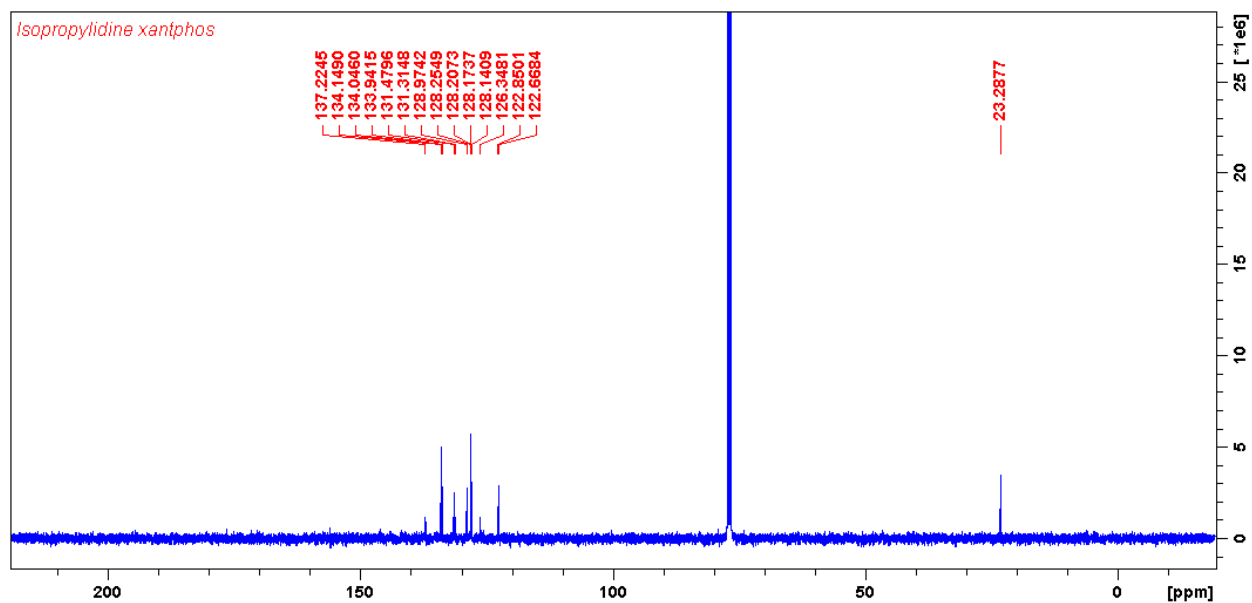


Figure 13: ^{13}C NMR of ligand (4,5-bis(diphenylphosphino) 10-isopropylidene xanthene) 2.10

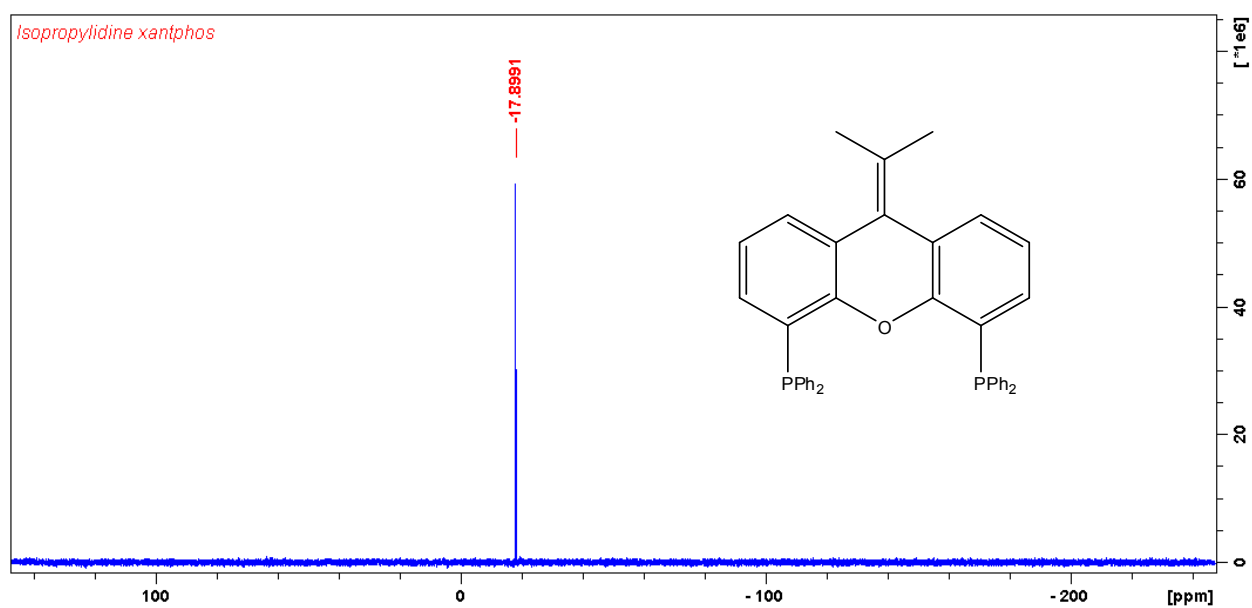


Figure 14: ^{31}P NMR of ligand (4,5-bis(diphenylphosphino) 10-isopropylidene xanthene) 2.10

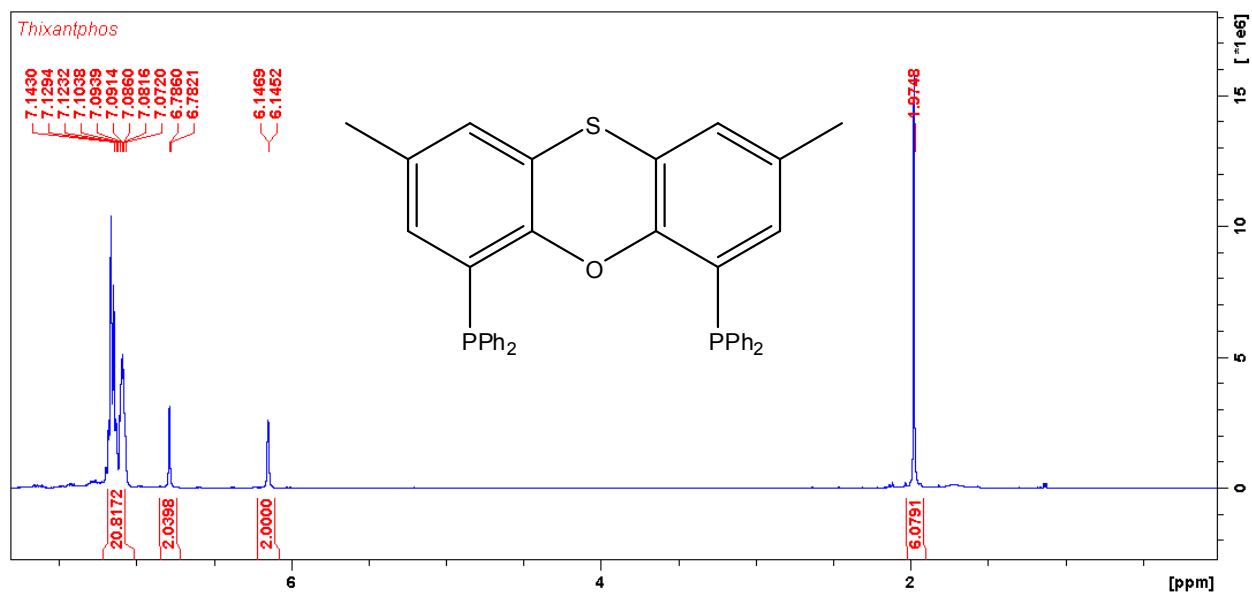


Figure 15: ¹H NMR of ligand 2.7

Appendix B

Standards used for GC calibration

Table 1: Standards used for GC calibration and the suppliers

Multi component standards	Supplier
Octane	Fluka
Octanol	Sigma Aldrich
Octanoic acid	Sigma Aldrich
2-octanol	Sigma Aldrich
3-octanol	Fluka
4-octanol	Fluka
2-octanone	Fluka
3-octanone	Fluka
4-octanone	Sigma Aldrich
Octanal	Sigma Aldrich
Pentanoic acid	Merck

The standards in the above were all weighed into a 10 ml volumetric flask and diluted into a mark by THF solvent. This multicomponent standard mixture was used for GC calibration.

RF values were calculated based on the following formula:

$$RF = ((\text{area of internal standard})(\text{mol of analyte})) / ((\text{area of analyte})(\text{mol of internal standard}))$$

Table 2: Mass of standards used in THF solvents and their respective RF values

Standards	Tetrahydrofuran	
	Mass/g	RF value
Octane	0.0100	0.389
1-octanol	0.0127	0.638
2-octanol	0.0130	0.709
3-octanol	0.0134	0.901
4-octanol	0.0109	0.715
2-octanone	0.0155	0.459
3-octanone	0.0150	0.461
4-octanone	0.0126	0.577
Octanal	0.0138	0.989
Octanoic acid	0.0129	0.453

Optimization of substrate to oxidant (TBHP) ratio in Tetrahydrofuran solvent and using complex 2.11

Table 3: Quantities used in the blank runs for the optimization of the substrate to oxidant (TBHP) ratio

Ratio	octane		<i>t</i> -BuOOH		Pentanoic acid	
	Mass /g	mol x 10 ⁻⁴	Mass /g	mol x 10 ⁻³	Mass /g	mol x 10 ⁻⁵
1:7.5	0.0441	3.86	0.389	4.32	0.0094	9.20
1:10	0.0439	3.84	0.511	5.67	0.0161	15.7

Table 4: Quantities used in the optimization of the substrate to oxidant (TBHP) ratio using catalyst 2.11

Ratio	Catalyst		Octane		<i>t</i> -BuOOH		Pentanoic acid	
	Mass /g	mol x 10 ⁻⁶	Mass /g	mol x 10 ⁻⁴	Mass /g	mol x 10 ⁻³	Mass /g	mol x 10 ⁻⁴
1:7.5	0.0031	4.37	0.0397	3.47	0.384	4.26	0.0108	1.05
1:10	0.0029	4.09	0.0423	3.70	0.513	5.69	0.0103	1.00

Optimization of substrate to oxidant (TBHP) ratio in Tetrahydrofuran solvent and using complex 2.11

Table 5: Quantities used in the blank runs for the substrate to oxidant (*m*-CPBA) ratio

Ratio	Octane		<i>m</i> -CPBA		Pentanoic acid	
	Mass /g	mol x 10 ⁻⁴	Mass /g	mol x 10 ⁻³	Mass /g	mol x 10 ⁻⁵
1:7.5	0.0478	4.18	0.554	3.21	0.0189	18.5
1:10	0.0478	4.18	0.702	4.06	0.0259	25.3

Table 6: Quantities used in the optimization of the substrate to oxidant (*m*-CPBA) ratio using catalyst 2.11

Ratio	Catalyst		Octane		<i>m</i> -CPBA		Pentanoic acid	
	Mass /g	mol x 10 ⁻⁶	Mass /g	mol x 10 ⁻⁴	Mass /g	mol x 10 ⁻³	Mass /g	mol x 10 ⁻⁴
1:7.5	0.0033	4.65	0.0483	4.20	0.550	3.18	0.0128	1.25
1:10	0.0035	4.94	0.0473	4.14	0.746	4.32	0.0204	1.99

Optimization of substrate to oxidant (H₂O₂) ratio in Tetrahydrofuran solvent and using complex 2.11

Table 7: Quantities used in the blank runs for the optimization of the substrate to oxidant (H₂O₂) ratio

Ratio	Octane		H ₂ O ₂		Pentanoic acid	
	Mass/g	Mol x 10 ⁻⁴	Mass/g	Mol x 10 ⁻³	Mass/g	Mol x 10 ⁻⁴
1:7.5	0.0457	4.00	0.2944	8.65	0.0129	1.26
1:10	0.0445	3.89	0.4143	12.1	0.0203	1.98

Table 8: Quantities used in the optimization of the substrate to oxidant (H₂O₂) ratio using catalyst 2.11

Ratio	Catalyst		Octane		H ₂ O ₂		Pentanoic acid	
	Mass/g	Mol x 10 ⁻⁶	Mass/g	Mol x 10 ⁻⁴	Mass/g	Mol x 10 ⁻³	Mass/g	Mol x 10 ⁻⁴
1:7.5	0.0029	4.09	0.0489	4.28	0.290	8.52	0.0129	1.26
1:7.5	0.0031	4.37	0.0481	4.21	0.284	8.34	0.0094	0.92

Catalytic testing in the presence of TBHP

Table 9: Mass and molar quantities used in the catalytic testing in THF with TBHP as the respective oxidant

Ratio	Catalyst		Octane		<i>t</i> -BuOOH		Pentanoic acid	
	Mass /g	mol x 10 ⁻⁶	Mass /g	mol x 10 ⁻⁴	Mass /g	mol x 10 ⁻³	Mass /g	mol x 10 ⁻⁴
2.11	0.0026	3.66	0.0476	4.17	0.488	5.41	0.0120	1.17
2.12	0.0029	3.79	0.0468	4.10	0.512	5.68	0.0107	1.04
2.13	0.0026	2.96	0.0471	4.13	0.513	5.69	0.0091	0.891
2.14	0.0025	3.44	0.0482	4.22	0.504	5.59	0.0145	1.41
2.15	0.0031	4.30	0.0463	4.05	0.549	6.09	0.0109	1.06
2.16	0.0036	5.08	0.0484	4.24	0.495	5.49	0.0124	1.21
2.17	0.0035	4.57	0.0480	4.20	0.507	5.62	0.0186	1.82
2.18	0.0032	3.65	0.0479	4.19	0.497	5.51	0.0107	1.04
2.19	0.0031	4.26	0.0468	4.10	0.506	5.61	0.0201	1.96
2.20	0.0034	4.72	0.0472	4.13	0.510	5.65	0.0111	1.09

Calculations of selectivity parameters

Table 10: Calculated reactivities from the % selectivity of the alcohols and ketones for catalyst 2.12

Alcohols/ketones	% Selectivity	Number of hydrogens	Normalized
2 octanone	55	16	3
3-octanol	17	17	1
4-octanol	28	17	2

Ratio = 3: 1: 2

Structure diagram of 4,5-(di-*p*-tolylphosphine)-9,9-dimethyl xanthene

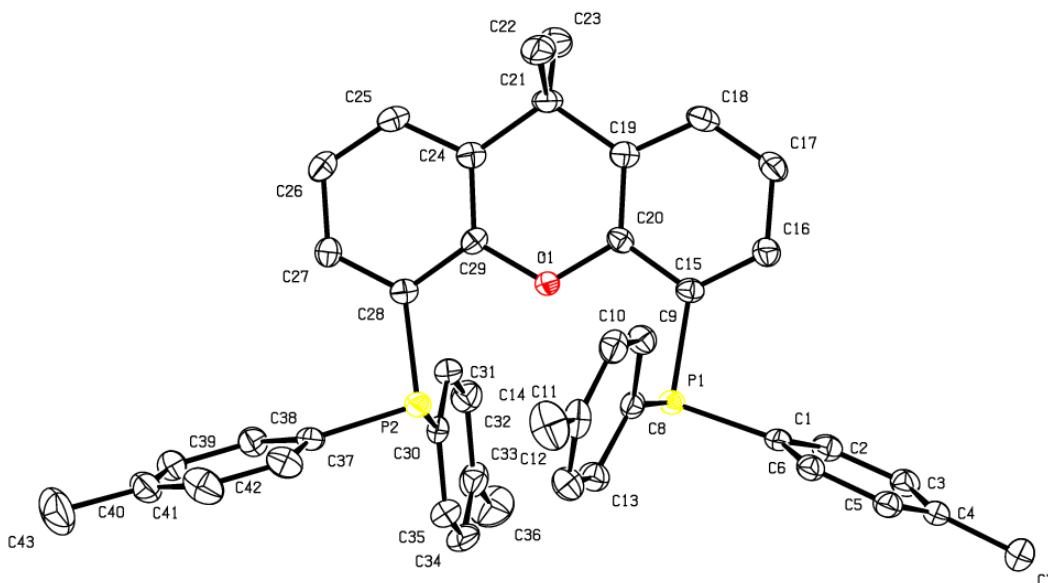


Table 11: Crystal data and structure refinement for (4, 5-bis(di-*p*-tolylphosphino)-9,9-dimethyl xanthene)

Empirical formula	C ₄₃ H ₄₀ O P ₂	
Formula weight	634.69	
Temperature	173(2) K	
Wavelength	0.71073 Å	
Crystal system	Triclinic	
Space group	P-1	
Unit cell dimensions	a = 9.8811(6) Å	a = 97.650(3)°.
	b = 9.9770(6) Å	b = 96.262(2)°.
	c = 18.3504(11) Å	g = 94.637(2)°.
Volume	1773.88(19) Å ³	

Z	2
Density (calculated)	1.188 Mg/m ³
Absorption coefficient	0.155 mm ⁻¹
F(000)	672
Crystal size	0.48 x 0.23 x 0.13 mm ³
Theta range for data collection	2.07 to 25.00°.
Index ranges	-11<=h<=11, -11<=k<=11, -21<=l<=21
Reflections collected	25830
Independent reflections	6054 [R(int) = 0.0332]
Completeness to theta = 25.00°	96.8 %
Absorption correction	Semi-empirical from equivalents
Max. and min. transmission	0.9802 and 0.9295
Refinement method	Full-matrix least-squares on F ²
Data / restraints / parameters	6054 / 0 / 421
Goodness-of-fit on F ²	1.060
Final R indices [I>2sigma(I)]	R1 = 0.0349, wR2 = 0.0904
R indices (all data)	R1 = 0.0398, wR2 = 0.0938
Largest diff. peak and hole	0.377 and -0.297 e.Å ⁻³

Table 12: Atomic coordinates and isotropic displacement parameters for (4,5-bis(di-*p*-tolylphosphino)-9,9-dimethyl xanthene)

	x	y	z	U(eq)
C(1)	7105(2)	7484(2)	671(1)	19(1)
C(2)	8309(2)	7964(2)	418(1)	22(1)
C(3)	8269(2)	8681(2)	-181(1)	24(1)
C(4)	7032(2)	8972(2)	-536(1)	23(1)
C(5)	5830(2)	8480(2)	-287(1)	23(1)
C(6)	5863(2)	7737(2)	300(1)	21(1)
C(7)	6989(2)	9805(2)	-1168(1)	31(1)
C(8)	5468(2)	6284(2)	1645(1)	19(1)
C(9)	4707(2)	5074(2)	1320(1)	24(1)
C(10)	3337(2)	4838(2)	1408(1)	27(1)
C(11)	2670(2)	5806(2)	1805(1)	29(1)
C(12)	3430(2)	7012(2)	2134(1)	30(1)
C(13)	4815(2)	7241(2)	2065(1)	25(1)
C(14)	1166(2)	5543(3)	1875(1)	45(1)
C(15)	7700(2)	4997(2)	1162(1)	19(1)
C(16)	7794(2)	4542(2)	424(1)	23(1)
C(17)	8063(2)	3215(2)	200(1)	27(1)
C(18)	8216(2)	2330(2)	717(1)	25(1)
C(19)	8143(2)	2747(2)	1469(1)	20(1)
C(20)	7911(2)	4087(2)	1675(1)	18(1)
C(21)	8270(2)	1747(2)	2028(1)	22(1)
C(22)	7055(2)	638(2)	1837(1)	32(1)
C(23)	9627(2)	1095(2)	1991(1)	32(1)
C(24)	8215(2)	2476(2)	2807(1)	20(1)
C(25)	8333(2)	1755(2)	3411(1)	23(1)
C(26)	8255(2)	2379(2)	4123(1)	24(1)
C(27)	8070(2)	3751(2)	4250(1)	21(1)
C(28)	7938(2)	4511(2)	3668(1)	18(1)
C(29)	8003(2)	3836(2)	2952(1)	17(1)
C(30)	9379(2)	7144(2)	3877(1)	20(1)

C(31)	10539(2)	6464(2)	3797(1)	22(1)
C(32)	11824(2)	7176(2)	3858(1)	27(1)
C(33)	11995(2)	8591(2)	4009(1)	30(1)
C(34)	10834(2)	9265(2)	4091(1)	31(1)
C(35)	9552(2)	8564(2)	4025(1)	28(1)
C(36)	13400(2)	9360(2)	4092(1)	46(1)
C(37)	7230(2)	6590(2)	4733(1)	20(1)
C(38)	8198(2)	6731(2)	5358(1)	23(1)
C(39)	7804(2)	6878(2)	6065(1)	28(1)
C(40)	6431(2)	6889(2)	6170(1)	32(1)
C(41)	5478(2)	6778(2)	5549(1)	36(1)
C(42)	5863(2)	6633(2)	4841(1)	28(1)
C(43)	5991(3)	7017(3)	6940(1)	54(1)
O(1)	7841(1)	4639(1)	2399(1)	20(1)
P(1)	7271(1)	6699(1)	1526(1)	18(1)
P(2)	7621(1)	6321(1)	3772(1)	19(1)

Table 13: Bond lengths [\AA] and angles [$^\circ$] for (4,5-bis(di-*p*-tolylphosphino)-9,9-dimethyl xanthene)

C(1)-C(6)	1.395(2)
C(1)-C(2)	1.397(2)
C(1)-P(1)	1.8413(16)
C(2)-C(3)	1.387(2)
C(2)-H(2)	0.9500
C(3)-C(4)	1.392(2)
C(3)-H(3)	0.9500
C(4)-C(5)	1.395(2)
C(4)-C(7)	1.512(2)
C(5)-C(6)	1.386(2)
C(5)-H(5)	0.9500
C(6)-H(6)	0.9500

C(7)-H(7A)	0.9800
C(7)-H(7B)	0.9800
C(7)-H(7C)	0.9800
C(8)-C(13)	1.390(2)
C(8)-C(9)	1.394(2)
C(8)-P(1)	1.8395(16)
C(9)-C(10)	1.385(2)
C(9)-H(9)	0.9500
C(10)-C(11)	1.387(3)
C(10)-H(10)	0.9500
C(11)-C(12)	1.392(3)
C(11)-C(14)	1.510(3)
C(12)-C(13)	1.392(2)
C(12)-H(12)	0.9500
C(13)-H(13)	0.9500
C(14)-H(14A)	0.9800
C(14)-H(14B)	0.9800
C(14)-H(14C)	0.9800
C(15)-C(16)	1.387(2)
C(15)-C(20)	1.402(2)
C(15)-P(1)	1.8402(16)
C(16)-C(17)	1.388(2)
C(16)-H(16)	0.9500
C(17)-C(18)	1.384(2)
C(17)-H(17)	0.9500
C(18)-C(19)	1.400(2)
C(18)-H(18)	0.9500
C(19)-C(20)	1.384(2)
C(19)-C(21)	1.526(2)
C(20)-O(1)	1.3798(18)
C(21)-C(24)	1.524(2)
C(21)-C(23)	1.541(2)
C(21)-C(22)	1.542(2)
C(22)-H(22A)	0.9800
C(22)-H(22B)	0.9800
C(22)-H(22C)	0.9800

C(23)-H(23A)	0.9800
C(23)-H(23B)	0.9800
C(23)-H(23C)	0.9800
C(24)-C(29)	1.385(2)
C(24)-C(25)	1.398(2)
C(25)-C(26)	1.382(2)
C(25)-H(25)	0.9500
C(26)-C(27)	1.388(2)
C(26)-H(26)	0.9500
C(27)-C(28)	1.391(2)
C(27)-H(27)	0.9500
C(28)-C(29)	1.405(2)
C(28)-P(2)	1.8464(16)
C(29)-O(1)	1.3788(18)
C(30)-C(31)	1.390(2)
C(30)-C(35)	1.399(2)
C(30)-P(2)	1.8390(17)
C(31)-C(32)	1.390(2)
C(31)-H(31)	0.9500
C(32)-C(33)	1.394(3)
C(32)-H(32)	0.9500
C(33)-C(34)	1.388(3)
C(33)-C(36)	1.513(3)
C(34)-C(35)	1.382(3)
C(34)-H(34)	0.9500
C(35)-H(35)	0.9500
C(36)-H(36A)	0.9800
C(36)-H(36B)	0.9800
C(36)-H(36C)	0.9800
C(37)-C(42)	1.390(2)
C(37)-C(38)	1.396(2)
C(37)-P(2)	1.8351(16)
C(38)-C(39)	1.388(2)
C(38)-H(38)	0.9500
C(39)-C(40)	1.392(3)
C(39)-H(39)	0.9500

C(40)-C(41)	1.383(3)
C(40)-C(43)	1.515(3)
C(41)-C(42)	1.386(3)
C(41)-H(41)	0.9500
C(42)-H(42)	0.9500
C(43)-H(43A)	0.9800
C(43)-H(43B)	0.9800
C(43)-H(43C)	0.9800
C(6)-C(1)-C(2)	117.97(15)
C(6)-C(1)-P(1)	124.35(12)
C(2)-C(1)-P(1)	117.43(12)
C(3)-C(2)-C(1)	120.88(15)
C(3)-C(2)-H(2)	119.6
C(1)-C(2)-H(2)	119.6
C(2)-C(3)-C(4)	121.19(15)
C(2)-C(3)-H(3)	119.4
C(4)-C(3)-H(3)	119.4
C(3)-C(4)-C(5)	117.81(15)
C(3)-C(4)-C(7)	121.26(15)
C(5)-C(4)-C(7)	120.92(16)
C(6)-C(5)-C(4)	121.22(16)
C(6)-C(5)-H(5)	119.4
C(4)-C(5)-H(5)	119.4
C(5)-C(6)-C(1)	120.88(15)
C(5)-C(6)-H(6)	119.6
C(1)-C(6)-H(6)	119.6
C(4)-C(7)-H(7A)	109.5
C(4)-C(7)-H(7B)	109.5
H(7A)-C(7)-H(7B)	109.5
C(4)-C(7)-H(7C)	109.5
H(7A)-C(7)-H(7C)	109.5
H(7B)-C(7)-H(7C)	109.5
C(13)-C(8)-C(9)	118.09(15)
C(13)-C(8)-P(1)	118.40(12)
C(9)-C(8)-P(1)	123.48(13)

C(10)-C(9)-C(8)	120.90(16)
C(10)-C(9)-H(9)	119.6
C(8)-C(9)-H(9)	119.6
C(9)-C(10)-C(11)	121.30(16)
C(9)-C(10)-H(10)	119.4
C(11)-C(10)-H(10)	119.4
C(10)-C(11)-C(12)	117.85(16)
C(10)-C(11)-C(14)	120.34(18)
C(12)-C(11)-C(14)	121.81(18)
C(11)-C(12)-C(13)	121.15(17)
C(11)-C(12)-H(12)	119.4
C(13)-C(12)-H(12)	119.4
C(8)-C(13)-C(12)	120.66(16)
C(8)-C(13)-H(13)	119.7
C(12)-C(13)-H(13)	119.7
C(11)-C(14)-H(14A)	109.5
C(11)-C(14)-H(14B)	109.5
H(14A)-C(14)-H(14B)	109.5
C(11)-C(14)-H(14C)	109.5
H(14A)-C(14)-H(14C)	109.5
H(14B)-C(14)-H(14C)	109.5
C(16)-C(15)-C(20)	118.06(15)
C(16)-C(15)-P(1)	125.05(12)
C(20)-C(15)-P(1)	116.87(11)
C(15)-C(16)-C(17)	120.61(15)
C(15)-C(16)-H(16)	119.7
C(17)-C(16)-H(16)	119.7
C(18)-C(17)-C(16)	119.81(15)
C(18)-C(17)-H(17)	120.1
C(16)-C(17)-H(17)	120.1
C(17)-C(18)-C(19)	121.54(15)
C(17)-C(18)-H(18)	119.2
C(19)-C(18)-H(18)	119.2
C(20)-C(19)-C(18)	117.08(15)
C(20)-C(19)-C(21)	122.00(14)
C(18)-C(19)-C(21)	120.89(14)

O(1)-C(20)-C(19)	123.10(14)
O(1)-C(20)-C(15)	114.06(13)
C(19)-C(20)-C(15)	122.83(14)
C(24)-C(21)-C(19)	110.14(13)
C(24)-C(21)-C(23)	110.01(13)
C(19)-C(21)-C(23)	109.74(14)
C(24)-C(21)-C(22)	108.45(14)
C(19)-C(21)-C(22)	108.65(13)
C(23)-C(21)-C(22)	109.82(14)
C(21)-C(22)-H(22A)	109.5
C(21)-C(22)-H(22B)	109.5
H(22A)-C(22)-H(22B)	109.5
C(21)-C(22)-H(22C)	109.5
H(22A)-C(22)-H(22C)	109.5
H(22B)-C(22)-H(22C)	109.5
C(21)-C(23)-H(23A)	109.5
C(21)-C(23)-H(23B)	109.5
H(23A)-C(23)-H(23B)	109.5
C(21)-C(23)-H(23C)	109.5
H(23A)-C(23)-H(23C)	109.5
H(23B)-C(23)-H(23C)	109.5
C(29)-C(24)-C(25)	117.13(15)
C(29)-C(24)-C(21)	122.87(14)
C(25)-C(24)-C(21)	119.97(14)
C(26)-C(25)-C(24)	121.38(15)
C(26)-C(25)-H(25)	119.3
C(24)-C(25)-H(25)	119.3
C(25)-C(26)-C(27)	120.01(15)
C(25)-C(26)-H(26)	120.0
C(27)-C(26)-H(26)	120.0
C(26)-C(27)-C(28)	120.87(15)
C(26)-C(27)-H(27)	119.6
C(28)-C(27)-H(27)	119.6
C(27)-C(28)-C(29)	117.38(14)
C(27)-C(28)-P(2)	124.35(12)
C(29)-C(28)-P(2)	118.23(12)

O(1)-C(29)-C(24)	122.24(14)
O(1)-C(29)-C(28)	114.55(13)
C(24)-C(29)-C(28)	123.21(14)
C(31)-C(30)-C(35)	117.72(16)
C(31)-C(30)-P(2)	124.89(13)
C(35)-C(30)-P(2)	117.36(13)
C(32)-C(31)-C(30)	120.86(16)
C(32)-C(31)-H(31)	119.6
C(30)-C(31)-H(31)	119.6
C(31)-C(32)-C(33)	121.29(17)
C(31)-C(32)-H(32)	119.4
C(33)-C(32)-H(32)	119.4
C(34)-C(33)-C(32)	117.65(17)
C(34)-C(33)-C(36)	121.26(18)
C(32)-C(33)-C(36)	121.08(18)
C(35)-C(34)-C(33)	121.33(17)
C(35)-C(34)-H(34)	119.3
C(33)-C(34)-H(34)	119.3
C(34)-C(35)-C(30)	121.14(17)
C(34)-C(35)-H(35)	119.4
C(30)-C(35)-H(35)	119.4
C(33)-C(36)-H(36A)	109.5
C(33)-C(36)-H(36B)	109.5
H(36A)-C(36)-H(36B)	109.5
C(33)-C(36)-H(36C)	109.5
H(36A)-C(36)-H(36C)	109.5
H(36B)-C(36)-H(36C)	109.5
C(42)-C(37)-C(38)	117.93(15)
C(42)-C(37)-P(2)	117.18(13)
C(38)-C(37)-P(2)	124.88(12)
C(39)-C(38)-C(37)	120.96(16)
C(39)-C(38)-H(38)	119.5
C(37)-C(38)-H(38)	119.5
C(38)-C(39)-C(40)	120.89(17)
C(38)-C(39)-H(39)	119.6
C(40)-C(39)-H(39)	119.6

C(41)-C(40)-C(39)	117.91(16)
C(41)-C(40)-C(43)	120.91(19)
C(39)-C(40)-C(43)	121.19(19)
C(40)-C(41)-C(42)	121.58(17)
C(40)-C(41)-H(41)	119.2
C(42)-C(41)-H(41)	119.2
C(41)-C(42)-C(37)	120.70(17)
C(41)-C(42)-H(42)	119.6
C(37)-C(42)-H(42)	119.6
C(40)-C(43)-H(43A)	109.5
C(40)-C(43)-H(43B)	109.5
H(43A)-C(43)-H(43B)	109.5
C(40)-C(43)-H(43C)	109.5
H(43A)-C(43)-H(43C)	109.5
H(43B)-C(43)-H(43C)	109.5
C(29)-O(1)-C(20)	119.51(12)
C(8)-P(1)-C(15)	99.46(7)
C(8)-P(1)-C(1)	101.56(7)
C(15)-P(1)-C(1)	100.66(7)
C(37)-P(2)-C(30)	101.09(7)
C(37)-P(2)-C(28)	100.93(7)
C(30)-P(2)-C(28)	100.97(7)

Table 14: Anisotropic displacement parameters for (4, 5-bis(di-*p*-tolylphosphino)-9,9-dimethyl xanthene)

	U ¹¹	U ²²	U ³³	U ²³	U ¹³	U ¹²
C(1)	23(1)	13(1)	18(1)	-1(1)	2(1)	2(1)
C(2)	21(1)	20(1)	23(1)	-1(1)	0(1)	2(1)
C(3)	28(1)	19(1)	24(1)	-1(1)	7(1)	-2(1)
C(4)	34(1)	16(1)	18(1)	0(1)	4(1)	2(1)
C(5)	27(1)	20(1)	21(1)	0(1)	-1(1)	5(1)
C(6)	23(1)	18(1)	20(1)	-1(1)	2(1)	0(1)

C(7)	41(1)	28(1)	25(1)	8(1)	5(1)	4(1)
C(8)	22(1)	19(1)	17(1)	5(1)	1(1)	2(1)
C(9)	26(1)	23(1)	22(1)	1(1)	1(1)	1(1)
C(10)	29(1)	27(1)	22(1)	4(1)	-2(1)	-6(1)
C(11)	24(1)	40(1)	22(1)	10(1)	3(1)	0(1)
C(12)	31(1)	33(1)	29(1)	3(1)	11(1)	7(1)
C(13)	28(1)	22(1)	26(1)	1(1)	6(1)	1(1)
C(14)	28(1)	65(2)	41(1)	2(1)	7(1)	-5(1)
C(15)	18(1)	16(1)	20(1)	0(1)	0(1)	2(1)
C(16)	26(1)	23(1)	19(1)	2(1)	0(1)	4(1)
C(17)	34(1)	26(1)	18(1)	-2(1)	2(1)	7(1)
C(18)	28(1)	20(1)	25(1)	-4(1)	1(1)	6(1)
C(19)	19(1)	19(1)	22(1)	1(1)	-1(1)	3(1)
C(20)	16(1)	19(1)	17(1)	-1(1)	0(1)	2(1)
C(21)	26(1)	15(1)	24(1)	1(1)	-1(1)	4(1)
C(22)	43(1)	19(1)	29(1)	1(1)	-3(1)	-5(1)
C(23)	39(1)	30(1)	29(1)	4(1)	4(1)	17(1)
C(24)	17(1)	18(1)	22(1)	2(1)	-1(1)	1(1)
C(25)	25(1)	16(1)	29(1)	5(1)	0(1)	3(1)
C(26)	26(1)	23(1)	24(1)	9(1)	0(1)	1(1)
C(27)	20(1)	23(1)	19(1)	4(1)	1(1)	2(1)
C(28)	15(1)	16(1)	21(1)	2(1)	-1(1)	1(1)
C(29)	14(1)	18(1)	20(1)	5(1)	-1(1)	1(1)
C(30)	28(1)	19(1)	14(1)	5(1)	2(1)	2(1)
C(31)	28(1)	18(1)	21(1)	2(1)	4(1)	1(1)
C(32)	27(1)	27(1)	28(1)	6(1)	4(1)	2(1)
C(33)	36(1)	28(1)	24(1)	7(1)	1(1)	-7(1)
C(34)	46(1)	16(1)	31(1)	6(1)	3(1)	-2(1)
C(35)	37(1)	20(1)	27(1)	7(1)	5(1)	5(1)
C(36)	42(1)	37(1)	56(1)	7(1)	1(1)	-14(1)
C(37)	23(1)	15(1)	21(1)	0(1)	3(1)	4(1)
C(38)	22(1)	25(1)	23(1)	3(1)	2(1)	4(1)
C(39)	37(1)	24(1)	22(1)	2(1)	1(1)	3(1)
C(40)	42(1)	24(1)	29(1)	-1(1)	15(1)	-1(1)
C(41)	26(1)	37(1)	45(1)	-5(1)	14(1)	-4(1)
C(42)	22(1)	27(1)	32(1)	-3(1)	0(1)	1(1)

C(43)	65(2)	61(2)	38(1)	1(1)	27(1)	-1(1)
O(1)	29(1)	15(1)	15(1)	2(1)	1(1)	4(1)
P(1)	20(1)	15(1)	17(1)	1(1)	0(1)	1(1)
P(2)	23(1)	18(1)	17(1)	2(1)	0(1)	6(1)

Table 15: Hydrogen coordinates and isotropic displacement parameters for (4,5-bis(di-*p*-tolylphosphino)-9,9-dimethyl xanthene)

	x	y	z	U(eq)
H(2)	9167	7798	659	26
H(3)	9101	8979	-351	28
H(5)	4973	8656	-525	28
H(6)	5030	7395	452	25
H(7A)	6669	9212	-1635	46
H(7B)	7907	10235	-1191	46
H(7C)	6362	10508	-1086	46
H(9)	5133	4402	1033	28
H(10)	2846	3996	1191	32
H(12)	2996	7690	2411	36
H(13)	5320	8060	2306	30
H(14A)	672	5161	1389	68
H(14B)	807	6398	2053	68
H(14C)	1041	4898	2226	68
H(16)	7673	5144	67	28
H(17)	8141	2916	-306	32
H(18)	8375	1417	557	30
H(22A)	6200	1049	1899	48
H(22B)	7163	-50	2168	48
H(22C)	7032	210	1322	48
H(23A)	9622	567	1500	48
H(23B)	9730	494	2370	48

H(23C)	10392	1809	2078	48
H(25)	8470	818	3331	28
H(26)	8328	1868	4524	29
H(27)	8032	4176	4742	25
H(31)	10452	5500	3698	27
H(32)	12601	6690	3797	32
H(34)	10923	10229	4195	37
H(35)	8776	9053	4081	33
H(36A)	13378	10098	3790	69
H(36B)	14062	8740	3928	69
H(36C)	13671	9739	4614	69
H(38)	9141	6726	5299	28
H(39)	8481	6971	6483	33
H(41)	4537	6801	5610	43
H(42)	5185	6561	4425	34
H(43A)	5291	7656	6976	81
H(43B)	6782	7350	7307	81
H(43C)	5614	6125	7034	81

Table 16: Torsion angles for (4,5-bis(di-*p*-tolylphosphino) 9,9-dimethyl xanthene)

C(6)-C(1)-C(2)-C(3)	0.6(2)
P(1)-C(1)-C(2)-C(3)	-173.90(12)
C(1)-C(2)-C(3)-C(4)	1.5(2)
C(2)-C(3)-C(4)-C(5)	-2.2(2)
C(2)-C(3)-C(4)-C(7)	177.33(16)
C(3)-C(4)-C(5)-C(6)	0.7(2)
C(7)-C(4)-C(5)-C(6)	-178.78(15)
C(4)-C(5)-C(6)-C(1)	1.4(2)
C(2)-C(1)-C(6)-C(5)	-2.0(2)
P(1)-C(1)-C(6)-C(5)	172.05(12)
C(13)-C(8)-C(9)-C(10)	0.4(2)
P(1)-C(8)-C(9)-C(10)	-177.65(12)

C(8)-C(9)-C(10)-C(11)	1.6(3)
C(9)-C(10)-C(11)-C(12)	-1.9(3)
C(9)-C(10)-C(11)-C(14)	178.16(17)
C(10)-C(11)-C(12)-C(13)	0.2(3)
C(14)-C(11)-C(12)-C(13)	-179.91(17)
C(9)-C(8)-C(13)-C(12)	-2.2(2)
P(1)-C(8)-C(13)-C(12)	176.03(13)
C(11)-C(12)-C(13)-C(8)	1.9(3)
C(20)-C(15)-C(16)-C(17)	1.2(2)
P(1)-C(15)-C(16)-C(17)	-176.96(13)
C(15)-C(16)-C(17)-C(18)	1.1(3)
C(16)-C(17)-C(18)-C(19)	-1.7(3)
C(17)-C(18)-C(19)-C(20)	-0.1(2)
C(17)-C(18)-C(19)-C(21)	178.08(16)
C(18)-C(19)-C(20)-O(1)	-178.74(14)
C(21)-C(19)-C(20)-O(1)	3.1(2)
C(18)-C(19)-C(20)-C(15)	2.5(2)
C(21)-C(19)-C(20)-C(15)	-175.61(14)
C(16)-C(15)-C(20)-O(1)	178.04(14)
P(1)-C(15)-C(20)-O(1)	-3.62(18)
C(16)-C(15)-C(20)-C(19)	-3.1(2)
P(1)-C(15)-C(20)-C(19)	175.23(12)
C(20)-C(19)-C(21)-C(24)	-4.3(2)
C(18)-C(19)-C(21)-C(24)	177.66(14)
C(20)-C(19)-C(21)-C(23)	-125.55(16)
C(18)-C(19)-C(21)-C(23)	56.4(2)
C(20)-C(19)-C(21)-C(22)	114.36(17)
C(18)-C(19)-C(21)-C(22)	-63.7(2)
C(19)-C(21)-C(24)-C(29)	3.2(2)
C(23)-C(21)-C(24)-C(29)	124.26(16)
C(22)-C(21)-C(24)-C(29)	-115.61(17)
C(19)-C(21)-C(24)-C(25)	-179.07(14)
C(23)-C(21)-C(24)-C(25)	-58.0(2)
C(22)-C(21)-C(24)-C(25)	62.16(19)
C(29)-C(24)-C(25)-C(26)	-0.6(2)
C(21)-C(24)-C(25)-C(26)	-178.47(15)

C(24)-C(25)-C(26)-C(27)	-0.7(3)
C(25)-C(26)-C(27)-C(28)	1.1(2)
C(26)-C(27)-C(28)-C(29)	-0.2(2)
C(26)-C(27)-C(28)-P(2)	177.49(12)
C(25)-C(24)-C(29)-O(1)	-178.56(14)
C(21)-C(24)-C(29)-O(1)	-0.7(2)
C(25)-C(24)-C(29)-C(28)	1.5(2)
C(21)-C(24)-C(29)-C(28)	179.38(14)
C(27)-C(28)-C(29)-O(1)	178.90(13)
P(2)-C(28)-C(29)-O(1)	1.11(18)
C(27)-C(28)-C(29)-C(24)	-1.2(2)
P(2)-C(28)-C(29)-C(24)	-178.99(12)
C(35)-C(30)-C(31)-C(32)	-0.3(2)
P(2)-C(30)-C(31)-C(32)	177.51(12)
C(30)-C(31)-C(32)-C(33)	0.6(3)
C(31)-C(32)-C(33)-C(34)	-0.4(3)
C(31)-C(32)-C(33)-C(36)	178.62(17)
C(32)-C(33)-C(34)-C(35)	-0.1(3)
C(36)-C(33)-C(34)-C(35)	-179.12(17)
C(33)-C(34)-C(35)-C(30)	0.4(3)
C(31)-C(30)-C(35)-C(34)	-0.2(2)
P(2)-C(30)-C(35)-C(34)	-178.18(13)
C(42)-C(37)-C(38)-C(39)	1.4(2)
P(2)-C(37)-C(38)-C(39)	-177.41(13)
C(37)-C(38)-C(39)-C(40)	-0.1(3)
C(38)-C(39)-C(40)-C(41)	-1.3(3)
C(38)-C(39)-C(40)-C(43)	178.58(18)
C(39)-C(40)-C(41)-C(42)	1.2(3)
C(43)-C(40)-C(41)-C(42)	-178.64(19)
C(40)-C(41)-C(42)-C(37)	0.2(3)
C(38)-C(37)-C(42)-C(41)	-1.5(3)
P(2)-C(37)-C(42)-C(41)	177.43(14)
C(24)-C(29)-O(1)-C(20)	-1.0(2)
C(28)-C(29)-O(1)-C(20)	178.88(13)
C(19)-C(20)-O(1)-C(29)	-0.2(2)
C(15)-C(20)-O(1)-C(29)	178.64(13)

C(13)-C(8)-P(1)-C(15)	166.10(13)
C(9)-C(8)-P(1)-C(15)	-15.81(15)
C(13)-C(8)-P(1)-C(1)	-90.87(14)
C(9)-C(8)-P(1)-C(1)	87.22(14)
C(16)-C(15)-P(1)-C(8)	101.83(15)
C(20)-C(15)-P(1)-C(8)	-76.38(13)
C(16)-C(15)-P(1)-C(1)	-1.94(16)
C(20)-C(15)-P(1)-C(1)	179.85(12)
C(6)-C(1)-P(1)-C(8)	4.47(15)
C(2)-C(1)-P(1)-C(8)	178.56(12)
C(6)-C(1)-P(1)-C(15)	106.54(14)
C(2)-C(1)-P(1)-C(15)	-79.37(13)
C(42)-C(37)-P(2)-C(30)	153.51(13)
C(38)-C(37)-P(2)-C(30)	-27.63(16)
C(42)-C(37)-P(2)-C(28)	-102.87(14)
C(38)-C(37)-P(2)-C(28)	75.99(15)
C(31)-C(30)-P(2)-C(37)	110.29(14)
C(35)-C(30)-P(2)-C(37)	-71.89(13)
C(31)-C(30)-P(2)-C(28)	6.71(15)
C(35)-C(30)-P(2)-C(28)	-175.46(12)
C(27)-C(28)-P(2)-C(37)	-10.36(15)
C(29)-C(28)-P(2)-C(37)	167.27(12)
C(27)-C(28)-P(2)-C(30)	93.34(14)
C(29)-C(28)-P(2)-C(30)	-89.03(13)

Table 17: Hydrogen bonds for (4, 5-bis(di-*p*-tolylphosphino)-9,9-dimethyl xanthene)

D-H...A	d(D-H)	d(H...A)	d(D...A)	<(DHA)
---------	--------	----------	----------	--------

Structure diagram of (Co((4,5-di-*p*-tolylphosphine)-9,9-dimethyl xanthene)Cl₂)

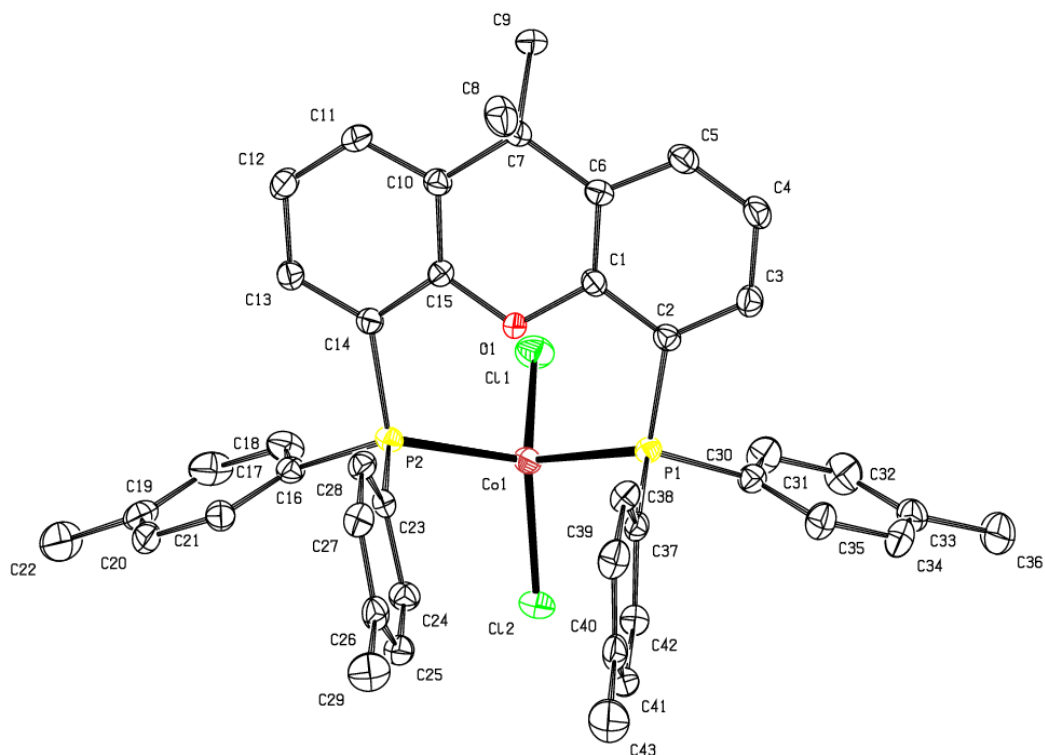


Table 18: Crystal data and structure refinement for (Co(4,5-bis(di-*p*-tolylphosphino)-9,9-dimethyl xanthene)Cl₂)

Empirical formula	C ₄₃ H ₄₀ Cl ₂ Co O P ₂	
Formula weight	764.52	
Temperature	173(2) K	
Wavelength	0.71073 Å	
Crystal system	Triclinic	
Space group	P-1	
Unit cell dimensions	a = 10.2166(3) Å	a = 74.7610(10)°.
	b = 11.0261(3) Å	b = 86.7170(10)°.
	c = 17.6982(5) Å	g = 83.0110(10)°.
Volume	1908.63(9) Å ³	
Z	2	
Density (calculated)	1.330 Mg/m ³	

Absorption coefficient	0.706 mm ⁻¹
F(000)	794
Crystal size	0.25 x 0.24 x 0.12 mm ³
Theta range for data collection	1.19 to 28.00°.
Index ranges	-13<=h<=13, -14<=k<=14, -23<=l<=23
Reflections collected	54347
Independent reflections	9060 [R(int) = 0.0258]
Completeness to theta = 28.00°	98.2 %
Absorption correction	Semi-empirical from equivalents
Max. and min. transmission	0.9201 and 0.8432
Refinement method	Full-matrix least-squares on F ²
Data / restraints / parameters	9060 / 0 / 448
Goodness-of-fit on F ²	1.077
Final R indices [I>2sigma(I)]	R1 = 0.0488, wR2 = 0.1178
R indices (all data)	R1 = 0.0563, wR2 = 0.1225
Largest diff. peak and hole	2.070 and -0.748 e.Å ⁻³

Table 19: Atomic coordinates and equivalent isotropic displacement parameters for (Co(4,5-bis(di-*p*-tolylphosphino)-9,9-dimethyl xanthene)Cl₂)

	x	y	z	U(eq)
C(1)	3432(3)	4349(2)	2139(2)	17(1)
C(2)	3328(2)	4281(2)	1368(2)	17(1)
C(3)	3261(3)	5407(3)	777(2)	20(1)
C(4)	3296(3)	6546(3)	967(2)	23(1)
C(5)	3358(3)	6581(3)	1742(2)	23(1)
C(6)	3412(3)	5476(2)	2353(2)	18(1)
C(7)	3434(3)	5510(2)	3211(2)	20(1)
C(8)	4784(3)	5863(3)	3377(2)	32(1)
C(9)	2317(3)	6489(3)	3371(2)	30(1)
C(10)	3238(3)	4206(2)	3746(2)	18(1)
C(11)	3015(3)	4006(3)	4556(2)	22(1)

C(12)	2864(3)	2814(3)	5037(2)	23(1)
C(13)	2923(3)	1775(3)	4723(2)	19(1)
C(14)	3143(2)	1934(2)	3921(2)	17(1)
C(15)	3311(3)	3145(2)	3456(2)	17(1)
C(16)	2649(3)	-637(2)	4169(2)	19(1)
C(17)	1298(3)	-690(3)	4301(2)	27(1)
C(18)	835(3)	-1683(3)	4873(2)	33(1)
C(19)	1703(3)	-2650(3)	5317(2)	30(1)
C(20)	3049(3)	-2587(3)	5182(2)	26(1)
C(21)	3524(3)	-1596(3)	4616(2)	21(1)
C(22)	1186(5)	-3748(3)	5920(2)	47(1)
C(23)	4931(3)	233(2)	3249(2)	16(1)
C(24)	5251(3)	-648(3)	2807(2)	21(1)
C(25)	6560(3)	-1065(3)	2677(2)	23(1)
C(26)	7581(3)	-601(3)	2963(2)	22(1)
C(27)	7254(3)	315(3)	3378(2)	22(1)
C(28)	5942(3)	721(3)	3525(2)	20(1)
C(29)	9000(3)	-1063(3)	2828(2)	33(1)
C(30)	2425(3)	3102(3)	263(2)	20(1)
C(31)	1056(3)	3191(3)	251(2)	28(1)
C(32)	419(3)	3500(3)	-459(2)	33(1)
C(33)	1117(3)	3732(3)	-1169(2)	28(1)
C(34)	2483(3)	3637(3)	-1152(2)	31(1)
C(35)	3144(3)	3322(3)	-448(2)	26(1)
C(36)	397(4)	4079(4)	-1928(2)	41(1)
C(37)	4862(3)	2069(2)	1058(2)	18(1)
C(38)	5970(3)	2570(3)	1224(2)	21(1)
C(39)	7229(3)	1987(3)	1119(2)	27(1)
C(40)	7416(3)	911(3)	838(2)	25(1)
C(41)	6306(3)	395(3)	693(2)	25(1)
C(42)	5044(3)	957(3)	805(2)	22(1)
C(43)	8775(3)	323(4)	673(2)	40(1)
O(1)	3572(2)	3191(2)	2681(1)	21(1)
P(1)	3194(1)	2736(1)	1206(1)	16(1)
P(2)	3199(1)	683(1)	3418(1)	16(1)
Cl(1)	87(1)	2297(1)	2493(1)	29(1)

Cl(2)	2031(1)	-320(1)	1719(1)	24(1)
Co(1)	2025(1)	1340(1)	2212(1)	18(1)

Table 20: Bond lengths [\AA] and angles [$^\circ$] for (Co(4,5-bis(di-*p*-tolylphosphino)-9,9-dimethyl xanthene)Cl₂)

C(1)-O(1)	1.378(3)
C(1)-C(6)	1.389(4)
C(1)-C(2)	1.397(4)
C(2)-C(3)	1.394(4)
C(2)-P(1)	1.821(3)
C(3)-C(4)	1.388(4)
C(3)-H(3)	0.9500
C(4)-C(5)	1.386(4)
C(4)-H(4)	0.9500
C(5)-C(6)	1.397(4)
C(5)-H(5)	0.9500
C(6)-C(7)	1.531(4)
C(7)-C(10)	1.529(4)
C(7)-C(9)	1.540(4)
C(7)-C(8)	1.541(4)
C(8)-H(8A)	0.9800
C(8)-H(8B)	0.9800
C(8)-H(8C)	0.9800
C(9)-H(9A)	0.9800
C(9)-H(9B)	0.9800
C(9)-H(9C)	0.9800
C(10)-C(15)	1.388(4)
C(10)-C(11)	1.402(4)
C(11)-C(12)	1.386(4)
C(11)-H(11)	0.9500
C(12)-C(13)	1.393(4)
C(12)-H(12)	0.9500

C(13)-C(14)	1.392(4)
C(13)-H(13)	0.9500
C(14)-C(15)	1.397(4)
C(14)-P(2)	1.821(3)
C(15)-O(1)	1.372(3)
C(16)-C(17)	1.393(4)
C(16)-C(21)	1.398(4)
C(16)-P(2)	1.816(3)
C(17)-C(18)	1.392(4)
C(17)-H(17)	0.9500
C(18)-C(19)	1.396(5)
C(18)-H(18)	0.9500
C(19)-C(20)	1.389(5)
C(19)-C(22)	1.516(4)
C(20)-C(21)	1.389(4)
C(20)-H(20)	0.9500
C(21)-H(21)	0.9500
C(22)-H(22A)	0.9800
C(22)-H(22B)	0.9800
C(22)-H(22C)	0.9800
C(23)-C(28)	1.388(4)
C(23)-C(24)	1.400(4)
C(23)-P(2)	1.808(3)
C(24)-C(25)	1.387(4)
C(24)-H(24)	0.9500
C(25)-C(26)	1.390(4)
C(25)-H(25)	0.9500
C(26)-C(27)	1.395(4)
C(26)-C(29)	1.505(4)
C(27)-C(28)	1.393(4)
C(27)-H(27)	0.9500
C(28)-H(28)	0.9500
C(29)-H(29A)	0.9800
C(29)-H(29B)	0.9800
C(29)-H(29C)	0.9800
C(30)-C(31)	1.392(4)

C(30)-C(35)	1.399(4)
C(30)-P(1)	1.813(3)
C(31)-C(32)	1.389(4)
C(31)-H(31)	0.9500
C(32)-C(33)	1.388(5)
C(32)-H(32)	0.9500
C(33)-C(34)	1.389(5)
C(33)-C(36)	1.505(4)
C(34)-C(35)	1.393(4)
C(34)-H(34)	0.9500
C(35)-H(35)	0.9500
C(36)-H(36A)	0.9800
C(36)-H(36B)	0.9800
C(36)-H(36C)	0.9800
C(37)-C(38)	1.396(4)
C(37)-C(42)	1.400(4)
C(37)-P(1)	1.805(3)
C(38)-C(39)	1.391(4)
C(38)-H(38)	0.9500
C(39)-C(40)	1.390(4)
C(39)-H(39)	0.9500
C(40)-C(41)	1.394(4)
C(40)-C(43)	1.506(4)
C(41)-C(42)	1.389(4)
C(41)-H(41)	0.9500
C(42)-H(42)	0.9500
C(43)-H(43A)	0.9800
C(43)-H(43B)	0.9800
C(43)-H(43C)	0.9800
P(1)-Co(1)	2.3940(7)
P(2)-Co(1)	2.4050(8)
Cl(1)-Co(1)	2.2213(8)
Cl(2)-Co(1)	2.2248(7)
O(1)-C(1)-C(6)	122.0(2)
O(1)-C(1)-C(2)	114.2(2)
C(6)-C(1)-C(2)	123.7(2)

C(3)-C(2)-C(1)	117.9(2)
C(3)-C(2)-P(1)	124.3(2)
C(1)-C(2)-P(1)	117.75(19)
C(4)-C(3)-C(2)	119.8(3)
C(4)-C(3)-H(3)	120.1
C(2)-C(3)-H(3)	120.1
C(5)-C(4)-C(3)	120.6(3)
C(5)-C(4)-H(4)	119.7
C(3)-C(4)-H(4)	119.7
C(4)-C(5)-C(6)	121.5(3)
C(4)-C(5)-H(5)	119.3
C(6)-C(5)-H(5)	119.3
C(1)-C(6)-C(5)	116.3(2)
C(1)-C(6)-C(7)	121.9(2)
C(5)-C(6)-C(7)	121.8(2)
C(10)-C(7)-C(6)	109.8(2)
C(10)-C(7)-C(9)	109.5(2)
C(6)-C(7)-C(9)	109.2(2)
C(10)-C(7)-C(8)	108.6(2)
C(6)-C(7)-C(8)	109.2(2)
C(9)-C(7)-C(8)	110.5(2)
C(7)-C(8)-H(8A)	109.5
C(7)-C(8)-H(8B)	109.5
H(8A)-C(8)-H(8B)	109.5
C(7)-C(8)-H(8C)	109.5
H(8A)-C(8)-H(8C)	109.5
H(8B)-C(8)-H(8C)	109.5
C(7)-C(9)-H(9A)	109.5
C(7)-C(9)-H(9B)	109.5
H(9A)-C(9)-H(9B)	109.5
C(7)-C(9)-H(9C)	109.5
H(9A)-C(9)-H(9C)	109.5
H(9B)-C(9)-H(9C)	109.5
C(15)-C(10)-C(11)	116.3(2)
C(15)-C(10)-C(7)	121.6(2)
C(11)-C(10)-C(7)	122.1(2)

C(12)-C(11)-C(10)	121.6(2)
C(12)-C(11)-H(11)	119.2
C(10)-C(11)-H(11)	119.2
C(11)-C(12)-C(13)	120.5(3)
C(11)-C(12)-H(12)	119.8
C(13)-C(12)-H(12)	119.8
C(12)-C(13)-C(14)	119.8(2)
C(12)-C(13)-H(13)	120.1
C(14)-C(13)-H(13)	120.1
C(13)-C(14)-C(15)	118.2(2)
C(13)-C(14)-P(2)	125.1(2)
C(15)-C(14)-P(2)	116.75(19)
O(1)-C(15)-C(10)	122.7(2)
O(1)-C(15)-C(14)	113.6(2)
C(10)-C(15)-C(14)	123.7(2)
C(17)-C(16)-C(21)	119.0(3)
C(17)-C(16)-P(2)	118.2(2)
C(21)-C(16)-P(2)	122.8(2)
C(18)-C(17)-C(16)	120.1(3)
C(18)-C(17)-H(17)	120.0
C(16)-C(17)-H(17)	120.0
C(17)-C(18)-C(19)	121.2(3)
C(17)-C(18)-H(18)	119.4
C(19)-C(18)-H(18)	119.4
C(20)-C(19)-C(18)	118.3(3)
C(20)-C(19)-C(22)	121.0(3)
C(18)-C(19)-C(22)	120.7(3)
C(19)-C(20)-C(21)	121.1(3)
C(19)-C(20)-H(20)	119.5
C(21)-C(20)-H(20)	119.5
C(20)-C(21)-C(16)	120.4(3)
C(20)-C(21)-H(21)	119.8
C(16)-C(21)-H(21)	119.8
C(19)-C(22)-H(22A)	109.5
C(19)-C(22)-H(22B)	109.5
H(22A)-C(22)-H(22B)	109.5

C(19)-C(22)-H(22C)	109.5
H(22A)-C(22)-H(22C)	109.5
H(22B)-C(22)-H(22C)	109.5
C(28)-C(23)-C(24)	118.9(2)
C(28)-C(23)-P(2)	123.8(2)
C(24)-C(23)-P(2)	117.3(2)
C(25)-C(24)-C(23)	120.2(3)
C(25)-C(24)-H(24)	119.9
C(23)-C(24)-H(24)	119.9
C(24)-C(25)-C(26)	121.3(3)
C(24)-C(25)-H(25)	119.4
C(26)-C(25)-H(25)	119.4
C(25)-C(26)-C(27)	118.1(3)
C(25)-C(26)-C(29)	121.2(3)
C(27)-C(26)-C(29)	120.7(3)
C(28)-C(27)-C(26)	121.0(3)
C(28)-C(27)-H(27)	119.5
C(26)-C(27)-H(27)	119.5
C(23)-C(28)-C(27)	120.3(3)
C(23)-C(28)-H(28)	119.8
C(27)-C(28)-H(28)	119.8
C(26)-C(29)-H(29A)	109.5
C(26)-C(29)-H(29B)	109.5
H(29A)-C(29)-H(29B)	109.5
C(26)-C(29)-H(29C)	109.5
H(29A)-C(29)-H(29C)	109.5
H(29B)-C(29)-H(29C)	109.5
C(31)-C(30)-C(35)	119.0(3)
C(31)-C(30)-P(1)	118.0(2)
C(35)-C(30)-P(1)	123.0(2)
C(32)-C(31)-C(30)	120.2(3)
C(32)-C(31)-H(31)	119.9
C(30)-C(31)-H(31)	119.9
C(33)-C(32)-C(31)	121.6(3)
C(33)-C(32)-H(32)	119.2
C(31)-C(32)-H(32)	119.2

C(34)-C(33)-C(32)	117.9(3)
C(34)-C(33)-C(36)	121.8(3)
C(32)-C(33)-C(36)	120.3(3)
C(33)-C(34)-C(35)	121.6(3)
C(33)-C(34)-H(34)	119.2
C(35)-C(34)-H(34)	119.2
C(34)-C(35)-C(30)	119.8(3)
C(34)-C(35)-H(35)	120.1
C(30)-C(35)-H(35)	120.1
C(33)-C(36)-H(36A)	109.5
C(33)-C(36)-H(36B)	109.5
H(36A)-C(36)-H(36B)	109.5
C(33)-C(36)-H(36C)	109.5
H(36A)-C(36)-H(36C)	109.5
H(36B)-C(36)-H(36C)	109.5
C(38)-C(37)-C(42)	118.7(2)
C(38)-C(37)-P(1)	123.1(2)
C(42)-C(37)-P(1)	118.1(2)
C(39)-C(38)-C(37)	120.2(3)
C(39)-C(38)-H(38)	119.9
C(37)-C(38)-H(38)	119.9
C(40)-C(39)-C(38)	121.3(3)
C(40)-C(39)-H(39)	119.4
C(38)-C(39)-H(39)	119.4
C(39)-C(40)-C(41)	118.4(3)
C(39)-C(40)-C(43)	121.6(3)
C(41)-C(40)-C(43)	120.0(3)
C(42)-C(41)-C(40)	120.9(3)
C(42)-C(41)-H(41)	119.5
C(40)-C(41)-H(41)	119.5
C(41)-C(42)-C(37)	120.4(3)
C(41)-C(42)-H(42)	119.8
C(37)-C(42)-H(42)	119.8
C(40)-C(43)-H(43A)	109.5
C(40)-C(43)-H(43B)	109.5
H(43A)-C(43)-H(43B)	109.5

C(40)-C(43)-H(43C)	109.5
H(43A)-C(43)-H(43C)	109.5
H(43B)-C(43)-H(43C)	109.5
C(15)-O(1)-C(1)	118.7(2)
C(37)-P(1)-C(30)	105.94(12)
C(37)-P(1)-C(2)	105.89(12)
C(30)-P(1)-C(2)	103.97(12)
C(37)-P(1)-Co(1)	112.13(9)
C(30)-P(1)-Co(1)	112.62(9)
C(2)-P(1)-Co(1)	115.47(9)
C(23)-P(2)-C(16)	105.20(12)
C(23)-P(2)-C(14)	105.56(12)
C(16)-P(2)-C(14)	103.44(12)
C(23)-P(2)-Co(1)	111.47(9)
C(16)-P(2)-Co(1)	117.33(9)
C(14)-P(2)-Co(1)	112.81(9)
Cl(1)-Co(1)-Cl(2)	117.98(3)
Cl(1)-Co(1)-P(1)	110.89(3)
Cl(2)-Co(1)-P(1)	101.69(3)
Cl(1)-Co(1)-P(2)	105.87(3)
Cl(2)-Co(1)-P(2)	108.75(3)
P(1)-Co(1)-P(2)	111.76(3)

Table 21: Anisotropic displacement parameters for (Co(4,5-bis(di-*p*-tolylphosphino)-9,9-dimethyl xanthene)Cl₂)

	U ¹¹	U ²²	U ³³	U ²³	U ¹³	U ¹²
C(1)	17(1)	14(1)	17(1)	-2(1)	1(1)	0(1)
C(2)	16(1)	16(1)	19(1)	-4(1)	1(1)	0(1)
C(3)	21(1)	22(1)	17(1)	-2(1)	1(1)	-1(1)
C(4)	26(1)	17(1)	22(1)	1(1)	3(1)	-2(1)
C(5)	25(1)	16(1)	25(1)	-4(1)	3(1)	-2(1)
C(6)	18(1)	15(1)	21(1)	-6(1)	0(1)	0(1)
C(7)	27(1)	14(1)	20(1)	-5(1)	-3(1)	-1(1)
C(8)	41(2)	24(2)	31(2)	-2(1)	-9(1)	-13(1)
C(9)	45(2)	21(1)	23(2)	-10(1)	-2(1)	9(1)
C(10)	20(1)	16(1)	20(1)	-6(1)	-2(1)	-2(1)
C(11)	28(1)	21(1)	20(1)	-10(1)	0(1)	-3(1)
C(12)	29(1)	25(1)	17(1)	-7(1)	2(1)	-6(1)
C(13)	21(1)	18(1)	18(1)	-4(1)	-1(1)	-2(1)
C(14)	16(1)	16(1)	18(1)	-5(1)	-2(1)	-1(1)
C(15)	19(1)	17(1)	15(1)	-5(1)	-1(1)	-1(1)
C(16)	22(1)	16(1)	19(1)	-6(1)	2(1)	-5(1)
C(17)	23(1)	22(1)	35(2)	-9(1)	4(1)	-2(1)
C(18)	28(2)	30(2)	44(2)	-16(1)	16(1)	-11(1)
C(19)	47(2)	23(1)	23(2)	-12(1)	13(1)	-14(1)
C(20)	41(2)	21(1)	18(1)	-5(1)	-1(1)	-7(1)
C(21)	25(1)	19(1)	21(1)	-5(1)	-3(1)	-6(1)
C(22)	71(3)	32(2)	39(2)	-10(2)	27(2)	-23(2)
C(23)	18(1)	14(1)	15(1)	-1(1)	-1(1)	-1(1)
C(24)	23(1)	19(1)	24(1)	-7(1)	-2(1)	-4(1)
C(25)	27(1)	20(1)	22(1)	-6(1)	2(1)	-3(1)
C(26)	21(1)	23(1)	19(1)	-1(1)	4(1)	-3(1)
C(27)	19(1)	26(1)	21(1)	-6(1)	-1(1)	-6(1)
C(28)	22(1)	20(1)	18(1)	-6(1)	-1(1)	-4(1)
C(29)	21(1)	39(2)	41(2)	-14(2)	5(1)	-4(1)
C(30)	21(1)	20(1)	19(1)	-6(1)	-2(1)	-1(1)

C(31)	20(1)	36(2)	27(2)	-9(1)	-1(1)	0(1)
C(32)	22(1)	40(2)	36(2)	-9(1)	-9(1)	2(1)
C(33)	37(2)	22(1)	26(2)	-7(1)	-14(1)	3(1)
C(34)	38(2)	35(2)	18(1)	-6(1)	-2(1)	-2(1)
C(35)	22(1)	34(2)	21(1)	-6(1)	-1(1)	-1(1)
C(36)	52(2)	38(2)	32(2)	-9(2)	-21(2)	4(2)
C(37)	17(1)	21(1)	13(1)	-3(1)	1(1)	0(1)
C(38)	20(1)	26(1)	19(1)	-8(1)	0(1)	-2(1)
C(39)	19(1)	37(2)	22(1)	-6(1)	1(1)	-3(1)
C(40)	23(1)	31(2)	16(1)	0(1)	2(1)	6(1)
C(41)	32(2)	22(1)	19(1)	-5(1)	3(1)	4(1)
C(42)	23(1)	21(1)	20(1)	-5(1)	-1(1)	-1(1)
C(43)	27(2)	48(2)	40(2)	-8(2)	4(1)	12(2)
O(1)	34(1)	14(1)	13(1)	-3(1)	0(1)	0(1)
P(1)	15(1)	17(1)	16(1)	-6(1)	1(1)	-1(1)
P(2)	17(1)	14(1)	19(1)	-5(1)	-2(1)	-2(1)
Cl(1)	23(1)	29(1)	37(1)	-11(1)	4(1)	2(1)
Cl(2)	24(1)	18(1)	32(1)	-10(1)	-1(1)	-1(1)
Co(1)	19(1)	15(1)	19(1)	-4(1)	0(1)	0(1)

Table 22: Hydrogen coordinates and isotropic displacement parameters for (Co(4,5-bis(di-*p*-tolylphosphino)-9,9-dimethyl xanthene)Cl₂)

	x	y	z	U(eq)
H(3)	3192	5395	246	25
H(4)	3277	7310	563	27
H(5)	3364	7372	1860	27
H(8A)	4807	5873	3928	48
H(8B)	4919	6702	3041	48
H(8C)	5484	5237	3267	48
H(9A)	1463	6223	3296	45
H(9B)	2414	7315	3009	45

H(9C)	2361	6550	3912	45
H(11)	2965	4704	4781	26
H(12)	2720	2705	5585	28
H(13)	2814	961	5055	23
H(17)	691	-47	4001	32
H(18)	-89	-1704	4964	39
H(20)	3655	-3232	5482	32
H(21)	4448	-1571	4532	26
H(22A)	1928	-4304	6196	70
H(22B)	699	-4226	5657	70
H(22C)	597	-3425	6297	70
H(24)	4569	-962	2594	25
H(25)	6763	-1680	2387	28
H(27)	7937	667	3562	26
H(28)	5739	1334	3816	23
H(29A)	9341	-1658	3308	50
H(29B)	9521	-342	2682	50
H(29C)	9062	-1489	2404	50
H(31)	555	3039	729	34
H(32)	-516	3554	-458	39
H(34)	2979	3790	-1631	37
H(35)	4080	3258	-450	31
H(36A)	-262	3491	-1900	61
H(36B)	1028	4028	-2360	61
H(36C)	-44	4943	-2018	61
H(38)	5865	3311	1409	26
H(39)	7974	2330	1241	32
H(41)	6415	-353	514	30
H(42)	4299	586	710	26
H(43A)	9002	629	115	61
H(43B)	8790	-599	810	61
H(43C)	9417	557	985	61

Table 23: Torsion angles for (Co(4,5-di-*p*-tolylphosphino)-9,9-dimethyl xanthene)Cl₂

O(1)-C(1)-C(2)-C(3)	-176.3(2)
C(6)-C(1)-C(2)-C(3)	3.1(4)
O(1)-C(1)-C(2)-P(1)	7.1(3)
C(6)-C(1)-C(2)-P(1)	-173.5(2)
C(1)-C(2)-C(3)-C(4)	-0.2(4)
P(1)-C(2)-C(3)-C(4)	176.2(2)
C(2)-C(3)-C(4)-C(5)	-1.9(4)
C(3)-C(4)-C(5)-C(6)	1.2(4)
O(1)-C(1)-C(6)-C(5)	175.6(2)
C(2)-C(1)-C(6)-C(5)	-3.7(4)
O(1)-C(1)-C(6)-C(7)	-4.9(4)
C(2)-C(1)-C(6)-C(7)	175.8(2)
C(4)-C(5)-C(6)-C(1)	1.5(4)
C(4)-C(5)-C(6)-C(7)	-177.9(3)
C(1)-C(6)-C(7)-C(10)	-9.8(4)
C(5)-C(6)-C(7)-C(10)	169.6(2)
C(1)-C(6)-C(7)-C(9)	-129.9(3)
C(5)-C(6)-C(7)-C(9)	49.6(3)
C(1)-C(6)-C(7)-C(8)	109.2(3)
C(5)-C(6)-C(7)-C(8)	-71.4(3)
C(6)-C(7)-C(10)-C(15)	11.9(4)
C(9)-C(7)-C(10)-C(15)	131.8(3)
C(8)-C(7)-C(10)-C(15)	-107.5(3)
C(6)-C(7)-C(10)-C(11)	-170.0(3)
C(9)-C(7)-C(10)-C(11)	-50.1(3)
C(8)-C(7)-C(10)-C(11)	70.6(3)
C(15)-C(10)-C(11)-C(12)	-0.5(4)
C(7)-C(10)-C(11)-C(12)	-178.7(3)
C(10)-C(11)-C(12)-C(13)	-0.4(4)
C(11)-C(12)-C(13)-C(14)	0.4(4)
C(12)-C(13)-C(14)-C(15)	0.6(4)
C(12)-C(13)-C(14)-P(2)	-178.1(2)
C(11)-C(10)-C(15)-O(1)	-177.6(2)

C(7)-C(10)-C(15)-O(1)	0.6(4)
C(11)-C(10)-C(15)-C(14)	1.6(4)
C(7)-C(10)-C(15)-C(14)	179.8(2)
C(13)-C(14)-C(15)-O(1)	177.6(2)
P(2)-C(14)-C(15)-O(1)	-3.6(3)
C(13)-C(14)-C(15)-C(10)	-1.6(4)
P(2)-C(14)-C(15)-C(10)	177.2(2)
C(21)-C(16)-C(17)-C(18)	0.3(4)
P(2)-C(16)-C(17)-C(18)	-179.7(2)
C(16)-C(17)-C(18)-C(19)	-0.9(5)
C(17)-C(18)-C(19)-C(20)	1.1(5)
C(17)-C(18)-C(19)-C(22)	-178.0(3)
C(18)-C(19)-C(20)-C(21)	-0.7(4)
C(22)-C(19)-C(20)-C(21)	178.4(3)
C(19)-C(20)-C(21)-C(16)	0.1(4)
C(17)-C(16)-C(21)-C(20)	0.1(4)
P(2)-C(16)-C(21)-C(20)	-179.9(2)
C(28)-C(23)-C(24)-C(25)	2.8(4)
P(2)-C(23)-C(24)-C(25)	-177.9(2)
C(23)-C(24)-C(25)-C(26)	-1.6(4)
C(24)-C(25)-C(26)-C(27)	-0.9(4)
C(24)-C(25)-C(26)-C(29)	179.5(3)
C(25)-C(26)-C(27)-C(28)	2.2(4)
C(29)-C(26)-C(27)-C(28)	-178.1(3)
C(24)-C(23)-C(28)-C(27)	-1.5(4)
P(2)-C(23)-C(28)-C(27)	179.3(2)
C(26)-C(27)-C(28)-C(23)	-1.1(4)
C(35)-C(30)-C(31)-C(32)	-0.3(5)
P(1)-C(30)-C(31)-C(32)	178.4(3)
C(30)-C(31)-C(32)-C(33)	-0.2(5)
C(31)-C(32)-C(33)-C(34)	0.5(5)
C(31)-C(32)-C(33)-C(36)	-179.3(3)
C(32)-C(33)-C(34)-C(35)	-0.2(5)
C(36)-C(33)-C(34)-C(35)	179.7(3)
C(33)-C(34)-C(35)-C(30)	-0.4(5)
C(31)-C(30)-C(35)-C(34)	0.6(4)

P(1)-C(30)-C(35)-C(34)	-178.0(2)
C(42)-C(37)-C(38)-C(39)	1.6(4)
P(1)-C(37)-C(38)-C(39)	178.0(2)
C(37)-C(38)-C(39)-C(40)	0.9(4)
C(38)-C(39)-C(40)-C(41)	-2.5(4)
C(38)-C(39)-C(40)-C(43)	175.9(3)
C(39)-C(40)-C(41)-C(42)	1.6(4)
C(43)-C(40)-C(41)-C(42)	-176.8(3)
C(40)-C(41)-C(42)-C(37)	0.9(4)
C(38)-C(37)-C(42)-C(41)	-2.5(4)
P(1)-C(37)-C(42)-C(41)	-179.1(2)
C(10)-C(15)-O(1)-C(1)	-16.7(4)
C(14)-C(15)-O(1)-C(1)	164.1(2)
C(6)-C(1)-O(1)-C(15)	18.8(4)
C(2)-C(1)-O(1)-C(15)	-161.8(2)
C(38)-C(37)-P(1)-C(30)	122.9(2)
C(42)-C(37)-P(1)-C(30)	-60.7(2)
C(38)-C(37)-P(1)-C(2)	12.9(3)
C(42)-C(37)-P(1)-C(2)	-170.7(2)
C(38)-C(37)-P(1)-Co(1)	-113.9(2)
C(42)-C(37)-P(1)-Co(1)	62.5(2)
C(31)-C(30)-P(1)-C(37)	157.1(2)
C(35)-C(30)-P(1)-C(37)	-24.2(3)
C(31)-C(30)-P(1)-C(2)	-91.5(2)
C(35)-C(30)-P(1)-C(2)	87.2(3)
C(31)-C(30)-P(1)-Co(1)	34.2(3)
C(35)-C(30)-P(1)-Co(1)	-147.1(2)
C(3)-C(2)-P(1)-C(37)	92.5(2)
C(1)-C(2)-P(1)-C(37)	-91.1(2)
C(3)-C(2)-P(1)-C(30)	-18.9(3)
C(1)-C(2)-P(1)-C(30)	157.5(2)
C(3)-C(2)-P(1)-Co(1)	-142.8(2)
C(1)-C(2)-P(1)-Co(1)	33.6(2)
C(28)-C(23)-P(2)-C(16)	-104.4(2)
C(24)-C(23)-P(2)-C(16)	76.4(2)
C(28)-C(23)-P(2)-C(14)	4.6(3)

C(24)-C(23)-P(2)-C(14)	-174.6(2)
C(28)-C(23)-P(2)-Co(1)	127.4(2)
C(24)-C(23)-P(2)-Co(1)	-51.8(2)
C(17)-C(16)-P(2)-C(23)	-166.2(2)
C(21)-C(16)-P(2)-C(23)	13.8(3)
C(17)-C(16)-P(2)-C(14)	83.3(2)
C(21)-C(16)-P(2)-C(14)	-96.7(2)
C(17)-C(16)-P(2)-Co(1)	-41.6(2)
C(21)-C(16)-P(2)-Co(1)	138.3(2)
C(13)-C(14)-P(2)-C(23)	-101.4(2)
C(15)-C(14)-P(2)-C(23)	79.8(2)
C(13)-C(14)-P(2)-C(16)	8.8(3)
C(15)-C(14)-P(2)-C(16)	-169.9(2)
C(13)-C(14)-P(2)-Co(1)	136.6(2)
C(15)-C(14)-P(2)-Co(1)	-42.1(2)
C(37)-P(1)-Co(1)-Cl(1)	171.92(10)
C(30)-P(1)-Co(1)-Cl(1)	-68.71(10)
C(2)-P(1)-Co(1)-Cl(1)	50.51(10)
C(37)-P(1)-Co(1)-Cl(2)	-61.80(10)
C(30)-P(1)-Co(1)-Cl(2)	57.57(10)
C(2)-P(1)-Co(1)-Cl(2)	176.79(10)
C(37)-P(1)-Co(1)-P(2)	54.05(10)
C(30)-P(1)-Co(1)-P(2)	173.42(10)
C(2)-P(1)-Co(1)-P(2)	-67.36(10)
C(23)-P(2)-Co(1)-Cl(1)	-166.03(9)
C(16)-P(2)-Co(1)-Cl(1)	72.60(10)
C(14)-P(2)-Co(1)-Cl(1)	-47.48(10)
C(23)-P(2)-Co(1)-Cl(2)	66.26(9)
C(16)-P(2)-Co(1)-Cl(2)	-55.10(10)
C(14)-P(2)-Co(1)-Cl(2)	-175.18(9)
C(23)-P(2)-Co(1)-P(1)	-45.20(9)
C(16)-P(2)-Co(1)-P(1)	-166.56(10)
C(14)-P(2)-Co(1)-P(1)	73.36(10)

Structure diagram of complex (Ni(4,5-bis(di-*p*-tolylphosphino)-9,9-dimethyl xanthene)Cl₂)

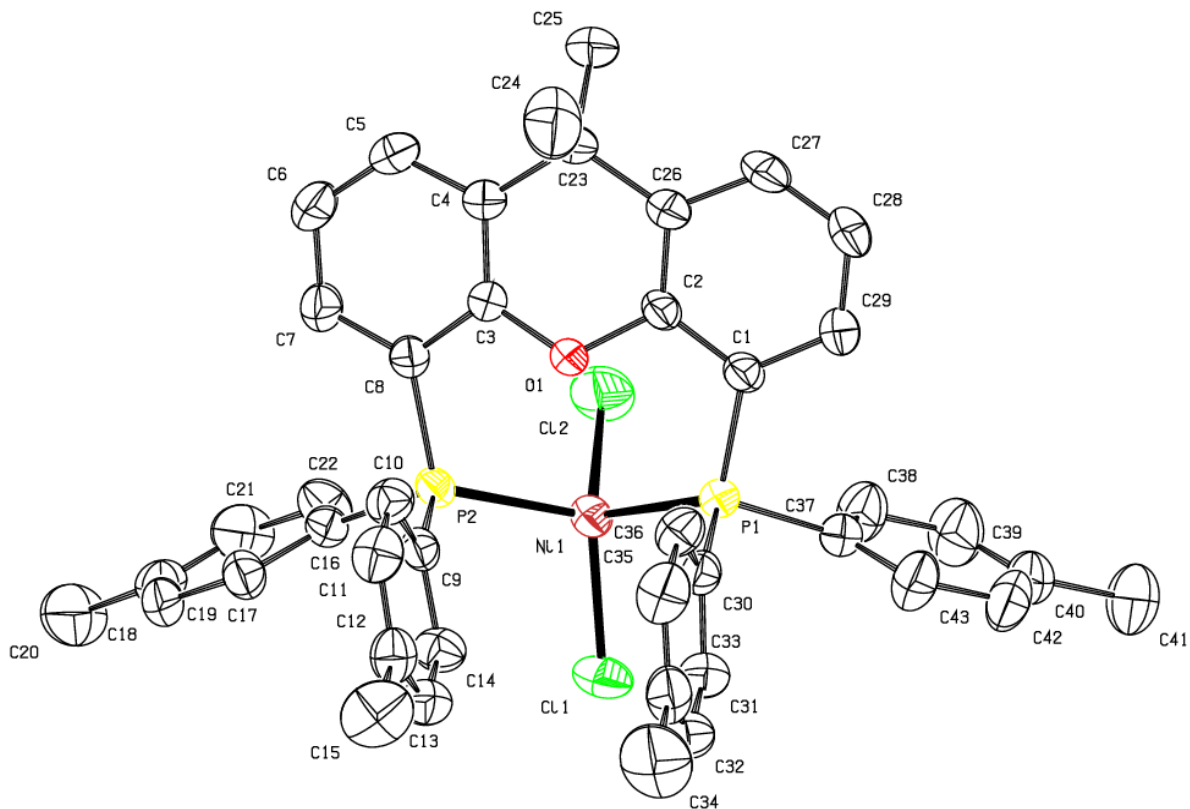


Table 24: Crystal data and structure refinement for (Ni(4,5-bis(di-*p*-tolylphosphino)-9,9-dimethyl xanthene)Cl₂)

Empirical formula	C ₄₃ H ₄₀ Cl ₂ Ni O P ₂	
Formula weight	764.30	
Temperature	173(2) K	
Wavelength	0.71073 Å	
Crystal system	Triclinic	
Space group	P -1	
Unit cell dimensions	a = 10.2501(3) Å	a = 73.9650(10)°.
	b = 11.1611(3) Å	b = 86.322(2)°.
	c = 17.7687(5) Å	g = 83.512(2)°.

Volume	1940.03(10) Å ³
Z	2
Density (calculated)	1.308 Mg/m ³
Absorption coefficient	0.752 mm ⁻¹
F(000)	796
Crystal size	0.586 x 0.529 x 0.382 mm ³
Theta range for data collection	1.193 to 28.393°.
Index ranges	-13<=h<=12, -14<=k<=14, -23<=l<=23
Reflections collected	58526
Independent reflections	9650 [R(int) = 0.0311]
Completeness to theta = 25.242°	100.0 %
Absorption correction	Semi-empirical from equivalents
Max. and min. transmission	0.750 and 0.637
Refinement method	Full-matrix least-squares on F ²
Data / restraints / parameters	9650 / 2 / 448
Goodness-of-fit on F ²	1.014
Final R indices [I>2sigma(I)]	R1 = 0.0327, wR2 = 0.0786
R indices (all data)	R1 = 0.0512, wR2 = 0.0878
Extinction coefficient	n/a
Largest diff. peak and hole	0.419 and -0.256 e.Å ⁻³

Table 25: Atomic coordinates and equivalent isotropic displacement parameters for (Ni(4,5-bis(di-*p*-tolylphosphino)-9,9-dimethyl xanthene)Cl₂)

	x	y	z	U(eq)
C(1)	3402(2)	4222(2)	1366(1)	32(1)
C(2)	3546(2)	4324(1)	2118(1)	32(1)
C(3)	3455(2)	3135(2)	3433(1)	33(1)
C(4)	3307(2)	4184(2)	3710(1)	38(1)
C(5)	2996(2)	3974(2)	4509(1)	49(1)
C(6)	2837(2)	2791(2)	4984(1)	51(1)
C(7)	2954(2)	1771(2)	4678(1)	43(1)

C(8)	3265(2)	1933(2)	3887(1)	34(1)
C(9)	5061(2)	263(2)	3221(1)	33(1)
C(10)	6070(2)	746(2)	3494(1)	42(1)
C(11)	7364(2)	321(2)	3373(1)	48(1)
C(12)	7696(2)	-596(2)	2989(1)	46(1)
C(13)	6684(2)	-1056(2)	2706(1)	47(1)
C(14)	5390(2)	-625(2)	2811(1)	42(1)
C(15)	9103(2)	-1082(3)	2878(2)	76(1)
C(16)	2752(2)	-600(2)	4120(1)	36(1)
C(17)	3599(2)	-1567(2)	4558(1)	43(1)
C(18)	3102(2)	-2544(2)	5125(1)	52(1)
C(19)	1773(3)	-2597(2)	5274(1)	56(1)
C(20)	1229(4)	-3682(2)	5876(2)	92(1)
C(21)	938(3)	-1620(2)	4846(1)	62(1)
C(22)	1419(2)	-636(2)	4272(1)	52(1)
C(23)	3510(2)	5475(2)	3166(1)	46(1)
C(24)	4878(3)	5801(3)	3292(2)	82(1)
C(25)	2431(3)	6453(2)	3340(1)	78(1)
C(26)	3437(2)	5443(2)	2316(1)	38(1)
C(27)	3263(2)	6526(2)	1699(1)	48(1)
C(28)	3178(2)	6468(2)	938(1)	49(1)
C(29)	3223(2)	5327(2)	768(1)	41(1)
C(30)	4988(2)	2040(2)	1090(1)	35(1)
C(31)	5191(2)	986(2)	808(1)	45(1)
C(32)	6447(2)	468(2)	691(1)	53(1)
C(33)	7531(2)	956(2)	867(1)	54(1)
C(34)	8897(3)	399(3)	712(2)	92(1)
C(35)	7327(2)	1974(2)	1170(1)	55(1)
C(36)	6069(2)	2525(2)	1276(1)	44(1)
C(37)	2541(2)	3009(2)	309(1)	37(1)
C(38)	1194(2)	3160(2)	299(1)	57(1)
C(39)	549(3)	3506(3)	-403(2)	69(1)
C(40)	1240(3)	3685(2)	-1110(1)	61(1)
C(41)	523(3)	4062(3)	-1874(2)	94(1)
C(42)	2580(3)	3526(2)	-1094(1)	67(1)
C(43)	3247(2)	3186(2)	-397(1)	55(1)

O(1)	3828(1)	3195(1)	2669(1)	37(1)
P(1)	3315(1)	2665(1)	1248(1)	31(1)
P(2)	3336(1)	722(1)	3374(1)	32(1)
Cl(1)	2260(1)	-311(1)	1745(1)	52(1)
Cl(2)	367(1)	2401(1)	2560(1)	66(1)
Ni(1)	2127(1)	1319(1)	2229(1)	33(1)

Table 26: Bond lengths [\AA] and angles [$^\circ$] for (Ni(4,5-bis(di-*p*-tolylphosphino)-9,9-dimethyl xanthene)Cl₂)

C(1)-C(2)	1.390(2)
C(1)-C(29)	1.390(2)
C(1)-P(1)	1.8200(16)
C(2)-O(1)	1.3793(18)
C(2)-C(26)	1.379(2)
C(3)-O(1)	1.3723(19)
C(3)-C(4)	1.380(2)
C(3)-C(8)	1.389(2)
C(4)-C(5)	1.396(3)
C(4)-C(23)	1.526(2)
C(5)-C(6)	1.377(3)
C(5)-H(5)	0.9500
C(6)-C(7)	1.381(3)
C(6)-H(6)	0.9500
C(7)-C(8)	1.387(2)
C(7)-H(7)	0.9500
C(8)-P(2)	1.8205(17)
C(9)-C(14)	1.385(2)
C(9)-C(10)	1.389(2)
C(9)-P(2)	1.8091(18)
C(10)-C(11)	1.381(3)
C(10)-H(10)	0.9500
C(11)-C(12)	1.380(3)

C(11)-H(11)	0.9500
C(12)-C(13)	1.386(3)
C(12)-C(15)	1.503(3)
C(13)-C(14)	1.378(3)
C(13)-H(13)	0.9500
C(14)-H(14)	0.9500
C(15)-H(15A)	0.9800
C(15)-H(15B)	0.9800
C(15)-H(15C)	0.9800
C(16)-C(22)	1.379(3)
C(16)-C(17)	1.391(3)
C(16)-P(2)	1.8193(17)
C(17)-C(18)	1.385(3)
C(17)-H(17)	0.9500
C(18)-C(19)	1.376(3)
C(18)-H(18)	0.9500
C(19)-C(21)	1.383(3)
C(19)-C(20)	1.511(3)
C(20)-H(20A)	0.9800
C(20)-H(20B)	0.9800
C(20)-H(20C)	0.9800
C(21)-C(22)	1.389(3)
C(21)-H(21)	0.9500
C(22)-H(22)	0.9500
C(23)-C(26)	1.527(3)
C(23)-C(24)	1.533(3)
C(23)-C(25)	1.542(3)
C(24)-H(24A)	0.9800
C(24)-H(24B)	0.9800
C(24)-H(24C)	0.9800
C(25)-H(25A)	0.9800
C(25)-H(25B)	0.9800
C(25)-H(25C)	0.9800
C(26)-C(27)	1.392(2)
C(27)-C(28)	1.380(3)
C(27)-H(27)	0.9500

C(28)-C(29)	1.383(3)
C(28)-H(28)	0.9500
C(29)-H(29)	0.9500
C(30)-C(36)	1.382(3)
C(30)-C(31)	1.391(3)
C(30)-P(1)	1.8109(18)
C(31)-C(32)	1.378(3)
C(31)-H(31)	0.9500
C(32)-C(33)	1.379(3)
C(32)-H(32)	0.9500
C(33)-C(35)	1.376(3)
C(33)-C(34)	1.507(3)
C(34)-H(34A)	0.9800
C(34)-H(34B)	0.9800
C(34)-H(34C)	0.9800
C(35)-C(36)	1.390(3)
C(35)-H(35)	0.9500
C(36)-H(36)	0.9500
C(37)-C(38)	1.373(3)
C(37)-C(43)	1.384(3)
C(37)-P(1)	1.8191(18)
C(38)-C(39)	1.386(3)
C(38)-H(38)	0.9500
C(39)-C(40)	1.377(4)
C(39)-H(39)	0.9500
C(40)-C(42)	1.365(4)
C(40)-C(41)	1.517(3)
C(41)-H(41A)	0.9800
C(41)-H(41B)	0.9800
C(41)-H(41C)	0.9800
C(42)-C(43)	1.392(3)
C(42)-H(42)	0.9500
C(43)-H(43)	0.9500
P(1)-Ni(1)	2.3398(5)
P(2)-Ni(1)	2.3469(5)
Cl(1)-Ni(1)	2.2048(5)

Cl(2)-Ni(1)	2.1964(6)
C(2)-C(1)-C(29)	117.49(15)
C(2)-C(1)-P(1)	117.81(12)
C(29)-C(1)-P(1)	124.46(13)
O(1)-C(2)-C(26)	121.36(15)
O(1)-C(2)-C(1)	114.31(14)
C(26)-C(2)-C(1)	124.32(15)
O(1)-C(3)-C(4)	121.99(15)
O(1)-C(3)-C(8)	113.66(14)
C(4)-C(3)-C(8)	124.35(15)
C(3)-C(4)-C(5)	115.83(16)
C(3)-C(4)-C(23)	120.89(15)
C(5)-C(4)-C(23)	123.27(16)
C(6)-C(5)-C(4)	121.55(17)
C(6)-C(5)-H(5)	119.2
C(4)-C(5)-H(5)	119.2
C(5)-C(6)-C(7)	120.78(17)
C(5)-C(6)-H(6)	119.6
C(7)-C(6)-H(6)	119.6
C(6)-C(7)-C(8)	119.78(17)
C(6)-C(7)-H(7)	120.1
C(8)-C(7)-H(7)	120.1
C(7)-C(8)-C(3)	117.66(16)
C(7)-C(8)-P(2)	125.56(13)
C(3)-C(8)-P(2)	116.63(12)
C(14)-C(9)-C(10)	118.29(17)
C(14)-C(9)-P(2)	117.90(14)
C(10)-C(9)-P(2)	123.81(14)
C(11)-C(10)-C(9)	120.32(18)
C(11)-C(10)-H(10)	119.8
C(9)-C(10)-H(10)	119.8
C(12)-C(11)-C(10)	121.62(18)
C(12)-C(11)-H(11)	119.2
C(10)-C(11)-H(11)	119.2
C(11)-C(12)-C(13)	117.67(19)

C(11)-C(12)-C(15)	121.5(2)
C(13)-C(12)-C(15)	120.9(2)
C(14)-C(13)-C(12)	121.27(18)
C(14)-C(13)-H(13)	119.4
C(12)-C(13)-H(13)	119.4
C(13)-C(14)-C(9)	120.76(17)
C(13)-C(14)-H(14)	119.6
C(9)-C(14)-H(14)	119.6
C(12)-C(15)-H(15A)	109.5
C(12)-C(15)-H(15B)	109.5
H(15A)-C(15)-H(15B)	109.5
C(12)-C(15)-H(15C)	109.5
H(15A)-C(15)-H(15C)	109.5
H(15B)-C(15)-H(15C)	109.5
C(22)-C(16)-C(17)	118.43(17)
C(22)-C(16)-P(2)	118.94(14)
C(17)-C(16)-P(2)	122.62(15)
C(18)-C(17)-C(16)	120.2(2)
C(18)-C(17)-H(17)	119.9
C(16)-C(17)-H(17)	119.9
C(19)-C(18)-C(17)	121.8(2)
C(19)-C(18)-H(18)	119.1
C(17)-C(18)-H(18)	119.1
C(18)-C(19)-C(21)	117.60(19)
C(18)-C(19)-C(20)	121.8(2)
C(21)-C(19)-C(20)	120.6(2)
C(19)-C(20)-H(20A)	109.5
C(19)-C(20)-H(20B)	109.5
H(20A)-C(20)-H(20B)	109.5
C(19)-C(20)-H(20C)	109.5
H(20A)-C(20)-H(20C)	109.5
H(20B)-C(20)-H(20C)	109.5
C(19)-C(21)-C(22)	121.4(2)
C(19)-C(21)-H(21)	119.3
C(22)-C(21)-H(21)	119.3
C(16)-C(22)-C(21)	120.5(2)

C(16)-C(22)-H(22)	119.7
C(21)-C(22)-H(22)	119.7
C(4)-C(23)-C(26)	109.39(14)
C(4)-C(23)-C(24)	108.54(18)
C(26)-C(23)-C(24)	108.83(19)
C(4)-C(23)-C(25)	109.70(18)
C(26)-C(23)-C(25)	109.38(17)
C(24)-C(23)-C(25)	111.0(2)
C(23)-C(24)-H(24A)	109.5
C(23)-C(24)-H(24B)	109.5
H(24A)-C(24)-H(24B)	109.5
C(23)-C(24)-H(24C)	109.5
H(24A)-C(24)-H(24C)	109.5
H(24B)-C(24)-H(24C)	109.5
C(23)-C(25)-H(25A)	109.5
C(23)-C(25)-H(25B)	109.5
H(25A)-C(25)-H(25B)	109.5
C(23)-C(25)-H(25C)	109.5
H(25A)-C(25)-H(25C)	109.5
H(25B)-C(25)-H(25C)	109.5
C(2)-C(26)-C(27)	116.14(16)
C(2)-C(26)-C(23)	121.27(15)
C(27)-C(26)-C(23)	122.59(15)
C(28)-C(27)-C(26)	121.32(17)
C(28)-C(27)-H(27)	119.3
C(26)-C(27)-H(27)	119.3
C(27)-C(28)-C(29)	120.80(17)
C(27)-C(28)-H(28)	119.6
C(29)-C(28)-H(28)	119.6
C(28)-C(29)-C(1)	119.74(17)
C(28)-C(29)-H(29)	120.1
C(1)-C(29)-H(29)	120.1
C(36)-C(30)-C(31)	118.55(17)
C(36)-C(30)-P(1)	122.84(14)
C(31)-C(30)-P(1)	118.52(14)
C(32)-C(31)-C(30)	120.4(2)

C(32)-C(31)-H(31)	119.8
C(30)-C(31)-H(31)	119.8
C(31)-C(32)-C(33)	121.3(2)
C(31)-C(32)-H(32)	119.4
C(33)-C(32)-H(32)	119.4
C(35)-C(33)-C(32)	118.21(19)
C(35)-C(33)-C(34)	121.3(2)
C(32)-C(33)-C(34)	120.5(2)
C(33)-C(34)-H(34A)	109.5
C(33)-C(34)-H(34B)	109.5
H(34A)-C(34)-H(34B)	109.5
C(33)-C(34)-H(34C)	109.5
H(34A)-C(34)-H(34C)	109.5
H(34B)-C(34)-H(34C)	109.5
C(33)-C(35)-C(36)	121.3(2)
C(33)-C(35)-H(35)	119.3
C(36)-C(35)-H(35)	119.3
C(30)-C(36)-C(35)	120.17(19)
C(30)-C(36)-H(36)	119.9
C(35)-C(36)-H(36)	119.9
C(38)-C(37)-C(43)	118.67(18)
C(38)-C(37)-P(1)	118.31(15)
C(43)-C(37)-P(1)	122.94(16)
C(37)-C(38)-C(39)	120.9(2)
C(37)-C(38)-H(38)	119.5
C(39)-C(38)-H(38)	119.5
C(40)-C(39)-C(38)	121.0(2)
C(40)-C(39)-H(39)	119.5
C(38)-C(39)-H(39)	119.5
C(42)-C(40)-C(39)	117.7(2)
C(42)-C(40)-C(41)	121.8(2)
C(39)-C(40)-C(41)	120.5(3)
C(40)-C(41)-H(41A)	109.5
C(40)-C(41)-H(41B)	109.5
H(41A)-C(41)-H(41B)	109.5
C(40)-C(41)-H(41C)	109.5

H(41A)-C(41)-H(41C)	109.5
H(41B)-C(41)-H(41C)	109.5
C(40)-C(42)-C(43)	122.3(2)
C(40)-C(42)-H(42)	118.9
C(43)-C(42)-H(42)	118.9
C(37)-C(43)-C(42)	119.4(2)
C(37)-C(43)-H(43)	120.3
C(42)-C(43)-H(43)	120.3
C(3)-O(1)-C(2)	117.23(13)
C(30)-P(1)-C(37)	105.89(8)
C(30)-P(1)-C(1)	106.62(8)
C(37)-P(1)-C(1)	102.34(8)
C(30)-P(1)-Ni(1)	114.08(6)
C(37)-P(1)-Ni(1)	110.87(6)
C(1)-P(1)-Ni(1)	115.95(6)
C(9)-P(2)-C(16)	104.77(8)
C(9)-P(2)-C(8)	106.19(8)
C(16)-P(2)-C(8)	102.87(8)
C(9)-P(2)-Ni(1)	114.32(6)
C(16)-P(2)-Ni(1)	113.94(6)
C(8)-P(2)-Ni(1)	113.65(6)
Cl(2)-Ni(1)-Cl(1)	128.87(3)
Cl(2)-Ni(1)-P(1)	108.62(2)
Cl(1)-Ni(1)-P(1)	99.58(2)
Cl(2)-Ni(1)-P(2)	102.95(2)
Cl(1)-Ni(1)-P(2)	107.39(2)
P(1)-Ni(1)-P(2)	108.403(18)

Table 27: Anisotropic displacement parameters for (Ni(4,5-bis(di-*p*-tolylphosphino)-9,9-dimethyl xanthene)Cl₂)

	U ¹¹	U ²²	U ³³	U ²³	U ¹³	U ¹²
C(1)	36(1)	26(1)	33(1)	-5(1)	3(1)	-2(1)
C(2)	38(1)	24(1)	32(1)	-3(1)	2(1)	-2(1)
C(3)	40(1)	30(1)	28(1)	-8(1)	-3(1)	-1(1)
C(4)	49(1)	31(1)	35(1)	-11(1)	-2(1)	-3(1)
C(5)	69(2)	44(1)	39(1)	-21(1)	1(1)	-5(1)
C(6)	71(2)	53(1)	31(1)	-14(1)	5(1)	-8(1)
C(7)	53(1)	40(1)	33(1)	-5(1)	-1(1)	-8(1)
C(8)	39(1)	31(1)	30(1)	-6(1)	-5(1)	-3(1)
C(9)	38(1)	28(1)	30(1)	-2(1)	-4(1)	-5(1)
C(10)	45(1)	43(1)	40(1)	-14(1)	-3(1)	-9(1)
C(11)	41(1)	59(1)	47(1)	-12(1)	-5(1)	-16(1)
C(12)	39(1)	53(1)	40(1)	-4(1)	3(1)	-8(1)
C(13)	48(1)	45(1)	51(1)	-17(1)	1(1)	-2(1)
C(14)	41(1)	39(1)	52(1)	-17(1)	-7(1)	-7(1)
C(15)	41(1)	104(2)	88(2)	-36(2)	8(1)	-5(1)
C(16)	45(1)	29(1)	34(1)	-8(1)	-3(1)	-7(1)
C(17)	50(1)	36(1)	39(1)	-4(1)	-7(1)	-7(1)
C(18)	81(2)	36(1)	35(1)	-3(1)	-5(1)	-7(1)
C(19)	88(2)	41(1)	40(1)	-13(1)	19(1)	-20(1)
C(20)	138(3)	59(2)	72(2)	-7(1)	49(2)	-30(2)
C(21)	58(2)	58(1)	69(2)	-16(1)	23(1)	-19(1)
C(22)	46(1)	44(1)	60(1)	-7(1)	3(1)	-4(1)
C(23)	71(1)	28(1)	40(1)	-13(1)	-5(1)	-5(1)
C(24)	113(2)	68(2)	68(2)	-3(1)	-23(2)	-49(2)
C(25)	140(3)	42(1)	48(1)	-18(1)	1(1)	23(1)
C(26)	48(1)	28(1)	38(1)	-9(1)	0(1)	-3(1)
C(27)	66(1)	23(1)	51(1)	-7(1)	2(1)	-3(1)
C(28)	67(1)	30(1)	42(1)	3(1)	0(1)	-3(1)
C(29)	52(1)	35(1)	32(1)	-3(1)	0(1)	-4(1)
C(30)	35(1)	39(1)	28(1)	-6(1)	0(1)	0(1)

C(31)	48(1)	43(1)	47(1)	-16(1)	0(1)	0(1)
C(32)	61(2)	48(1)	45(1)	-14(1)	6(1)	12(1)
C(33)	47(1)	62(1)	39(1)	-2(1)	7(1)	14(1)
C(34)	54(2)	107(2)	99(2)	-18(2)	15(2)	26(2)
C(35)	36(1)	76(2)	50(1)	-14(1)	-1(1)	-5(1)
C(36)	39(1)	54(1)	40(1)	-16(1)	1(1)	-5(1)
C(37)	43(1)	35(1)	34(1)	-9(1)	-4(1)	-2(1)
C(38)	45(1)	76(2)	46(1)	-13(1)	-7(1)	2(1)
C(39)	52(2)	87(2)	63(2)	-13(1)	-21(1)	7(1)
C(40)	80(2)	51(1)	50(1)	-13(1)	-28(1)	7(1)
C(41)	121(3)	96(2)	61(2)	-17(2)	-48(2)	16(2)
C(42)	84(2)	79(2)	33(1)	-12(1)	-5(1)	2(1)
C(43)	51(1)	75(2)	36(1)	-12(1)	-1(1)	-1(1)
O(1)	59(1)	24(1)	27(1)	-6(1)	0(1)	1(1)
P(1)	34(1)	29(1)	29(1)	-8(1)	0(1)	-2(1)
P(2)	37(1)	25(1)	32(1)	-5(1)	-4(1)	-3(1)
Cl(1)	55(1)	35(1)	71(1)	-22(1)	-5(1)	-4(1)
Cl(2)	54(1)	66(1)	74(1)	-23(1)	8(1)	15(1)
Ni(1)	34(1)	30(1)	35(1)	-6(1)	-3(1)	-4(1)

Table 28: Hydrogen coordinates and isotropic displacement parameters for (Ni(4,5-bis(di-*p*-tolylphosphino)-9,9-dimethyl xanthene)Cl₂)

	x	y	z	U(eq)
H(5)	2891	4663	4731	59
H(6)	2644	2675	5528	62
H(7)	2822	962	5008	51
H(10)	5869	1371	3765	50
H(11)	8042	668	3558	58
H(13)	6887	-1680	2434	57

H(14)	4717	-940	2600	51
H(15A)	9641	-376	2704	114
H(15B)	9165	-1549	2482	114
H(15C)	9422	-1637	3375	114
H(17)	4522	-1557	4467	51
H(18)	3695	-3195	5420	62
H(20A)	671	-3367	6262	139
H(20B)	1956	-4260	6140	139
H(20C)	708	-4125	5616	139
H(21)	17	-1623	4946	75
H(22)	824	19	3982	62
H(24A)	5546	5175	3170	123
H(24B)	4942	5806	3839	123
H(24C)	5021	6631	2947	123
H(25A)	2552	7277	2981	118
H(25B)	2490	6488	3882	118
H(25C)	1566	6214	3268	118
H(27)	3202	7320	1804	57
H(28)	3088	7221	526	59
H(29)	3131	5298	245	49
H(31)	4459	622	695	54
H(32)	6569	-239	485	64
H(34A)	8904	-510	811	138
H(34B)	9508	581	1059	138
H(34C)	9169	765	165	138
H(35)	8061	2307	1308	66
H(36)	5951	3236	1477	52
H(38)	696	3026	779	68
H(39)	-384	3621	-397	83
H(41A)	-1	4869	-1923	141
H(41B)	-56	3423	-1877	141
H(41C)	1164	4138	-2314	141
H(42)	3073	3651	-1576	80
H(43)	4180	3078	-406	66

Table 29: Torsion angles for (Ni(4,5-bis(di-*p*-tolylphosphino)-9,9-dimethyl xanthene)Cl₂)

C(29)-C(1)-C(2)-O(1)	-174.93(16)
P(1)-C(1)-C(2)-O(1)	10.4(2)
C(29)-C(1)-C(2)-C(26)	4.4(3)
P(1)-C(1)-C(2)-C(26)	-170.21(15)
O(1)-C(3)-C(4)-C(5)	-176.53(17)
C(8)-C(3)-C(4)-C(5)	2.6(3)
O(1)-C(3)-C(4)-C(23)	2.1(3)
C(8)-C(3)-C(4)-C(23)	-178.78(18)
C(3)-C(4)-C(5)-C(6)	-0.6(3)
C(23)-C(4)-C(5)-C(6)	-179.2(2)
C(4)-C(5)-C(6)-C(7)	-1.4(4)
C(5)-C(6)-C(7)-C(8)	1.5(3)
C(6)-C(7)-C(8)-C(3)	0.4(3)
C(6)-C(7)-C(8)-P(2)	-175.08(16)
O(1)-C(3)-C(8)-C(7)	176.66(16)
C(4)-C(3)-C(8)-C(7)	-2.5(3)
O(1)-C(3)-C(8)-P(2)	-7.5(2)
C(4)-C(3)-C(8)-P(2)	173.34(15)
C(14)-C(9)-C(10)-C(11)	-1.6(3)
P(2)-C(9)-C(10)-C(11)	178.12(14)
C(9)-C(10)-C(11)-C(12)	-0.7(3)
C(10)-C(11)-C(12)-C(13)	1.9(3)
C(10)-C(11)-C(12)-C(15)	-178.3(2)
C(11)-C(12)-C(13)-C(14)	-0.8(3)
C(15)-C(12)-C(13)-C(14)	179.4(2)
C(12)-C(13)-C(14)-C(9)	-1.5(3)
C(10)-C(9)-C(14)-C(13)	2.7(3)
P(2)-C(9)-C(14)-C(13)	-177.03(15)
C(22)-C(16)-C(17)-C(18)	0.7(3)
P(2)-C(16)-C(17)-C(18)	179.25(14)
C(16)-C(17)-C(18)-C(19)	0.2(3)
C(17)-C(18)-C(19)-C(21)	-1.3(3)
C(17)-C(18)-C(19)-C(20)	178.1(2)

C(18)-C(19)-C(21)-C(22)	1.6(3)
C(20)-C(19)-C(21)-C(22)	-177.9(2)
C(17)-C(16)-C(22)-C(21)	-0.4(3)
P(2)-C(16)-C(22)-C(21)	-179.03(17)
C(19)-C(21)-C(22)-C(16)	-0.7(4)
C(3)-C(4)-C(23)-C(26)	17.9(3)
C(5)-C(4)-C(23)-C(26)	-163.64(19)
C(3)-C(4)-C(23)-C(24)	-100.8(2)
C(5)-C(4)-C(23)-C(24)	77.7(3)
C(3)-C(4)-C(23)-C(25)	137.8(2)
C(5)-C(4)-C(23)-C(25)	-43.7(3)
O(1)-C(2)-C(26)-C(27)	174.63(17)
C(1)-C(2)-C(26)-C(27)	-4.7(3)
O(1)-C(2)-C(26)-C(23)	-5.2(3)
C(1)-C(2)-C(26)-C(23)	175.51(18)
C(4)-C(23)-C(26)-C(2)	-16.4(3)
C(24)-C(23)-C(26)-C(2)	102.1(2)
C(25)-C(23)-C(26)-C(2)	-136.5(2)
C(4)-C(23)-C(26)-C(27)	163.86(19)
C(24)-C(23)-C(26)-C(27)	-77.7(3)
C(25)-C(23)-C(26)-C(27)	43.7(3)
C(2)-C(26)-C(27)-C(28)	1.4(3)
C(23)-C(26)-C(27)-C(28)	-178.9(2)
C(26)-C(27)-C(28)-C(29)	2.0(3)
C(27)-C(28)-C(29)-C(1)	-2.3(3)
C(2)-C(1)-C(29)-C(28)	-0.8(3)
P(1)-C(1)-C(29)-C(28)	173.50(16)
C(36)-C(30)-C(31)-C(32)	-2.3(3)
P(1)-C(30)-C(31)-C(32)	-178.99(15)
C(30)-C(31)-C(32)-C(33)	1.6(3)
C(31)-C(32)-C(33)-C(35)	0.5(3)
C(31)-C(32)-C(33)-C(34)	-178.1(2)
C(32)-C(33)-C(35)-C(36)	-1.8(3)
C(34)-C(33)-C(35)-C(36)	176.8(2)
C(31)-C(30)-C(36)-C(35)	1.0(3)
P(1)-C(30)-C(36)-C(35)	177.52(15)

C(33)-C(35)-C(36)-C(30)	1.1(3)
C(43)-C(37)-C(38)-C(39)	-1.2(3)
P(1)-C(37)-C(38)-C(39)	175.61(19)
C(37)-C(38)-C(39)-C(40)	1.2(4)
C(38)-C(39)-C(40)-C(42)	-0.8(4)
C(38)-C(39)-C(40)-C(41)	179.9(3)
C(39)-C(40)-C(42)-C(43)	0.4(4)
C(41)-C(40)-C(42)-C(43)	179.7(2)
C(38)-C(37)-C(43)-C(42)	0.7(3)
P(1)-C(37)-C(43)-C(42)	-175.87(18)
C(40)-C(42)-C(43)-C(37)	-0.4(4)
C(4)-C(3)-O(1)-C(2)	-25.7(2)
C(8)-C(3)-O(1)-C(2)	155.10(15)
C(26)-C(2)-O(1)-C(3)	27.2(2)
C(1)-C(2)-O(1)-C(3)	-153.41(15)
C(36)-C(30)-P(1)-C(37)	126.24(15)
C(31)-C(30)-P(1)-C(37)	-57.21(16)
C(36)-C(30)-P(1)-C(1)	17.76(17)
C(31)-C(30)-P(1)-C(1)	-165.69(14)
C(36)-C(30)-P(1)-Ni(1)	-111.56(15)
C(31)-C(30)-P(1)-Ni(1)	64.99(15)
C(38)-C(37)-P(1)-C(30)	162.04(16)
C(43)-C(37)-P(1)-C(30)	-21.35(19)
C(38)-C(37)-P(1)-C(1)	-86.44(17)
C(43)-C(37)-P(1)-C(1)	90.17(18)
C(38)-C(37)-P(1)-Ni(1)	37.81(18)
C(43)-C(37)-P(1)-Ni(1)	-145.58(16)
C(2)-C(1)-P(1)-C(30)	-89.35(15)
C(29)-C(1)-P(1)-C(30)	96.41(17)
C(2)-C(1)-P(1)-C(37)	159.69(14)
C(29)-C(1)-P(1)-C(37)	-14.55(18)
C(2)-C(1)-P(1)-Ni(1)	38.89(16)
C(29)-C(1)-P(1)-Ni(1)	-135.35(15)
C(14)-C(9)-P(2)-C(16)	73.92(15)
C(10)-C(9)-P(2)-C(16)	-105.77(15)
C(14)-C(9)-P(2)-C(8)	-177.64(14)

C(10)-C(9)-P(2)-C(8)	2.68(17)
C(14)-C(9)-P(2)-Ni(1)	-51.51(15)
C(10)-C(9)-P(2)-Ni(1)	128.80(14)
C(22)-C(16)-P(2)-C(9)	-168.91(15)
C(17)-C(16)-P(2)-C(9)	12.54(17)
C(22)-C(16)-P(2)-C(8)	80.23(17)
C(17)-C(16)-P(2)-C(8)	-98.31(16)
C(22)-C(16)-P(2)-Ni(1)	-43.25(17)
C(17)-C(16)-P(2)-Ni(1)	138.21(14)
C(7)-C(8)-P(2)-C(9)	-104.27(17)
C(3)-C(8)-P(2)-C(9)	80.21(15)
C(7)-C(8)-P(2)-C(16)	5.52(19)
C(3)-C(8)-P(2)-C(16)	-169.99(14)
C(7)-C(8)-P(2)-Ni(1)	129.20(15)
C(3)-C(8)-P(2)-Ni(1)	-46.32(16)

Table 30: Hydrogen bonds for (Ni(4,5-bis(di-*p*-tolylphosphino)-9,9-dimethyl xanthene)Cl₂)

D-H...A	d(D-H)	d(H...A)	d(D...A)	<(DHA)
C(14)-H(14)...Cl(1)	0.95	2.94	3.765(2)	146
C(31)-H(31)...Cl(1)	0.95	2.93	3.592(2)	128